Politecnico di Milano

Facoltà di Ingegneria dei Sistemi

Corso di Laurea in Ingegneria Biomedica

Dipartimento di Bioingegneria

Signal transmission and processing
at the inner plexiform layer synapses
in the vertebrate retina

Relatore Politecnico di Milano:

Prof. ssa Maria Gabriella Signorini

Correlatore:

Ing. Federico Esposti, PhD

Candidato

Federico Capiaghi

751535

Anno Accademico 2010-2011

Index

Figure index

Graph index

Table index

Abstract

The thesis wants to have a better comprehension about the function of the Inner Plexiform Layer (IPL), one of the stratum in which the retina is subdivided. The retina is the neural machinery of the eye whose task is to translate the visual scene in a biological signal and perform the first stages of information processing in order to detect the relevant features of the visual scene before transmitting to the brain.

In the IPL as well as in the retina, there are two pathway in which the visual information is transmitted; one is the direct pathway in which the light stimulus is first converted by photoreceptors in an electrical signal, then sent to the bipolar cells (BCs) which deliver the visual information to the ganglion cells (GCs) that are the output of the retina system. The other pathway is the lateral one in which horizontal cells (HCs) send signals and feedbacks to the photoreceptors and the amacrine cells (ACs) do the same to the BCs. Therefore the neural activity observed in the IPL is a complex synaptic activity involving the BCs terminals with their connections to the GCs and the feedbacks received from the ACs.

Physiologically there are two types of BCs with opposite responses to a light stimulus; the ON BCs are depolarized in response to a light stimulus, while the OFF BCs are hyperpolarized in response to a light stimulus and they are depolarized when the light stimulus is gone.

The IPL activity is spatially organized and the IPL itself is divided in distinct layers; the spatial organization contributes directly to the visual information processing, as each layer represents a specific frequency: in the central layers the terminals with transient response are located and thus high frequency signals are there represented. Also the distribution of ON and OFF terminals is not random, but precisely stratified in the IPL. The similarities and differences between the ON and OFF populations and their spatial distribution in the IPL are key points to understand the IPL activity.

The thesis has two main purposes; one is the implementation of a set of tools for extracting quantitative parameters and indicators of different features in the BCs response, such as plasticity mechanism, ability to respond to dimmer light conditions, capacity to respond to

flashes following one another and so on. The other one is the employment of these tools in order to study and analyze quantitatively the peculiarities of the BCs terminals response.

We have used an optical method for recording the synaptic activity in the IPL, by employing a fluorescent reporter called SyGCaMP2. The optical techniques have a good spatial scope as well as a good resolution, therefore it is possible to study the activity of the entire network of synapses in the IPL without losing information about each single terminal activity. Furthermore optical method is not invasive, making possible to have *in vivo* recordings. Specifically the SyGCaMP2, a genetically encoded reporter developed in the Laboratory of Molecular Biology (LMB) by the Lagnado' group, is bound to the calcium channel of the BCs terminals. It is able to sense a calcium inflow into the terminal membrane; a light stimulation causes such an inflow, which in turn triggers the neurotransmitter release used to transmit the visual information to GCs. The calcium level is tracked by a variation on fluorescence level as the $\frac{\Delta F}{F_0}$ signal.

The BCs have ribbon synapses, whose characteristic is to respond to a stimulus not through an action potential, but through a graded potential variation enabling them to gradually release the neurotransmitter; therefore, also the calcium level gradually changes during light exposure and as a consequence the $\frac{\Delta F}{F_0}$ signal too. This signal has been extracted for each terminal and used as input to the algorithms expressly created in the current thesis to have quantitative analysis of the IPL terminals behavior.

The zebrafish, genetically modified in order to make them express the fluorescent reporter SYGCaMP2, were the model organisms; there are many advantages: fast growth from the egg to the adult, the easiness to be treated with genetic engineering techniques, the anatomical and morphological similarities to the human retina. The experimental set up was based on a two-photon microscope, used for fluorescence microscopy, whose output was the *in vivo* recording of the IPL activity.

The light stimulation triggers the calcium inflow in the IPL terminals. We have accurately modeled the stimulation protocol to be able to study the response features we were interested in. In the present work the focus is on how the IPL response changes for variations in the stimulus intensity from brighter light conditions to dimmer ones. The

second aspect is related to the plasticity mechanism, occurring for a stimulus repeated over the time. Therefore the protocol of stimulation consists in a train of four light flashes following one another repeated at different light intensity.

The output of the experiments were the *in vivo* recordings, preprocessed in order to reduce the noise by Kalman filtering and to detect the regions of interest (ROIs) corresponding to the BCs terminals. Each ROI have been then averaged and normalized in order to convert the 2D information in 1D information, because it is easier to apply algorithms to 1D signal than to the 2D one. I had implemented algorithms for obtaining quantitative information on the BCs terminals because in the retina there are many "features detectors"; visual system separates the visual content into distinct components as specific frequencies or specific light intensities. For this reason it is interesting to assess the "features detectors" and their differences between the ON and OFF populations.

The algorithms have as output many parameters and indicators; some of them take into account the variation of the terminals response when the light conditions are changed; some others indicate whether a specific terminal is plastic and changes its behavior for a repeated stimulation. The implemented algorithms treat the terminal as an analogue sensor; to assess the performances of an analogue sensor, a very well known input is provided to the sensor and then its output is measured. The same is done with a BCs terminal: a fixed stimulation pattern is provided and the terminal response is measured; from such response, the algorithms extrapolate the information interesting to assess the performances of that terminal.

We have organized the results in a big dataset. These data has been used for statistical studies on the ON and OFF populations and on related differences and similarities as well as for understanding whether the parameters and the features of the ON and OFF terminal responses have a peculiar spatial organization. We have employed many data mining tools: histograms, cumulative histograms, box-whiskers representations, statistical tests, clustering analysis.

The results have highlighted there are statistically significant differences between the ON and OFF populations, especially regarding the plasticity mechanism during a repeated stimulation, the capacity to respond to dimmer light flashes, the response precision and

repeatability. Furthermore the clustering analysis results in homogeneous groups of terminals, which act as filters to the light intensity of the stimulus; each group has an optimal response at defined ranges of light intensity. These filters are evenly sampled in the IPL. Therefore in each IPL stratum a specific frequency and the entire range of light intensities are represented. The retina is therefore able to process a visual signal at any frequency at any intensity and then transmit it to CSN where it become one piece of the big puzzle that is the visual scene.

We have attempted to identify models able to simulate the real responses to prove the high complexity of connections and feedback mechanisms in the IPL. The results have highlighted how the activity in the IPL is due to many factors, from the signal of the photoreceptors to the ACs influences to the feedback mechanisms of the neurotransmitter released. All these factors contributing to the overall terminal activity are composed in a non linear fashion.

The thesis has described quantitatively features related to the BCs terminals responses; for further researches on the IPL activity, it will be useful to isolate the distinct factors contributing to the terminal response and study them separately. Furthermore the results are interesting not only for the academic theories but also for applied science, e.g. the research on the retinal prosthesis. As a matter of fact, it requires a strategy for the software implementation: a refinement of the methods developed in the current thesis may improve the performances of the retinal devices, assuring patient a better quality of life.

The thesis organization is the following:

- Introduction: the chapter introduces the visual system; it focuses on the retina organization and function and describes briefly the state of the art in the methods for studying it. It finally introduces in detail the morphology and physiology of the Bipolar cells.

- Material and methods: the chapter describes at first the experimental setup; then the chapter explores the methods used to analyze the BCs dynamic in response to light stimulation, from the algorithms to the clustering analyzes, to the strategies to realize mathematical models for the BCs terminals.

- Results: the chapter exposes the results obtained by the previous analyzes, distinguishing the ON and OFF behaviors.

- Discussion: the chapter highlights the more significant neural activity features, looking for some correlations between the parameters calculated and for the main differences between the ON and OFF responses. It shows the distribution of the parameters in the IPL space and finally it debate about the model goodness.

- Conclusion: the chapter exposes which conclusions can be driven from the previous work and the possible future development and opportunities of the project.

- References: the chapter is a list of the papers and books used to complete the thesis.

- Appendix: the chapter reports the algorithms implemented and provides a brief description of them.

The thesis project has been taken place in the Lagnado's group of the Neurobiology division in the Laboratory of Molecular Biology (LMB), Cambridge (UK).

Abstract

L'obiettivo della tesi è avere una migliore comprensione dell'Inner Plexiform Layer (IPL), uno degli strati in cui la retina è suddivisa. La retina traduce la scena visiva in un segnale biologico e attua le prime fasi di elaborazione del segnale al fine di individuare le caratteristiche salienti della scena visiva prima di trasmettere il pacchetto informativo al cervello.

Nell'IPL così come nella retina esistono due vie per la trasmissione dell'informazione visiva; una è la via diretta in cui lo stimolo luminoso è, inizialmente, convertito in un segnale elettrico grazie all'azione dei fotorecettori, poi viene inviato alle cellule bipolari (BCs) che a loro volta inviano l'informazione visiva alle cellule gangliari (GCs) che rappresentano l'output della retina. La seconda via è quella laterale nella quale le cellule orizzontali (HCs) inviano segnali e feedback ai fotorecettori e le cellule amacrine (ACs) alle cellule bipolari. Quindi l'attività neuronale osservata nell'IPL è una complessa attività sinaptica che coinvolge le BCS e le loro connessioni con le GCs e i feedback ricevuti dalle ACs.

Fisiologicamente, ci sono principalmente due tipi di BCs che hanno risposte alla stimolazione luminosa opposte; le BCs ON si depolarizzano in risposta ad uno stimolo luminoso, mentre le BCs OFF si iperpolarizzano ed invece si depolarizzano quando non vi è più il suddetto stimolo.

L'attività nell'IPL è organizzata nello spazio e l'IPL stessa è organizzata in strati distinti; l'organizzazione spaziale contribuisce direttamente all'elaborazione dell'informazione visiva, dato che vi è una stratificazione delle frequenze nell'IPL: negli strati più centrali si trovano i terminali con la risposta transiente e che quindi sono in grado di riportare le alte frequenze del segnale. Inoltre la distribuzione dei terminali ON e OFF non è casuale ma è precisamente organizzata negli strati dell'IPL. Le similarità e differenze tra le popolazioni ON e OFF e la loro distribuzione all'interno dell'IPL sono punti chiave per capire cosa accade nell'IPL durante una stimolazione luminosa.

I principali obiettivi della tesi sono due; uno è l'implementazione di un set di strumenti per estrarre parametri ed indici quantitativi per le diverse caratteristiche della risposta nelle

BCs, come ad esempio meccanismi di plasticità, capacità di rispondere a condizioni luminose molto fioche, capacità di rispondere al susseguirsi di flash lumino e così via. L'altro obiettivo è quello di usare efficacemente tali strumenti in modo da potere studiare ed analizzare quantitativamente le differenze tra i terminali BCs ON e OFF, come i comportamenti nella risposta sono diversi e la distribuzione spaziale dei parametri calcolati.

Abbiamo usato un metodo ottico per registrare l'attività sinaptica nell'IPL, attraverso l'impiego di un reporter fluorescente, chiamato SyGCaMP2. Le tecniche ottiche hanno un buon FOV così come una buona risoluzione, quindi è possibile studiare l'attività dell'intera rete di sinapsi nell'IPL senza perdere l'informazione relative all'attività di ogni singola sinapsi. Inoltre il metodo ottico non è invasivo, rendendo possibile registrazioni *in vivo* dei fenomeni nell'IPL durante la stimolazione luminosa. In particolare il SyGCaMP2, un reporter geneticamente codificato sviluppato dal gruppo Lagnado presso LMB, è legato ai canali di calcio dei terminali BCs. È in grado di rilevare l'influsso di calcio dentro la membrana del terminale; tale influsso è determinato dalla stimolazione luminosa ed è il meccanismo che attiva il rilascio del neurotrasmettitore, usato per trasmettere l'informazione visiva al successivo strato di cellule, le GCs. Il livello di calcio è tracciato dalla variazione nel livello di fluorescenza, in particolare il segnale $\frac{\Delta F}{F_0}$.

Le sinapsi delle BCs sono sinapsi ribbon, la cui caratteristica è quella di rispondere allo stimolo non attraverso un potenziale d'azione, ma attraverso una variazione graduale del potenziale che permette loro di rilasciare in modo controllato il neurotrasmettitore; quindi anche il livello di calcio cambia gradualmente durante l'esposizione alla luce e, di conseguenza, anche il segnale $\frac{\Delta F}{F_0}$. Tale segnale viene poi estratto per ogni terminale e viene usato come input degli algoritmi che sono espressamente creati in questa tesi per fare un'analisi quantitativa del comportamento dei terminali nell'IPL.

Gli zebrafish, geneticamente modificati perché esprimessero il reporter fluorescente SyGCaMP2, sono stati utilizzati per gli esperimenti; molti sono i vantaggi: crescita rapida dalla fase di uovo a quella di individuo adulto, la facilità di trattamento con tecniche di ingegneria genetica, le similitudini anatomiche e fisiologiche con la retina dell'uomo. Il set up sperimentale si basa su un microscopio a due fotoni, usato per la microscopia a

fluorescenza, il cui output è la registrazione in vivo dell'attività dell'IPL in un certo periodo di tempo.

La stimolazione luminosa provoca l'influsso di calcio nei terminali dell'IPL. Particolare attenzione è stata data al protocollo di stimolazione, in modo da potere studiare le caratteristiche di interesse della risposta. Nel presente lavoro il focus è su come la risposta dei terminali dell'IPL cambia al variare dell'intensità dello stimolo luminoso. Il secondo aspetto è relativo ai meccanismi di plasticità mostrati dai terminali nel rispondere ad un stimolo ripetuto nel tempo. Quindi il protocollo di stimolazione è costituito da un treno di quattro flash luminosi successivi, ripetuti a diverse intensità luminose.

I risultati degli esperimenti sono state le registrazioni *in vivo*, sulle quali sono state svolte delle operazioni di preprocessing per la riduzione del rumore attraverso un filtraggio alla Kalman e l'individuazione delle regioni di interesse (ROI) corrispondenti ai terminali BCs. Ogni ROI è stata poi mediata e normalizzata in modo da convertire l'informazione 2D in 1D: è, infatti, più semplice applicare algoritmi ad un segnale 1D rispetto ad uno 2D. Abbiamo implementato algoritmi per estrarre informazione quantitativa dato che nella retina, vi sono numerosi "features detectors"; l'idea generale è che il sistema visivo separa il contenuto visivo nei suoi componenti, come ad esempio le specifiche frequenze e la specifica intensità di luce. Per questa ragione è interessante valutare i "features detectors" e le loro differenze tra popolazioni ON e OFF.

Gli algoritmi applicati al segnale $\frac{\Delta F}{F_0}$ hanno come uscita diversi parametri ed indicatori; alcuni considerano la risposta terminale quando le condizioni luminose vengono cambiate; altri indicano se uno specifico terminal è plastico e cambia il proprio comportamento per uno stimolo ripetuto nel tempo. In generale gli algoritmi implementati trattano i terminali come se fossero dei sensori elettrici analogici; per valutare le prestazioni di un sensore analogico, un ingresso conosciuto è inviato al sensore di cui si misura poi l'uscita. Lo stesso viene fatto con i terminali BCs: uno schema fisso di stimolazione viene somministrata al terminale e si misura poi la sua risposta; da tale risposta, gli algoritmi estraggono l'informazione utile per la valutazione delle prestazioni del terminale.

I risultati sono stati organizzati in un ampio dataset. Questi dati sono stati usati per studi statistici sulle popolazioni ON e OFF e sulle relative differenze e similitudini così come

per capire se i parametri e le caratteristiche della risposta dei terminali abbiano una peculiare organizzazione spaziale. Sono stati impiegati inoltre diversi metodi di data mining: istogrammi, istogrammi cumulative, grafici box-whisker, test statistici, analisi dei clusters.

I risultati hanno evidenziato che vi sono differenze statisticamente significative tra le popolazioni ON e OFF, specialmente riguardo il meccanismo di plasticità durante la ripetizione degli stimoli, la capacità di rispondere a bassi livelli di intensità luminosa, la precisione e la ripetibilità nella risposta. Inoltre l'analisi dei clusters fornisce una serie di gruppi di terminali omogenei, ognuno dei quali agisce come un filtro alle diverse intensità luminose; ogni gruppo ha la risposta ottima ad un definito range di intensità luminosa. Questi filtri si trovano equamente distribuiti all'interno dell'IPL. Quindi in ogni strato IPL è rappresentato una specifica frequenza e l'intero range di intensità luminosa. La retina può così elaborare un segnale luminoso a qualsiasi frequenza ed intensità e poi trasmetterlo al sistema nervoso centrale dove diventa un pezzo del grane puzzle che è la scena visiva.

Sono stati fatti dei tentavi di identificazione dei modelli per simulare la risposta reale dei terminali per mostrare l'alta complessità dei meccanismi di connessione e feedback nell'IPL. I risultati hanno provato che l'attività nell'IPL è dovuta a diversi fattori, dal segnale dei fotorecettori alle influenze delle ACs fino ai meccanismi di feedback da parte dello stesso neurotrasmettitore rilasciato. Tutti questi eventi che contribuiscono alla risposta del terminale sono combinati tra loro in modo non lineare.

La tesi ha dunque descritto quantitativamente alcune caratteristiche peculiari relative alla risposta dei terminali BCs; per ulteriori ricerche sull'attività nell'IPL, sarà utile isolare i singoli fattori che contribuiscono alla risposta dei terminali e studiarli separatamente. Inoltre i risultati possono essere interessanti non solo per le teorie accademiche ma anche la scienza applicata, per esempio la ricerca sulle protesi retiniche. Questi richiede, infatti, una strategia per l'implementazione della componente software: un raffinamento dei metodi sviluppati nella tesi possono migliorare le prestazioni dei dispositivi retinici, assicurando una migliore qualità della vita per i pazienti.

L'organizzazione della tesi è la seguente:

- Introduzione: il capitolo introduce il sistema visivo in generale; si focalizza sull'organizzazione e la funzione della retina e descrive brevemente lo stato dell'arte sui metodi fino ora applicati per studiarla. Infine spiega in dettaglio la morfologia e la fisiologia delle cellule bipolari.

- Materiali e metodi: inizialmente viene descritto il setup sperimentale; poi il capitolo esplora i metodi usati per analizzare la dinamica dei terminali BCs, dagli algoritmi alle analisi di cluster fino alle strategie per realizzare modelli matematici dei terminali.

- Risultati: il capitolo espone i risultati ottenuti dalla precedenti analisi, distinguendo le popolazioni ON e OFF.

- Discussione: il capitolo evidenzia le caratteristiche più significative dell'attività sinaptica, cercando delle correlazioni tra i parametri calcolati e tra le maggiori differenze nelle risposte ON e OFF. Espone inoltre la distribuzione dei parametri calcolati nello spazio IPL e discute la bontà dei modelli identificati.

- Conclusione: il capitolo espone quali conclusioni si possono derivare e quali futuri sviluppi potrebbe avere il lavoro svolto.

- Riferimenti: il capitolo è una lista delle pubblicazioni e dei libri utilizzati per svolgere la presente tesi.

- Appendice: il capitolo riporta gli algoritmi implementati e ne fornisce una breve descrizione

Il progetto di tesi ha avuto luogo nel gruppo del Dott. Lagnado della divisione di Neurobiologia press oil Laboratorio di Biologia Molecolare (LMB), Cambridge (UK).

I. INTRODUCTION

Since the early years of civilization, mankind has been struck by the vision sense: Parmenides, west philosophy father, was the first to address the question about the difference from what man sees and what actually is. This issue has been a fertile field for debate among philosophers and scientists and the modern neuroscience seems to confirm Parmenides' intuition: the vision sense has evolved not to record and reproduce the reality as an HIFI camera, but to perceive the reality and give a reasonable and reliable interpretation of it, thus allowing man to react the most effectively (Parker, 2003).

The sense of vision is made possible by two organs: the eye and the brain; as a matter of fact vision is the result of a sophisticated information processing taking place in the eyes and in the brain. The eyes are composed by many anatomical structures and play the key role as collector of light energy, converter from light energy to electric one and finally first signal processor (Chalpua & Werner, 2004).

Retina, a filmy piece of tissue about 0.4 mm stretched on the back of the eyeball, accomplishes the mentioned tasks, as it includes both the photoreceptors, cones and rods, which convert the light in a variation of ion concentration and thus in an electrical signal and the neural circuits formed by bipolar cells (BCs), amacrine cells (ACs), horizontal cells (HCs) and ganglion cells (GCs), which provide the first stage of signal processing (Williams, Cavada, & Reinoso-Suárez, 1993). In order to maximize performances, retina has evolved as a multilayered structure (Samuel M Wu, 2010), organized as follows:

- Outer nuclear layer (ONL): formed by photoreceptors
- Outer plexiform layer (OPL): formed by the synaptic links between photoreceptors and BCs and HCs.
- Inner nuclear layer (INL): formed by the BCs, HCs, ACs soma

- Inner plexiform layer (IPL): formed by the BCs terminal and ACs and GCs dendrites

- Ganglion cells layer: formed by GCs and displaced AC soma, and the GCs axons.

An abundant literature studied the patho-physiology of photoreceptors and ganglion cells, the main inputs and outputs of the retina (Boycott & Wassle, 1974) (Mollon & Bowmakler, 1992). This has been done through different approaches:

- Dissociated retina: neurons are removed at their embryonic state from the interested area, e.g. the retina. Once dissociated, the neurons are transferred *in vitro* to obtain a cell culture, where it is possible to observe the synaptogenesis and the following connectivity

- Electrophysiology: the electrical activity of neurons is measured directly as the trans-membrane voltage by, for example, patch clamp. Its strength is a reliable and accurate measure of the neuron electric signal, but with strong drawbacks: it is very challenging *in vivo* and it allows the recording of a very limited number of neurons at the same time

- MEA: the Multi Electrode Arrays are matrices whose inferior surface is covered by electric conductive traces, which permit both to stimulate and record the neurons laying on the retinal surface. The advantages are: good temporal resolution and multisite recording. In this case the main drawbacks are represented by the poor spatial resolution and the fact that measures are performed extracellularly which introduced other factors other than the net membrane potential in the measure.

This abundance of photoreceptor and GC literature is not mirrored by a rich literature on bipolar cells, since the possibility to study these cells is mainly reduced to *in vitro* recordings of dissociated BCs. The study of BC activity *in vivo* has been made possible just recently by a method introduced by (Dreosti *et al.*, 2009), which is the method employed in this thesis (see **Methods** section).

The aim of this thesis is to get a better comprehension of the IPL functionality as the place where the first step of the visual information processing occurs. To understand how the IPL works, we have considered two aspects: the dynamic features of the calcium activity occurring at the BC synapses in response to light and the localization of those synapses at the different strata composing the IPL.

The IPL is the place where the complex interactions among BCs terminals, ACs and GCs take place (Kaneko, 1970). Due to the high complexity of the IPL cellular and synaptic structure, a recording of the whole IPL at the single synapse resolution is required.

There have been many investigations on the BCc morphoanatomy and they results in the recognition of 17 BCs types with distinct morphologies in the zebrafish retina, and similar number for other species (Connaughton, Graham, & Nelson, 2004). The differences in BCs types are due to various factors: the presynaptic and postsynaptic connections, the glutamate receptors expressed, the dendrites arborization and so on; some receive inputs just from the cones, other just from the rods and some other again receive the glutamate signal by both the kind of photoreceptors; different morphological BCs types are innervated by different photoreceptors as well as they innervate different types of GCs and ACs. Finally there are mono or multi stratified BCs depending on the distribution of their synaptic boutons in the IPL.

From the physiological point of view, the BCs have two opposite behaviors: ON BCs respond to an increase in light intensity whereas OFF BCs respond to a decrease in light intensity. Both the types of BCs receive the signal from the photoreceptors in the form of the glutamate release: as the input is the same, there should be a different mechanism in sensing the glutamate and a consequent different response. The photoreceptors release glutamate during the absence of light, whereas they block the glutamate transmission during light stimulation. It means in the ON BCs the glutamate blocks a cation-permeable channel.

The ON BCs present both metabotropic and ionotropic receptors. The metabotropic receptors do not form ion channels themselves, but act as isolated antennae on the cell surface sensing glutamate and activating intracellular pathways and mechanisms that can indirectly affect membrane potential (Awatramani & M. M. Slaughter, 2001).

There is a metabotropic glutamate agonist, the 2-amino-4-phosphonobutric acid (APB or DL-AP4, with the L enantiomer being effective) that selectively blocks the light responses of ON BCs (M. Slaughter & Miller, 1985). Thus, ON BCs utilize a metabotropic pathway to sense light-induced variations in photoreceptor glutamate. The metabotropic receptor has been identified as mGluR6 (Nakajima et al., 1993). So the glutamate binding onto the mGluR6 induces the closure of the calcium channel with a related block in the calcium inflow.

As said before the ON BCs present also ionotropic receptors; when the glutamate released binds to these sites, the cell membrane become more permeable to the Cl^- ions and thus the BCs is hyperpolarized during the absence of light. Instead when the glutamate release is inhibited by a light stimulus the BCs is depolarized and the response occurs, as depicted in the figure 1, representing a typical ON response to a train of light flashes.

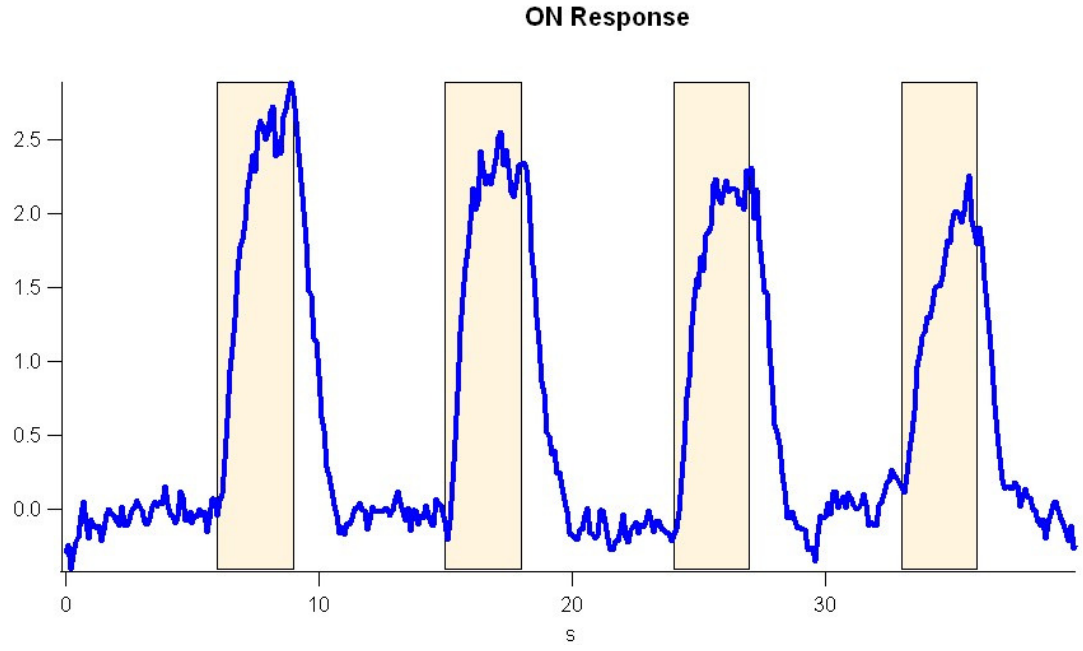

Figure 1: ON response to a train of light stimuli

The OFF BCs do not expose on their membrane metabotropic receptors, but they have only ionotropic ones. Two types of ionotropic channels are used by the OFF BCs in the generation of the light response: the kainite and the AMPA receptors (DeVries & Schwartz, 1999). Despite the kainite and AMPA receptors have different dynamics and thus provide different temporal characteristic to the OFF BCs, their general role is to

provide a calcium inflow, when the glutamate, released from photoreceptors, binds to their sites; this happen during the absence of a light stimulus, as depicted in the figure 2, showing a typical OFF response during a stimulation in the form of a train of light flashes.

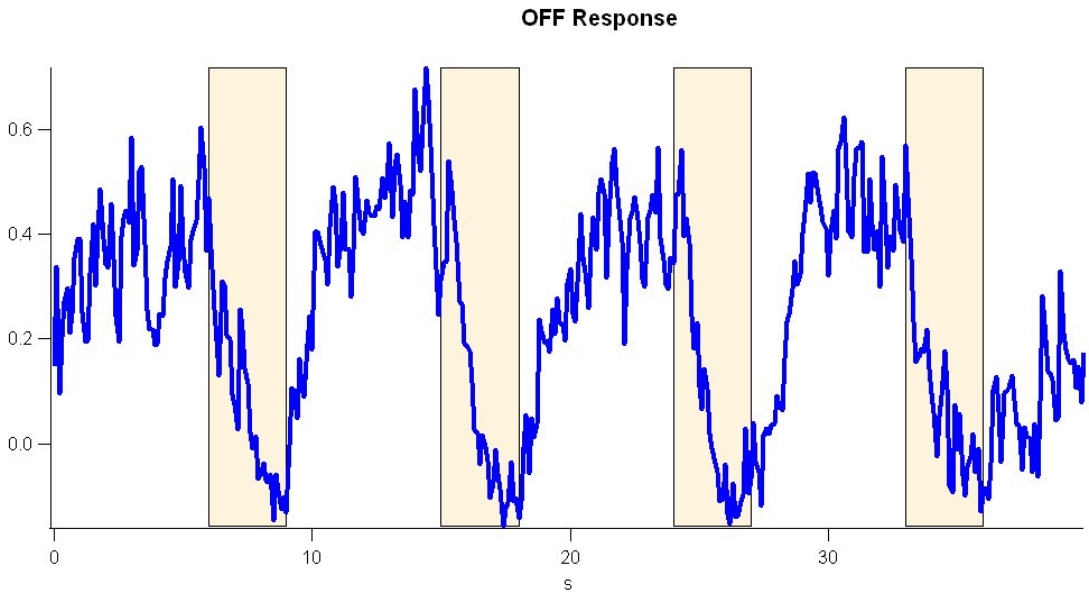

Figure 2: OFF response to a train of stimuli

ON BCs and OFF BCs are linked with distinguished GCs in order to keep the segregation of the ON and OFF channel along all the visual pathway.

II. MATERIAL AND METHODS

Experimental Setup

1. *Transgenic Zebrafish*

The model organism used in this work is Zebrafish (*Danio rerio*). Zebrafish are a tropical freshwater fish belonging to the minnow family (Cyprinidae) of order Cypriniformes, and is an important vertebrate model organism in scientific research for many reasons (Sprague, Doerry, Douglas, & Westerfield, 2001). First of all, the physiology and the anatomy of retina are highly conserved among vertebrates; for this reason the Zf retina is an excellent model for the human one. Moreover, some practical and economical motivations imposed Zf as one of the most used model organisms for vision research. Zf embryos develop very quickly: in 24 hours they evolve from a single cell of fertilized egg to a independently feeding fish, while a similar development process in the mouse last for almost 21 days (with clear economical implications, as well). Zf embryos transparency allows the observation of the inner organs (Karlsson, von Hpfsten, & Olsson, 2001), such as the retina, and thus to use fluorescent protein markers in order to label the interested anatomic targets. Finally, Zf has been proved as a convenient model organism for genetic engineering and molecular biology, allowing the development of many molecular biology tools for gene insertion, modification or knockdown (Baier, 2000).

For the sake of this study Zf larvae and embryos were grown in E2 medium at 28 °C and breed naturally. The fish used for the experiments came from a stable transgenic line expressing the genetically encoded calcium reporter GCaMP2 (Tallini et al., 2006), in its synaptically localized version SyGCaMP2 (Dreosti et al., 2009) under the Ribeye-A promoter.

2. *SyGCaMP2 reporter*

Neuroscientists are interested in a method able to monitor and represent the phenomena happening in a pool of neurons when activated by some sort of stimuli; as a matter of fact the variations in membrane potential are the basic phenomena that trigger vesicular release.

Given the difficulties in developing reliable and effective voltage sensitive optical dyes, one of the most widespread tools for optical monitoring the neuronal activity is calcium dyes. As known, calcium is the signaling ion involved in traducing the variations in membrane potential into vesicle release, thanks to voltage-activated calcium channels (Augustine, 2001).

The optical techniques exploit fluorescent reporters which are proteins emitting fluorescence when activated. In the eukaryote cells the Calmodulin (CaM), a calcium binding protein, is very common. The scientists have exploited the CaM to produce fluorescent reporter able to sense calcium; when the CaM binds calcium, it is subjected to a conformational change. Therefore a protein, which becomes susceptible to fluorescence for conformational change, is bound to the CaM: the result is a protein reporter susceptible to fluorescence in presence of calcium, e.g. GCaMP2.

We were interested in detecting the activation in single synapses due to a single stimulus; a promising location to sense the calcium inward movement is the presynaptic terminal, a small cellular compartment with high density of voltage sensitive calcium channel. Therefore the GCaMP2 does not have to spread all around the cytoplasm, but it should be concentrated at the synapses close to the neurotransmitter vesicles. The Lagnado group at LMB recently developed SyGCaMP2 (Dreosti, Odermatt, Dorostkar, & Lagnado, 2009), as the fusion of GCaMP2 to the synaptophysin, a transmembrane protein in the synaptic vesicles, specifically on its cytoplasmatic side.

Locating the gene codifying for the GCaMP2 downstream to the one codifying for the synaptophysin is necessary for producing the SyGCaMP2, but up to now there are not techniques able to place a gene next to another one. Therefore the portion of DNA codifying for the GCaMP2 and the synaptophysin is inserted in a plasmid and then inserted

in the synapses target. The plasmid are DNA molecular separated from the chromosomal DNA and able to replicate independently from it; thanks to these features they can be used in genetic engineering as the so called vectors: they carry genetic sequences we want the host to express.

The gene to be expressed needs a promoter that is a genetic sequence not codifying for any gene; instead it has a regulatory function by activating the gene expression if some conditions are verified. The promoter used is the Ribeye A, that activates the gene expression for the production of those proteins that in turn produce the ribbon synapses present in the BCs. The result is the SyGCaMP2 reporter, i.e. GCaMP2 molecules tethered to the synapses vesicles in the ribbon of the BCs. When the calcium binds the reporter, a conformational change occurs making the reporter susceptible to fluorescence. Therefore an incident radiation on the SyGCaMP2 generates a fluorescent phenomenon visible thanks to a fluorescent microscope.

The SyGCaMP2 has been tested both for *in vitro* and *in vivo* recordings, showing a striking ability to detect the single spikes at individual synapses as well as the activity in the ribbon synapses in the retina, which is more interesting for the present thesis. Indeed, retinal BCs are characterized by the ribbon synapses, i.e. synapses responding to a stimulus not with a spikes generation, but with a graded membrane potential. As a matter of fact the luminance changes vary around a mean level, and they are not signaled by a change in the rate of spiking as in the most of CSN, but as a graded variation in the membrane potential (Werblin & Dowling, 1969). Such a behavior means the BCs can continually grade the synaptic output and thus conveying more information: it is a typical mechanism easy to find in the neurons involved in the perception of complex sense such as vision and hearing (Parsons & Sterling, 2003). The finely graded release of the neurotransmitter requires high density pool of vesicle and ready and fast triggering mechanism; the ribbon is the structure suiting this task. For example, ribbon synapses in the BCs keep the segregation between the ON and OFF pathway, producing parallel channels of information flow. The advantages of the ribbon synapses are that small and large changes in luminescence can be transmitted with comparable sensitivity and the broader bandwidth of frequency transmitted (Juusola, French, UUsitalo, & Weckstrom, 1996).

For the thesis purpose Zf have been genetically modified to express the SyGCaMP2 under the Ribeye A promoter which have been able to detect the underlying calcium activity in the IPL, by sampling many hundreds of terminal simultaneously and providing a better temporal resolution and spatial field of view than the GECIs in the neuron soma. The signal produced by the reporter is the $\frac{\Delta F}{F_0}$, i.e. the variation in the fluorescence due to the cytoplasmatic calcium increase against the average fluorescence; the area characterized by a large magnitude of the signal $\frac{\Delta F}{F_0}$ accounts for terminals that are been stimulated and in which the machinery providing the neurotransmitter release, and the consequent signal transmission, is triggered (Lagnado, Gomis, & Job, 1996). This signal is finally recorded and imaged by using a custom-built two-photon microscope.

3. *Imaging IPL by two-photon microscopy*

In recent years many imaging techniques have been explored to obtain the best spatial and time resolution views of biological process occurring below the accessible organism surface. One of the most significant advancements has been represented by the introduction of fluorescence microscopy (Tsai et al., 2002), based on the fluorescence phenomenon which is governed by three events: excitation (or absorption), vibrational relaxation and emission. In the absorption phase some molecules in the probe are excited by a wavelength of light falling within the linear absorption mode of the molecule: the light photon is absorbed and the molecule is promoted to higher energy electron state; during the vibrational relaxation energy is loss and the molecule gets back to its equilibrium state and a photon is emitted at longer wavelength respect the one of the excitation photon. The microscopy exploits the phenomenon as described in figure 3

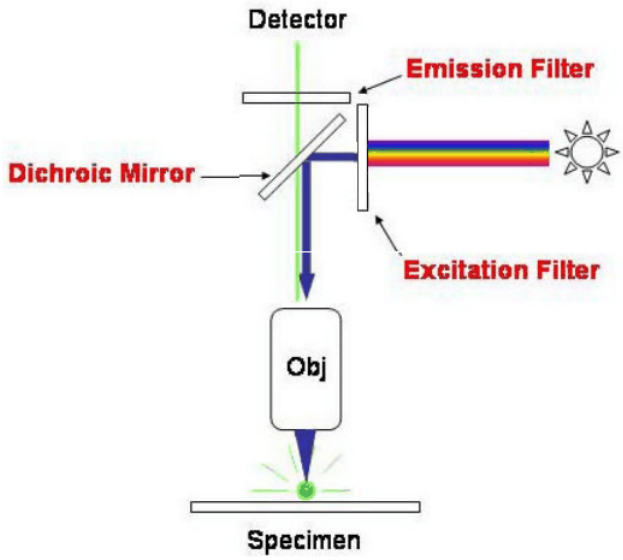

Figure 3: Example of fluorescence microscopy

As explained above, the image is made by the fluorescence of the molecules in the sample: so the image formation itself depends on the fluorescence event to happen when excitation light is provided. The probability of the excitation event is directly proportional to the photons spatial density, i.e. the light intensity. Therefore the one-photon absorption

fluorescence imaging technique requires strong light intensity, that means a high energy level which causes an important heat transfer with potential damage for the sample.

A better solution for the fluorescence imaging technique is the two-photon laser-scanning microscopy; the laser light has double wavelength of the one used in the traditional method, which means the photons carry half of the energy and the impact of a single photon cannot make the molecule to shift to the higher energy state. Hence, the excitation process requires the simultaneous absorption of two photons from the excitation beam; the probability of the simultaneous absorption of two photons scales with the square of the incident light intensity, and thus is significantly lower than the absorption probability in the one photon imaging. The problem is solved by the adoption of the pulsed technique for delivering the laser light to the sample, which allows to provide the needed large light intensity for the two photons absorption and to keep the average energy transferred in the safety limits of avoiding the heating and so the damaging the sample. The two-photon absorption microscopy has many advantages: since the heating damage depends on the average power of the incident beam and thus by the temporal variable as

$$P = \frac{E}{T} \quad P = Power;\ E = Energy;\ T = Time$$

the pulsed technique provides a lower temporal average energy and thus less heating damage; furthermore the excitation light penetrates to a depth dependent to the instantaneous peak power that is very high to increase the two photons absorption probability: the two-photons absorption microscopy can be used for thick preparations. Finally in the specific case studies, the laser has a wavelength outside the visible range and thus does not excite the photoreceptors.

The recordings used in the present thesis have been performed using a custom-built two-photon microscope installed in the LMB at the Neurobiology division floor. The microscope is equipped with a mode-locked Chameleon titanium sapphire laser tuned to 915 nm, produced by the Coherent firm; Chameleon is a kind of laser oscillator used for multiphoton microscopy and the mode-locked term refer to the technique for producing ultrafast pulses. The objective is an Olympus LUMPlanFI 40x water immersion, which captures the emitted fluorescence. The following step is the filtering by an HQ 535/50GFP

emission filter (Chroma Technology) and after that the fluorescence is detected by photomultipliers (Hamamatsu).

In order to record the IPL activity, the Zff has been immobilized on glass slide in 2% low-melting agar-agar that is a substance extracted from the agarophyte red algae, since its gelatinous consistency is used with a substrate purpose. The fish is then mounted with the pupil aiming to the microscope objective and to obtain a high quality recording the eye movements have to be prevented by injection of the neuromuscular blocker α-bungarotoxin (2 mg/ml).

The entire imaging process is managed by the software ScanImage v 3.0 running on a PC; the software controls the scanning phase, by generating the analog voltage for driving the scan mirrors, as well as the acquisition phase, by collecting the currents from the photomultipliers, converting it into voltage signals in order to obtain the raw data that, afterwards, are stored, as a stack of frames along the Z direction, in TIF files for easy portability and compatibility (Pologruto, Sabatini, & Svoboda, 2003). The acquisition rate was 10 Hz.

Each experiment is performed on one single fish stimulated by light pulses delivered through an optic fiber from an amber LED. The figure 4 shows the light stimulation.

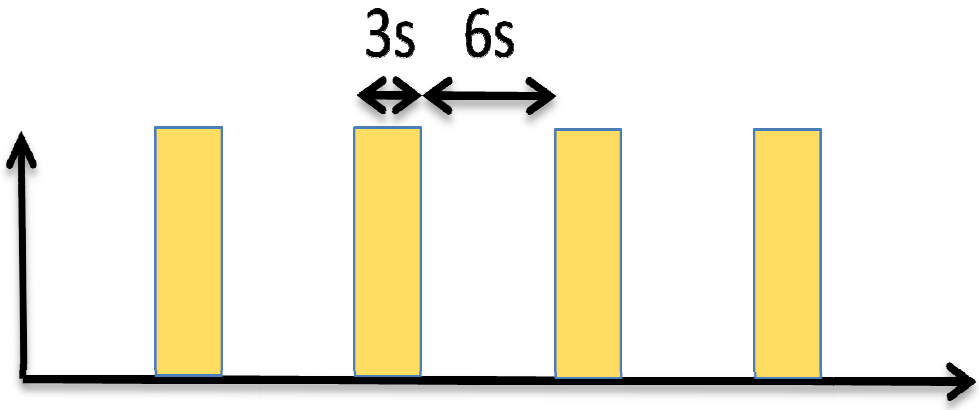

Figure 4: The stimulation pattern provided to the zebrafish retina during the experiment.

The stimulation protocol was composed by four 3 seconds long light flashes separated by 6 seconds of complete darkness. The emitted light intensity from the LED was 17 nW/mm^2 ;

the intensity was changed, by using an optical neutral density (ND) filter; this kind of disk filter has a constant attenuation effect, and therefore it is used to decrease the light intensity of the stimulus. Its capacity in reducing intensity is labeled by the optical density (or absorbance):

$$ND = \log_{10} \frac{I_0}{I}$$

I_0 = incident light intensity I = transmitted light intensity

The intensity range, with a log-spaced sampling, is from 17 nW/mm^2 to 1.7 pW/mm^2 (see table 1), so it is over four orders of magnitude; in the following part of thesis the light stimulus intensities will be represented by NDXX:

Intensity	ND
17 000 pW/mm^2	ND00
5380 pW/mm^2	ND05
1700 pW/mm^2	ND10
538 pW/mm^2	ND15
170 pW/mm^2	ND20
53.8 pW/mm^2	ND25
17 pW/mm^2	ND30
5.38 pW/mm^2	ND35
1.7 pW/mm^2	ND40

Table 1: Conversion between the intensities and the corresponding ND

The stimulation protocol allows to investigate two main aspects of the IPL synaptic activity: the presence of plasticity mechanism, explored through the four light flashes following one another, and the behavior at different light conditions, assessed by varying the light intensity. As a matter of fact the sequence scheme of stimulation clarifies the thesis targets, i.e. the analysis of the neuronal machinery in IPL behavior during dynamic stimulation with light intensities changes.

Signal Analysis

4. *Preprocessing*

The IPL imaging acquisition, by the two-photon microscope, had provided the raw data. The next step was to detect the synaptic terminals, i.e. the regions of interest ROIs, to evaluate their position in the IPL and finally to convert the 2D pixel information into 1D signal, more useful for extracting quantitative information on the calcium activity.

The sampling rate chosen was equal at 10 Hz over a time of 40 seconds; it means that for each light intensity the result was a movie representing the IPL strata of the retina during the light stimulations. The movie was a stack of 400 frames each of one depicting the IPL activity in a specific moment of the stimulation. So each image is a matrix of pixels and, depending on the temporal instant it has been detected, its grey level distribution would be more or less differentiated indicating synaptic activity in the IPL strata. The objective is to study this activity with the tools of the signal and data processing.

The image stack obtained during the acquisition phase needed some adjustment both for the size and for the noise corruption. Preprocessing stages were carried out in MacBiophotonics Image J, a software collecting many functions, macros and plugins for the image processing. The figure 5 illustrates a frame from the recording

Figure 5: One frame of the IPL activity recorded with a two-photon microscope

The raw data were corrupted from internal source of noise like the random fluorescence activity of some terminals as well as from external one like the shot noise always present in the optical imaging; as a matter of fact, the number of photons carrying the energy is sufficiently low so that the uncertainties due to the Poisson distribution, which describes the occurrence of random events, are significant high. . Kalman predictive filtering was applied on the stacks in order to reduce the noise components.

The figure 6 shows the result from the application of the Kalman Filter to a frame of the recording.

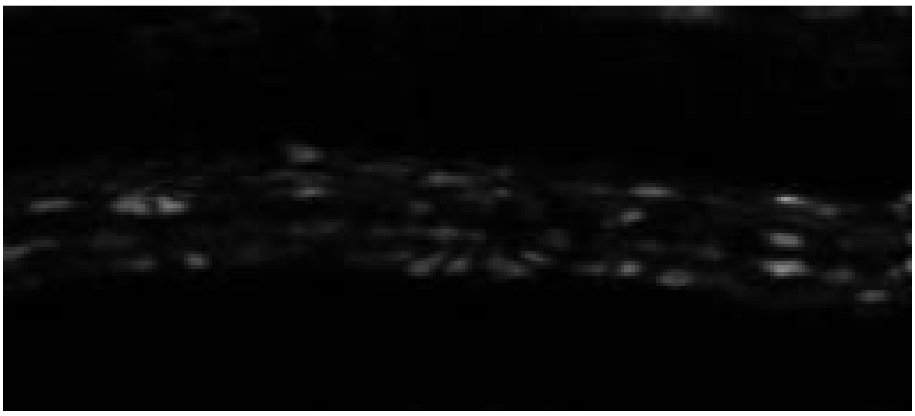

Figure 6: The same frame after the noise clearing by the application of the Kalman filter

The *in vivo* imaging techniques face the issue of the model organism movement and the related distortion. The solution adopted consisted in applying a rigid-body registration to the recording.

Once the previous preprocessing stages were completed, we have used a new software environment, Igor Pro (Wavemetrics), a commercial data analysis package popular amongst the electrophysiologists. The specific tool SARFIA (for Semi-Automated Routines for Functional Image Analysis) implemented in the Lagnado's Group performed the automatic detection of the synaptic terminals and the identification of terminals position in the IPL (Dorostkar, Dreosti, Odermatt, & Lagnado, 2010).

Background subtraction was applied in order to correct for the resting background fluorescence of the movie. A background area is manually selected, the average gray level intensity was computed and the latter was subtracted from the entire recording.

The terminals, labeled through a reporter protein as the SyGCaMP2, had different levels of brightness due to not homogeneous distribution of the reporter as well as the variance in the expression level; furthermore the brightness depended on the terminals location relative to the plane of focus. As a matter of fact, there were many pixels actually belonging to an activated terminal but, for the reasons above explained, they had a low contrast with the background areas and their intensity level needs to be enhanced. The solution was first of all making an average of all the frames in order to have a reference image less noisy and then filtering the image with a Laplacian mask, an operator for the edge detection, that represents the approximation to the second derivate (Burger & Burge, 2008):

$$\nabla^2 I = \frac{\partial^2 I}{\partial x^2} + \frac{\partial^2 I}{\partial y^2}$$

$$\begin{bmatrix} 0 & -1 & 0 \\ -1 & 4 & -1 \\ 0 & -1 & 0 \end{bmatrix} \qquad \begin{bmatrix} -1 & -1 & -1 \\ -1 & 8 & -1 \\ -1 & -1 & -1 \end{bmatrix} \qquad \begin{bmatrix} -2 & 1 & -2 \\ 1 & 8 & 1 \\ -2 & 1 & -2 \end{bmatrix}$$

The filter is rotationally symmetric, which means edges at all the orientation contribute to the result. The sing of the result can be positive or negative: if the pixels gray level of the initial image is higher, in the filtered image they will have negative values. The threshold value was assessed as a multiple of the standard deviation of all the pixels falling into the Laplacian mask. The advantage of using a second order derivative filter was that takes into account the relative and thus local variation in brightness more than the global one.

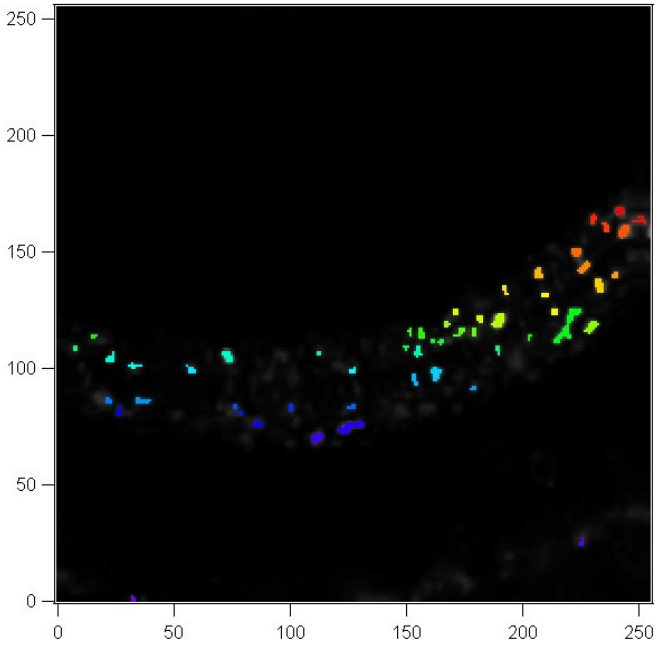

Figure 7: The colored zones represent the ROIs detected in the IPL

The figure 7 shows the final result that can be even more refined by the user who is able to select the minimum number of pixels required to have a ROI: it's a sort of low pass filter to counterbalance the effect of the Laplacian filtering. In this way the traces from the areas of interests were extracted and labeled. As the ROIs were saved as independent dataset, the ROIs mask has been calculated just for the first movie: the mask calculated for the recording at ND00 was applied then to the recordings at other ND.

There are two main reasons why the terminals location in the IPL is interesting; first of all, retina as well as other neuronal structures, such as the cerebral cortex or the hippocampus, is organized in distinct substrata called layers, thus correlating the organ spatial organization to its functions. Related to this feature, the scientific literature has shown that different types of BCs, typically ON and OFF, are localized in two separated layers, the sublamina b and the innermost layers of sublamina a for ON closer to the ganglion cells layers (GCL) , and the outer two layers of sublamina b for the OFF closer to the photoreceptors layers (Amthor, Takahashi, & Oyster, 1989).

The figure 8 depicts the layered structure of the retina.

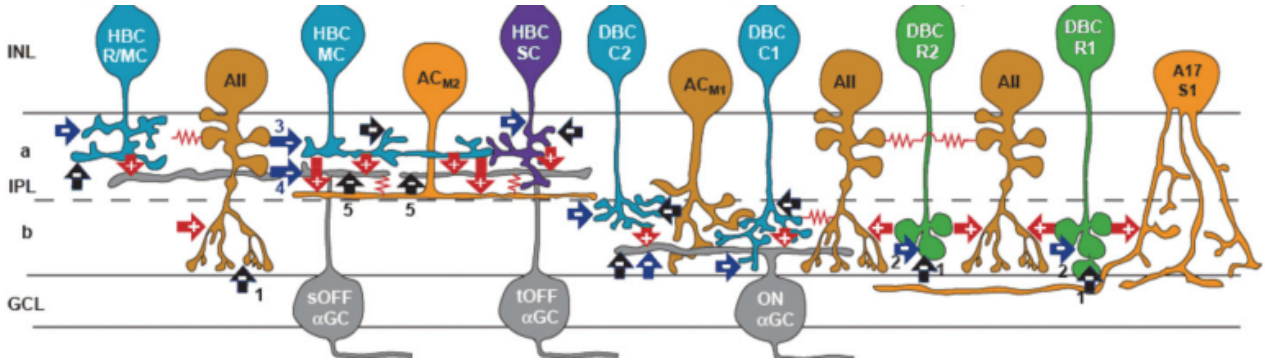

Figura 8: Spatial organization in the IPL

Two boundaries were fixed, with 0 labeling the border closest to the ganglion cells and the 100 the margin closest to the photoreceptors: the BCs terminal position fall inside these extremes. The localization of the terminals was carried out by superimposition of the ROIs mask on the average image. The localization algorithm calculated equispaced splines between the superior and inferior boundaries, manually drawn and smoothed using a locally weighted polynomial regression algorithm (Cleveland, 1979). The figure 9 shows the terminals detected, the boundary closest to the photoreceptors layers (red) and the one closest to the GCs bodies (cyan).

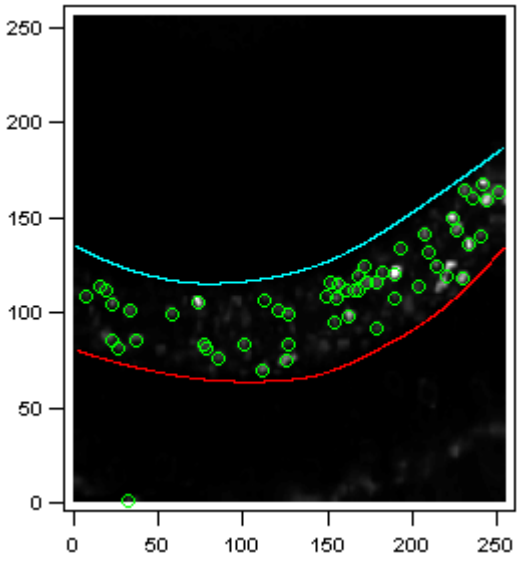

Figura 9: Procedure for the ROIs detection in the IPL

The red boundary was defined as c_{100}, while the cyan one as c_0: the remaining 99 layers were calculated as:

$$c_i = \frac{i \times c_{100} + (100 - i) \times c_0}{100}$$

For each ROI was calculated its center of mass $\vec{R}$, by weighing the position vector $\vec{r}$ of each pixel in the ROI for its brightness m_i:

$$\vec{R} = \frac{\sum(\vec{r} \times m_i)}{\sum m_i}$$

Finally the Euclidian distance was assessed between the ROI and each layer; the ROI was assigned to that layer from which it had the minimum distance.

The areas detected as ROIs but actually laying outside of the layered area, were labeled as outliers with the numbers -1 and 101.

The last stage in the preprocessing was the extraction of the $\frac{\Delta F}{F_0}$ signal varying across time from the terminals. Each ROI response was calculated as the average of all the pixel comprised in the ROI. The 2D information was thus converted into 1D signal to which it was easier to apply algorithm for extracting quantitative parameters and indicators useful for statistically studies about the terminal populations.

As the figure 10 show, it was possible an initial guess whether the BCs response is an ON or OFF one: the responses of the upper row belong to ON BCs terminals and the ones of the lower row to OFF BCs terminals

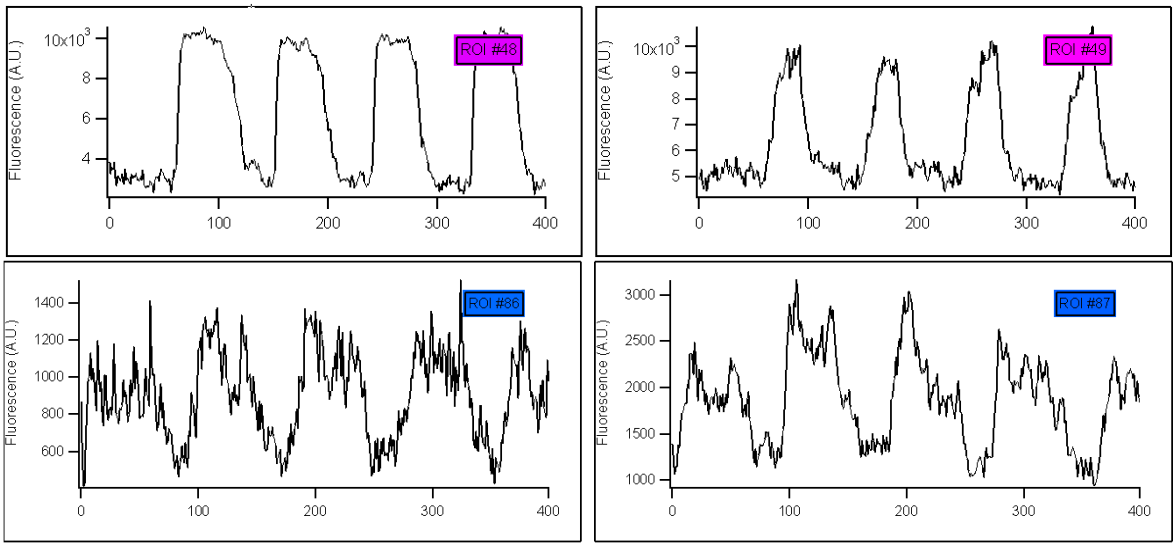

Figure 10: the fluorescence signal from each terminal at a specific ND

5. *Primary Parameters*

I have implemented algorithms (see the chapter **Appendix**) for extrapolating the $\frac{\Delta F}{F_0}$ signal some mathematical indicators for a quantitative description of the BCs dynamic activity. At first we analyzed primary statistics that are easier to calculate and give a general framework to study the neuronal response. First of all it was necessary to separate the ON BCs terminal and the OFF ones and a synoptic visualization with false colors of the $\frac{\Delta F}{F_0}$ signal over the recording time at each light stimulation intensity for each terminal has been useful.

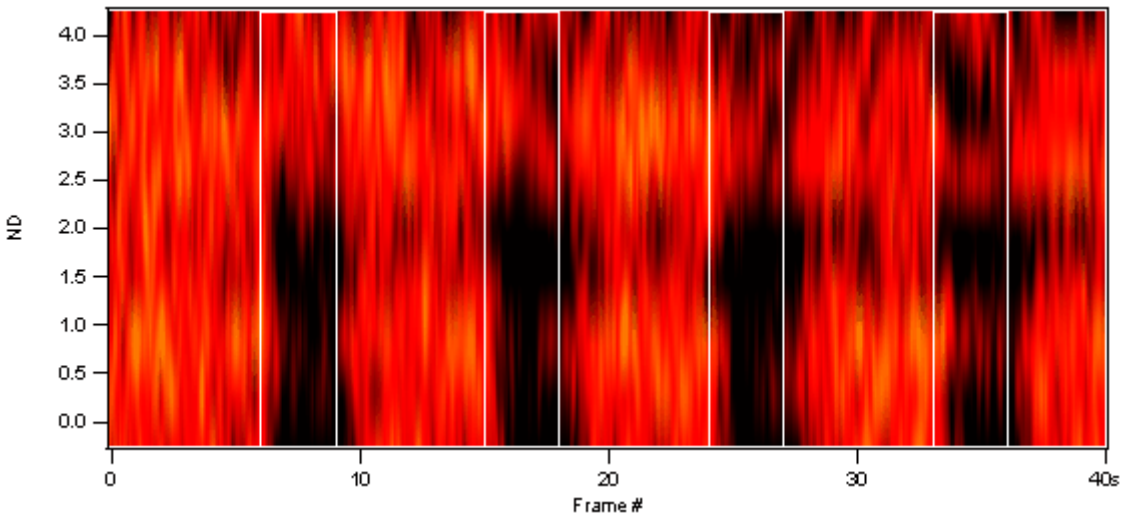

Figure 11: Synoptic representation of the activity of a specific terminal during the stimulation time for all the ND

In the figure 11, the darker colors represent higher value of $\frac{\Delta F}{F_0}$, while the white bars represent the light stimuli. This kind of representation allowed an easy survey on the response polarity and the luminance sensitivity. The figure 11 shows an ON BC terminal, which produces a calcium concentration increase in response to light stimulus. Once the classification has been made, the ON terminals and the OFF ones were saved in two different workspaces and they were approached separately in the next elaboration phases.

The approach employed in this work consisted in considering BC terminals as analog sensors, hence BC terminal responses were analyzed in terms of sensor performances. The

primary statistics considered were: response max average, area and slope and reliability over multiple presentations.

Max average

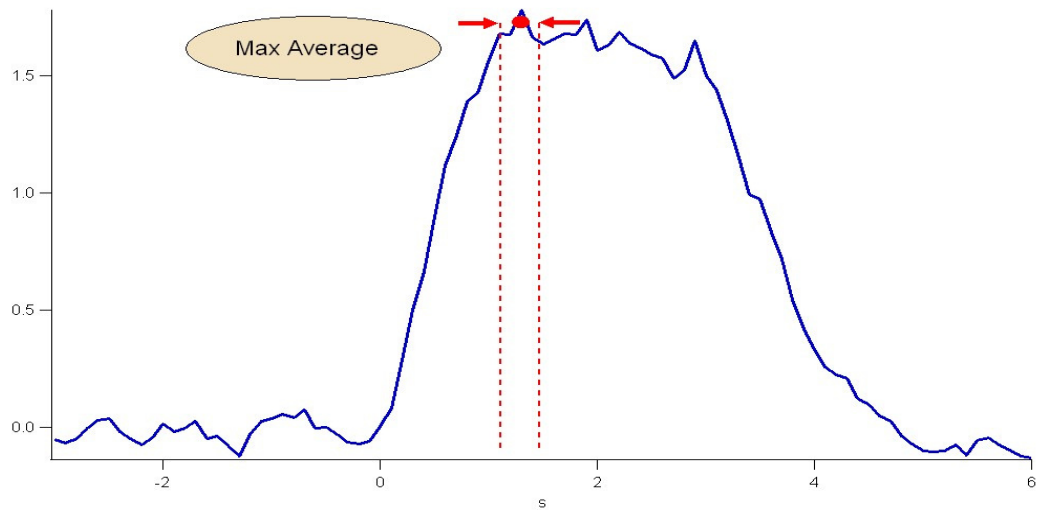

Figure 12: Representation of the max average parameter

The *max average* is calculated as the signal average in a window of 300 ms around the highest peak of the signal: it denotes the terminal brightness level which depends on how the fluorescence is strong and thus describes the calcium concentration at the terminal.

Figure 12 shows the response of a BC ON terminal to light; the arrows delimit the 300 ms time window centered around the maximum used to calculate the maximum average response (red dot).

.

Area

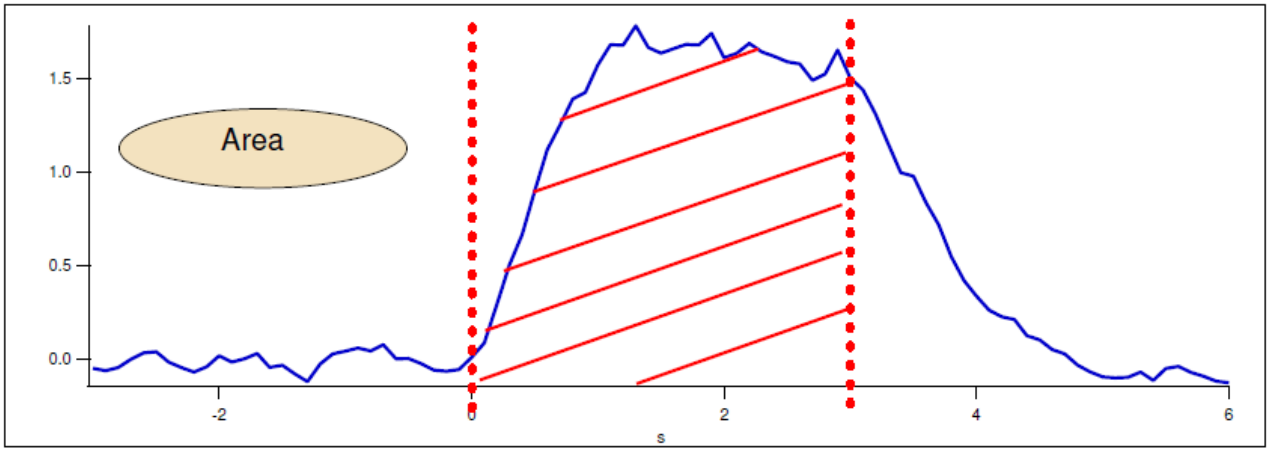

Figure 13: Representation of the Area parameter

The *area* parameter (figure 13) is the area under the response in the stimulus interval (3 seconds). Despite both the *area* and the *max average* are indicators of the fluoresce amplitude, the *area* conveys an additional information: a transient and a sustained response may have equal *max average* but they certainly have very different *area*. Furthermore the latter is more robust and dependable as it is an integral measure and thus the effect of a noise superimposed is corrected.

The *max average* and *area* parameter are interesting because are indicators of the gain in amplitude boosted at each stage of signal transfer in the visual pathway (Belgum & Copenhagen, 1988).

Reliability

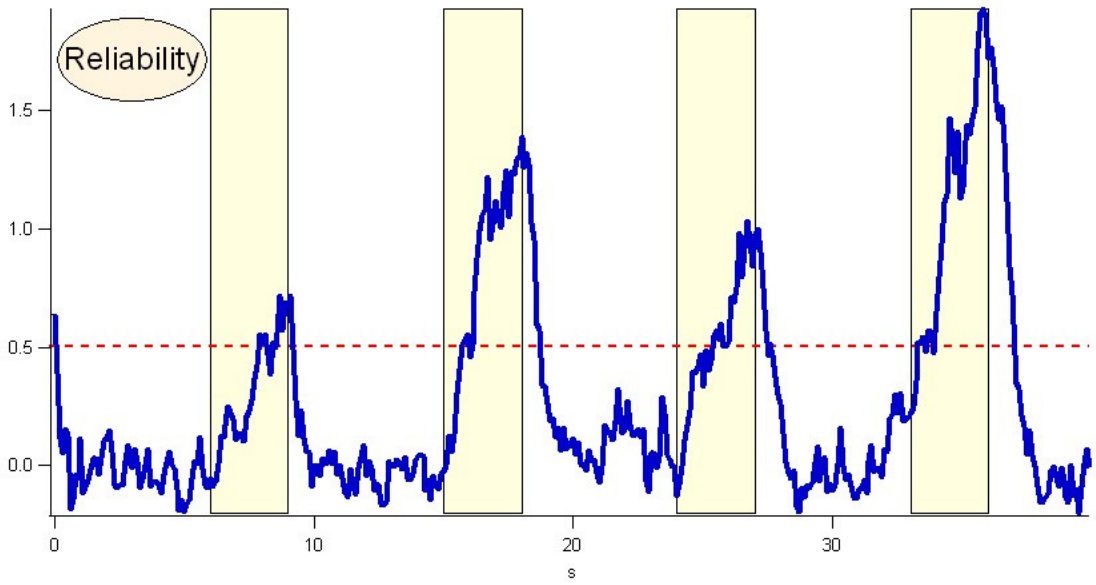

Figure 14: Representation of the Reliability parameter

Reliability is defined as the ability of a sensor to respond at each repeated stimulus. In the thesis the *reliability* is the ability of a terminal to respond to each of the four light flashes. The *reliability* employs the information from the *area* parameter by using the 0.5 *area* value as threshold: if the signal during the stimulation time has an *area* above 0.5 is considered as a response, otherwise it is not. So the maximum value of the *reliability* parameter is 4, if the terminal respond to each of the four light stimuli, while the minimum is 0 if it does never responds.

The figure 14 represents the terminal response to the stimulus and the threshold over which a response is considered reliable. The terminal has a reliability value equal to three, because it has a significant response for the last three flashes, but not for the first one.

Slope

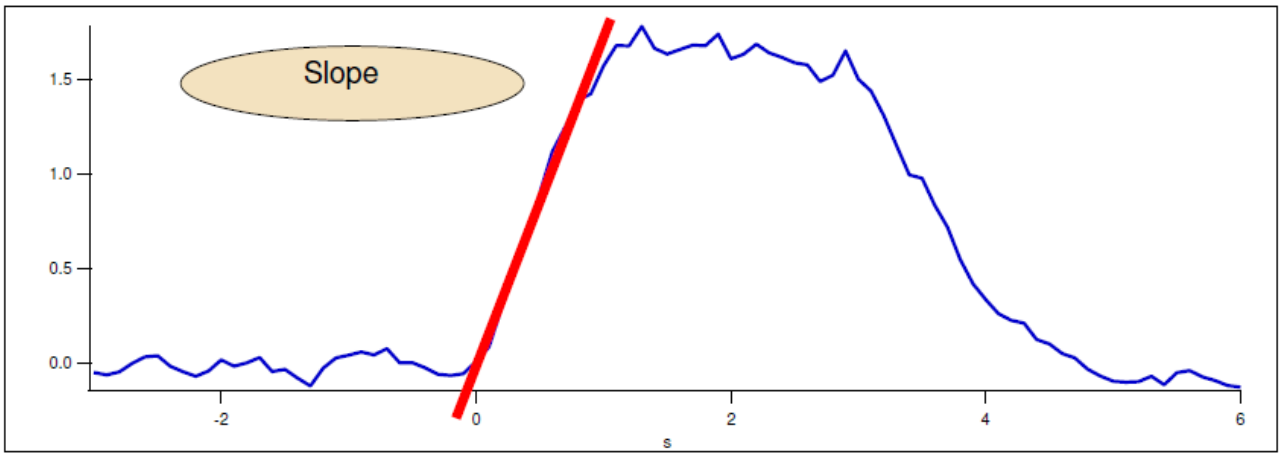

Figure 15: Representation of the Slope parameter

The *slope* indicates the response dynamic as it is a measure of how fast the signal reaches the steady state from the basal one. The *slope* is the ratio between the *max average* and the time spent for reaching the max peak from the baseline.

The figure 15 shows the slope of the terminal response.

For each terminal we have four values for the primary parameters, one for each light stimulus; I have averaged these values to study the overall response to a light step; together with the averaged value, I also calcluated the standard deviation represented as error bars. In the graph 1 primary statistics are drawn against the light intensity level (ND) and a blue rectangular is showed that represents the light intensities to which the terminal responds with a significant signal, again taking as reference value 0.5 of the *area* (see the first box of the graph 1).

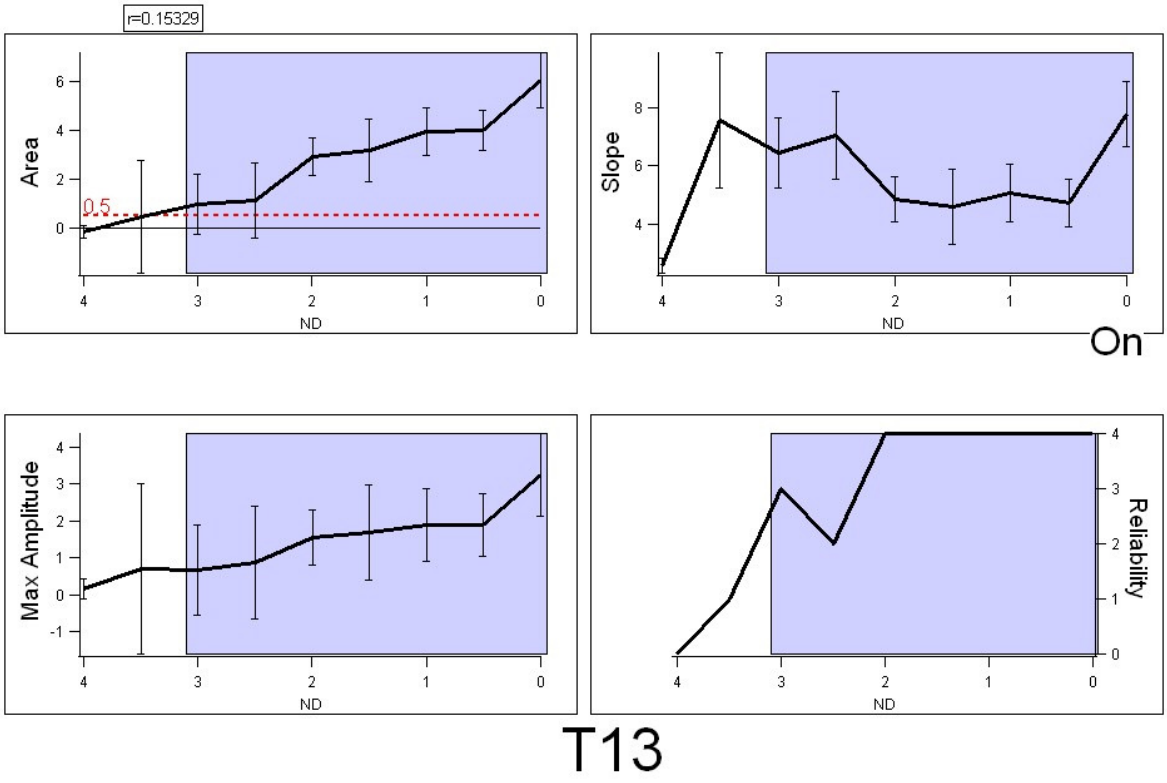

Graph 1: The trend of the four primary parameters over the stimulus light intensities

It is also interesting to evaluate how the primary statistics change over the train-stimulus pattern and thus study whether the terminal changes their calcium activity to respond to light inputs following one another. As before the primary statistics are graphed against the light intensity level, but now the four values for each stimulus are superimposed as showed in graph 2. The same layout also displayes the averaged terminal responses to a light step over the time at the different stimulus intensities. In a such a way a first description of the plasticity of the neuronal connections in the IPL is given and it will be further analyzed with the derived statistics in the following chapter.

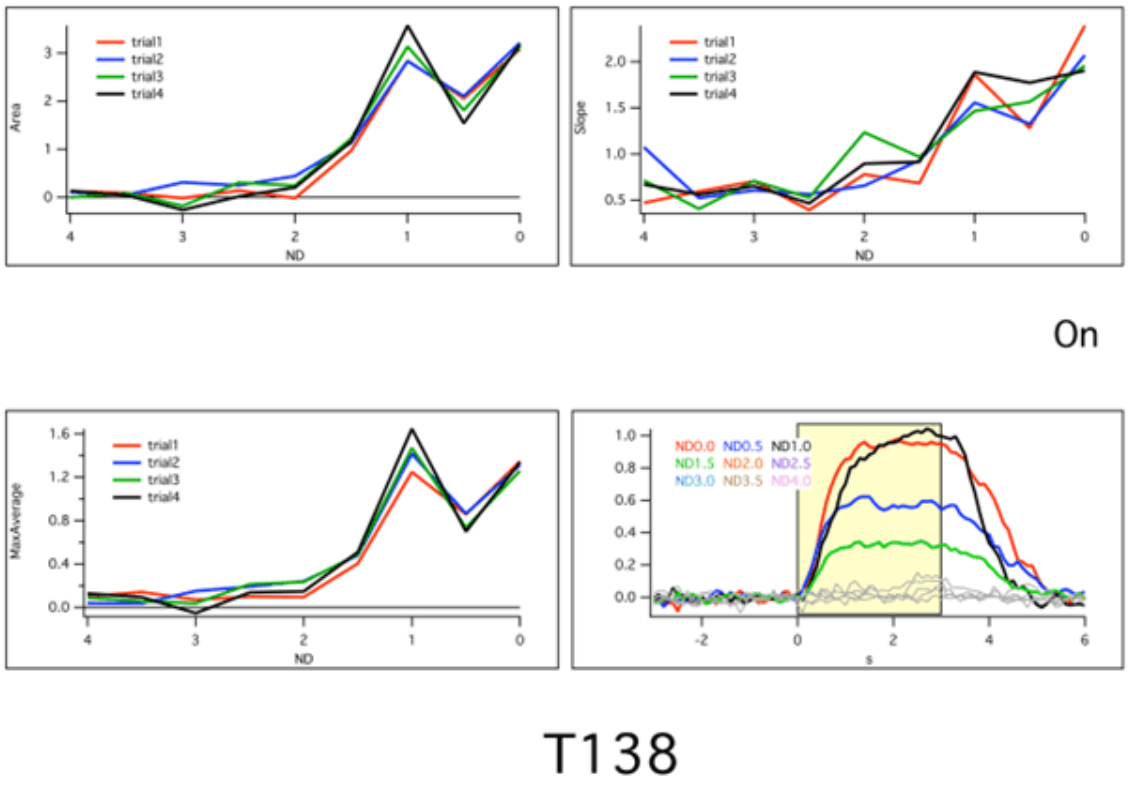

Graph 2: The trend of the four primary parameters for each flash and over the light intensities

6. *Derived Parameters*

A topic of particular interest for the thesis purpose, it is the dynamic activity in the IPL over the time in response not to a single stimulus but to a stimuli train, which better describes the plasticity of the neuronal machinery in the IPL, i.e. its ability in changing the rate and level of calcium flow. The primary parameters are not able to describe such a dynamical behavior because they were calculated as an average over the four stimuli, but they were still useful to derive new parameters which are better indicators of that behavior.

The derived parameters can be divided in two main categories, with a certain degrade of overlapping between them

- Measures focusing on the dynamic response to a train of four flashes
- Measures focusing on the assessment of the performances of the BCs terminal studied as an analogue sensor

The parameters belonging to the first category are:

Adaptation/Potentiation

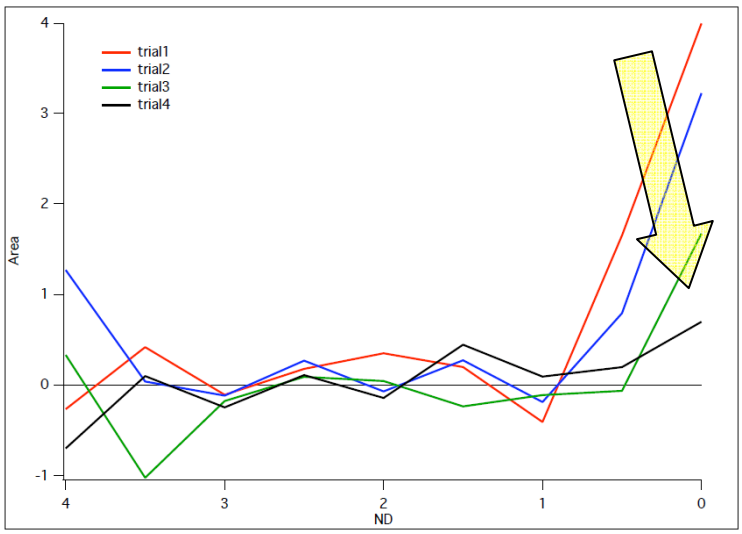

Graph 3: Representation of the Adaptation parameter

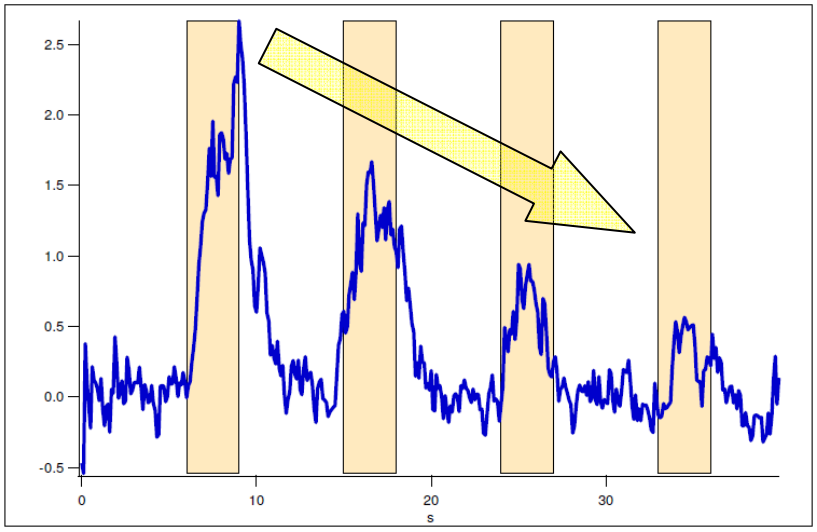

Figure 16: Visualization of the Adaptation parameter in the fluorescence signal

Adaptivity is a typical neuronal mechanism that induces neurons to reduce the neurotransmitter release in response to repeated stimuli. It is a vital strategy to avoid the neurons to run out of neurotransmitter, necessary for the signal transmission.

It is derived from the *area* parameter and it is calculated as the sum of the Manhattan distance between the *area* value at the first light step and the one at the second light step, between the second and the third and finally between the third and fourth light step. A positive value indicates adaptation.

The graph 3 represents the *area* parameter at each flash: it is clear how there is a decrease in this parameter moving from the first flash to the fourth one. The figure 16 shows the *adaptation* phenomenon during a terminal response to the stimulus.

The potentiation is the opposite phenomenon to adaptivity and it is computed in the same way: the sum over the Manhattan distance will have a negative value

In the graph 4 the *area* parameter at each flash is represented: it is clear how there is an increase in this parameter moving from the first flash to the fourth one. The figure 17 shows the *potentiation* phenomenon during a terminal response to the stimulus.

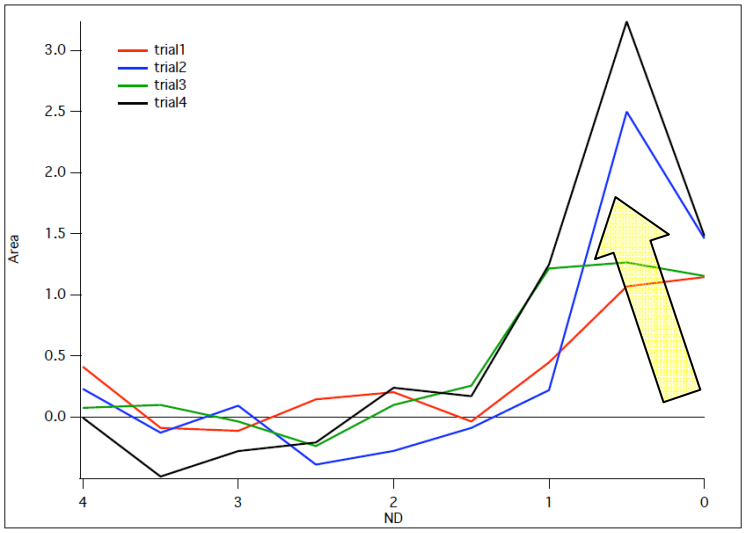

Graph 4: Representation of the Potentiation mechanism

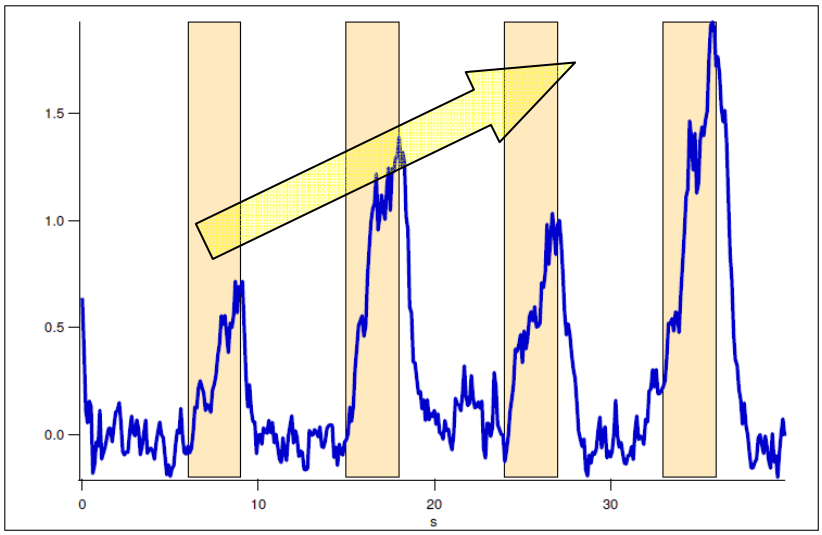

Figure 17: Visualization of the Adaptation parameter in the fluorescence signal

Peak Shift

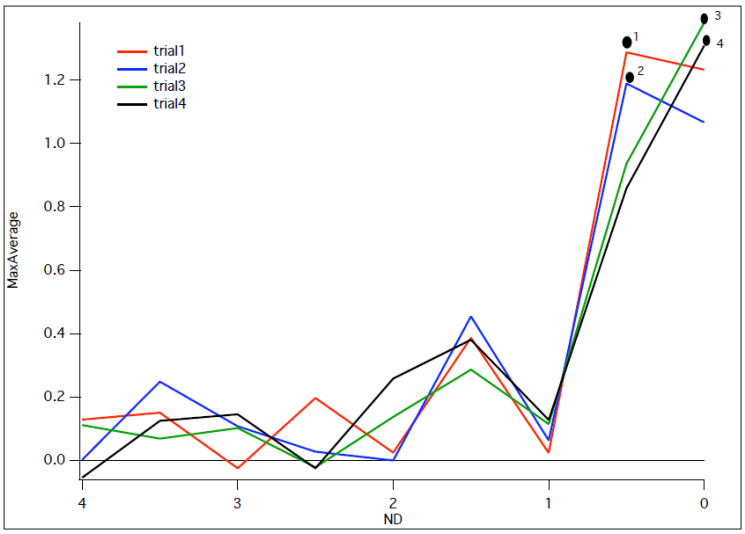

Graph 5: Representation of the Peak Shift parameter

The peak is the maximum in the terminal activity and occurs at the response to one of the four flashes; in graph 5 the peak is at the response to the third light step at the input intensity ND0, while at ND05 the peak is shifted toward the response to the first light step. The *peak shift* catches the activity peak moving among the responses to light steps and thus conveys an information of plasticity in the synaptic terminals.

Selectivity

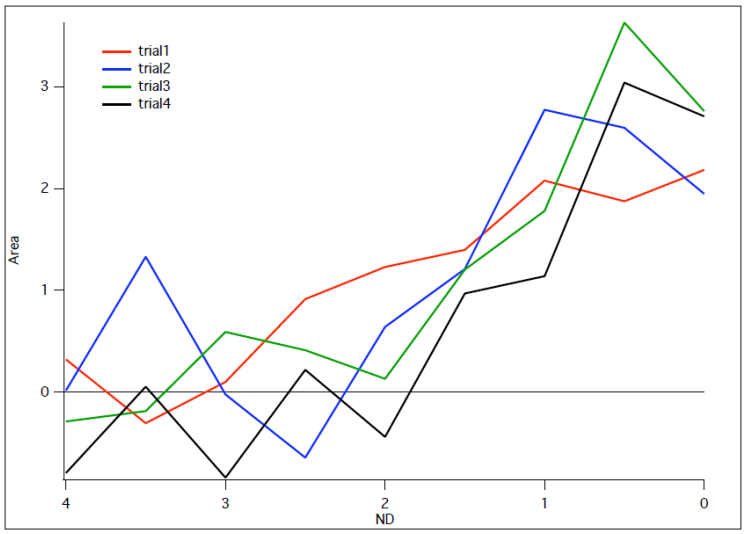

Graph 6: Representation of the Selectivity parameter

The *selectivity* feature belong to the second category too, because it evaluates the ability of the terminal to respond to some light intensity, while discarding others. Again the target is to study the terminal dynamic behavior and thus it is interesting not the absolute value, but how the *selectivity* is incresed or decreased in the responses to the four light steps following one another. The graph 6 depicts an example of *selectivity* increasing: from ND00 to ND15 the terminal has a good reponse at all the four light steps; at ND20 and ND25 just the activity at the first light step is high enough to be considered as a real response by the terminal: there is *selectivity* increase.

This parameter is assessed from *area*: for each response to light step, the difference between maximum *area* value and *area* value at the end of the responsive zone is calculated and it is divided by the *ND range* corressponding to those *area* values. By comptuing the difference between those values at the difference response to the four light steps, it is possible to assess if an increase or a decrease in the *selectivity* occurs.

The parameters belonging to the second category are:

Precision

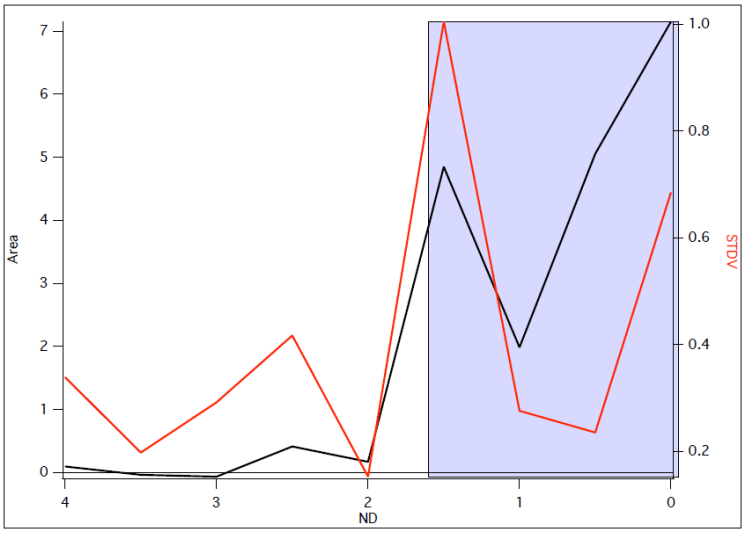

Graph 7: Representation of the Precision parameter

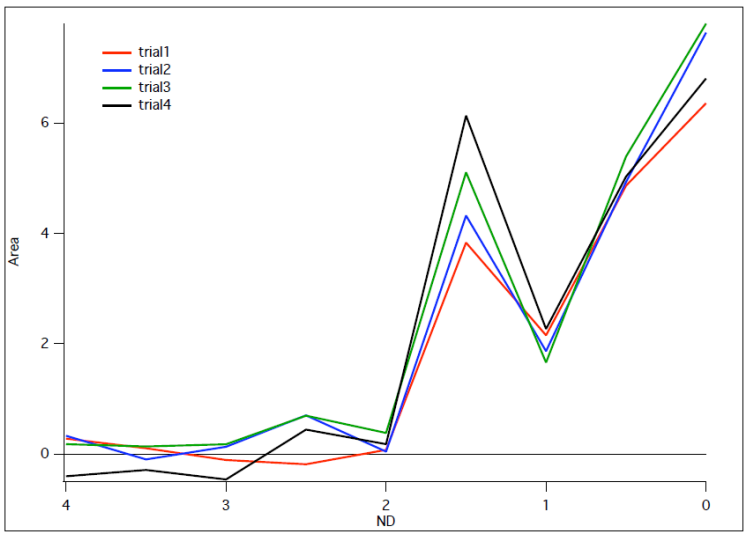

Graph 8: Representation of the Selectivity parameter

The *precision* assess how the good the BC terminal is to provide the same response to the same stimulus repeated over the time as the one used to stimulate the zebrafish retina.

I have evaluated it from the standard deviation of the *area* parameter: the smaller the standard deviation is and the more similar the terminal responses at the four light stimuli

are and thus the higher the *precision* is. In the graph 7 the standard deviation, depicted as the red line, in the responsive zone is small, so the four responses to the light steps are very similar as depicted in the graph 8, which illustrates the *area* parameter for the four flashes.

Slope Normalized

The *slope normalized* is a better indicator of the terminal dynamic than the *slope*, because it is normalized by the *max average* value, because it allows to compare terminals with different absolute value in the $\frac{\Delta F}{F_0}$. It indicates how fast the terminal responds to the light step. Therefore it is a description of the dynamics in the calcium inflow through the voltage gated calcium channels into the terminal membrane.

Reliability Aligned

More interesting than the general trend of the *reliability* is the *reliability aligned*. It describes how fast over the light intensities (ND) the reliability decreases to zero; as a matter of fact, a quick decrease to zero in *reliability* means the terminal responds just to the *ND range* is tuned to. We have made an assumption about the optimal range of response, assessed as the ND range to which the terminal respond with the maximum of *reliability*: the optimal range of response thus corresponds to the ND values to which the terminal is naturally tuned to. Therefore we have assumed that a decrease in reliability outside the optimal range is due to noise. Actually other factors, such as a signals from photoreceptors, HCs or ACs, may have the same effect in decreasing the reliability.

We have been individuated the last ND value in the optimal range of response for studying after how many other ND the *reliability* decreases definitely to zero; it was possible a direct compare between terminals, as the graph 9 shows: the terminal 5 is much more reliable than the terminal 59, because after the last maximum it decreases quite immediately to zero, while the terminal 59 has a rally-like trend before it stops to respond and the main cause it is more sensitive to the internal noise.

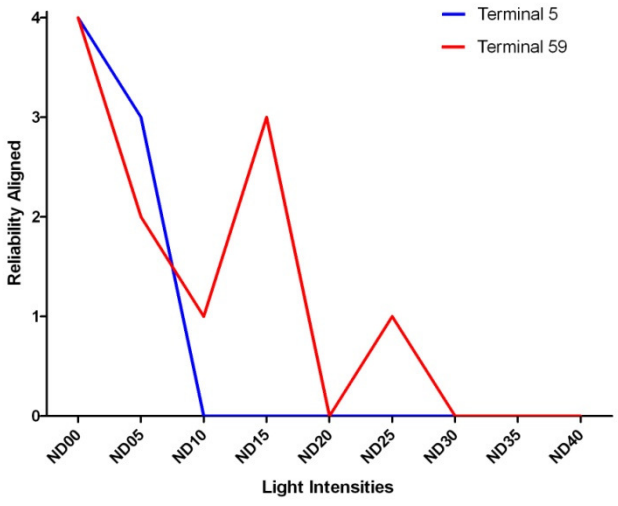

Graph 9: Representation of the Reliability Aligned parameter

ND Start, ND End, ND Range

These parameters represent respectevely the light intensity to which the terminal start to respond, finish to respond and the light instensity range over which the terminal is responsive. All together these parameters describe the luminance sensitivity of the terminal, i.e. its ability to respond to dimmer light intensities. The graph 10 depicts two terminals, one (terminal 9) high sensitivity as it responses also to very low intensity stimulus (ND3.5 = 5.38 pW/mm^2), while the other one (terminal 25) responses just to high level of light intensities.

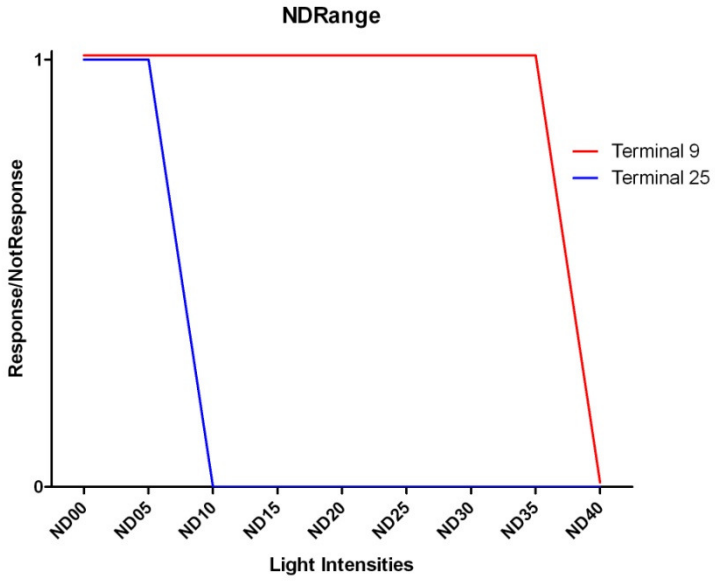

Graph 10: Representation of the ND Range parameter

At end two other parameters were studied, which conveys a more physical information such as the terminal dimension and the terminal localization in the IPL. As the single pixel dimension is known, it is easy to calculate the terminal size by considering the total number of pixel composing the terminal. The terminal position is assessed as explained in the **Preprocessing** chapter.

7. *Clustering*

The clustering belongs to the family of the machine learning algorithms, specifically, to the non supervised learning methods. The aim is to find similarity in some features of the dataset in order to identify homogeneous groups of data called clusters; in this way the data belonging to the same cluster share common and similar characteristics, and vice versa they are significantly different from data set in other clusters. Depending on the definition of metrics and the relative notions of distance and similarity between couple of data, many different clustering algorithms are available.

The one chosen for the present work has been the K-means one, because it provides the best experimental results. The K-means method requires as input the dataset, the number of clusters desired and a distance function; the function used in the present work has been the Euclidean distance. The algorithm workflow is simple: a number of centroids equal to the number of desired clusters is chosen randomly; the centroid of a cluster is defined as the average of the data belonging to that cluster. At each iteration, each data is assigned to the cluster whose centroid is closer and thus the distance between the centroid and the data is minimized; if no data is reallocated in a different cluster, the procedure stops and the clusters produced in the previous iteration are the final output of the algorithm (Pan, Lin, & Le, 2002).

We have used the software Multi Experiment Viewer 2.0 (MeV 2.0), that is a tool for the genomic data analysis and is well fitted for the data exploring and mining and especially for the different method of clustering analysis. The first step in the clustering procedure was the assessment of the ideal number of clusters to divide and then to merge the data; Figure Of Merit is a tool for estimating the predictive power of clustering algorithm: each sample is removed from the dataset and the clustering algorithm is performed on the remaining data; once the clusters are formed, it is assessed how well the removed data fit to the clusters scheme. Lower is the value of adjusted FOM better is the prediction power of the clustering algorithm, i.e. it fits to new data too. The procedure consisted in observing the FOM graph and in choosing, as initial guess about the number of clusters, the one at each there was a sharp variation on the first derivative. The graph 11 represents the figure

of merit, therefore the ideal number of cluster is two or seven and for obvious reason the first guess is the latter.

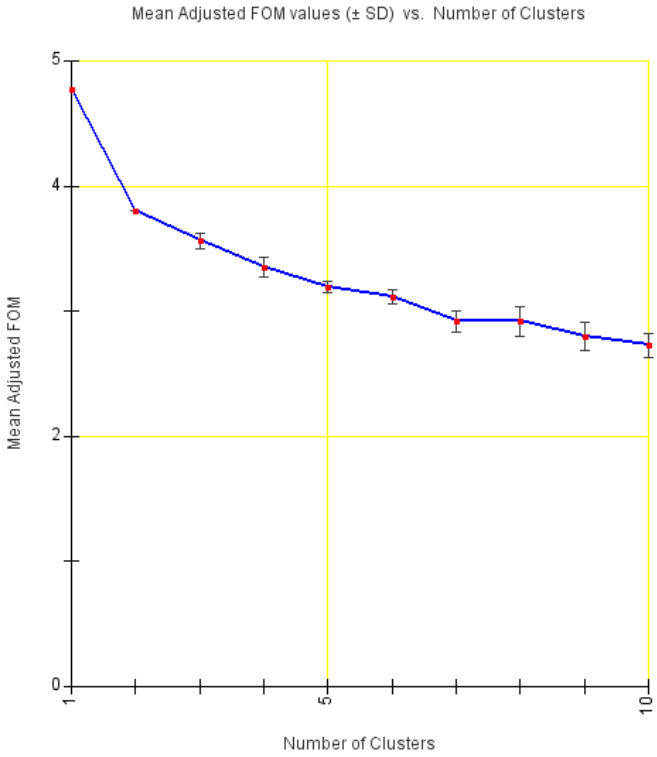

Graph 11: The trend of the Figure Of Merit

Since the final result was remarkably influenced by the initial random assignment of centroids, more the one clustering trial was provided also with some changes in the input parameter as the number of wanted clusters. The best cluster pattern was finally chosen.

The cluster schemes were then imported in Igor Pro to provide new data to be elaborated with the other parameters.

8. *Model identification*

The last part of the thesis deals with the model identification procedure to generate reliable models of the synaptic terminal in the IPL responses; it is just a draft and still needs more studies and works to obtain more significant results.

The approach to the model identification was the typical black box one, which describes the system behavior just from the stimulus and the response produced without a prior knowledge of the internal features of the system. All the neural mechanisms that produce the response in the IPL synapses are still not well known as, for example, the ACs feedbacks, and thus the black box models fits the thesis purpose.

We have chosen the Box-Jenkins (BJ) model structure, because it has more flexibility for modeling the noise; as a matter of fact it provides completely independent parameterization for the dynamics and the noise using rational polynomial functions (Ljung, 1999). We have assumed the only input received during the light exposure was a step light stimulus, without taking into consideration other factors contributing to the terminal response. For this reason we have assumed there was no noise in the input. The Box Jenkins model was useful to handle this kind of problem, because it allowed to independently set the parameters for the dynamics and those for the noise, as its mathematical structure shows:

$$y(t) = \sum_{i}^{nu} \frac{B_i(z)}{F_i(z)} u_i(t - nk_i) + \frac{C(z)}{D(z)} e(t)$$

The polynomials *B, F, C, D* contain the time shift operator z; ui is the i-th input, nu is the total number of input and nk is the i-th delay input that characterizes the delay response time and e is the white noise. For the assumption made the parameters related to the noise are set to zero.

The dataset available to feed the modeling algorithm were two

- The light step stimulus expressly implemented in MatLab, in graph 12

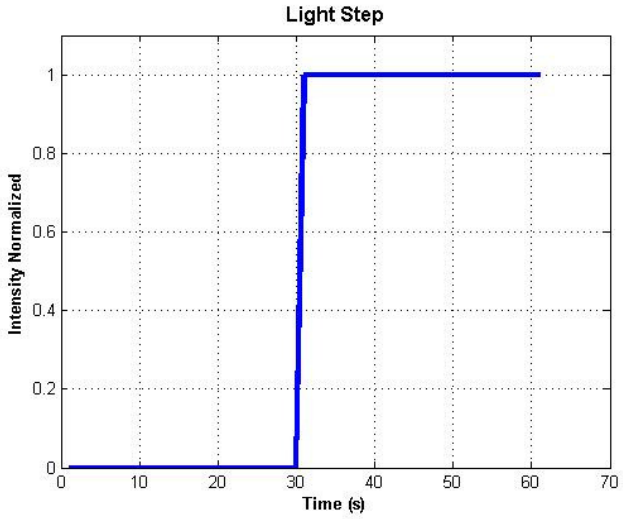

Graph 12: Stimulus provided as input to the model identification algorithm

- The single response to the light step by the terminal, taken from the waves saved in Igor Pro software, showed in the graph 13.

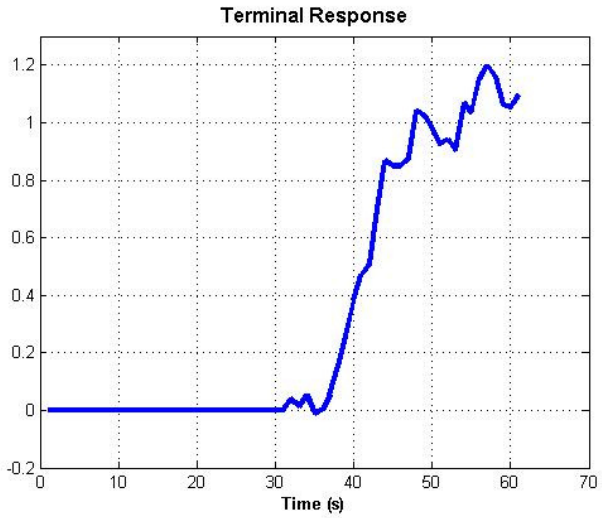

Graph 13: Terminal response used as input to the model identification algorithm

The BJ algorithm requires the information about the model order; it was given by a set of integer numbers of coefficents for each polynom used and so for *B, F, C, D* and also the number of samples which corresponded to the dead time, i.e. the delay natural systems faces to respond to the stimulus. In the case discussed in the thesis the coefficients for the noise parameterization were equal to zero and thus the noise effect were neglected.

An important step in the modeling process was the choosing of the optimal order. The number of coefficient of the polynomial at the numerator corresponds to the number of the zero of the systems while the ones at the denominator to the number of poles: added together they are the model order. It is an important feature of the model, as it represents the degrees of freedom of the model, i.e. the model capacity to simulate properly the real system. We have done many trials as well as we have considered the Akaike final prediction error (FPE) in order to choose the model order for the optimal parameterization. The Akaike FPE is criterion to measure how well a model fits the real phenomenon. We have looked for a tradeoff between a low Akaike FPE and an upper limit in the model order for avoiding a model too much precise in representing the terminal response. A model with higher order is better in simulating every features in the response of the specific terminal used in the training set for feeding the algorithm; nevertheless it loses the generalization capacity and it is not useful for further parameterization of new terminals response. Therefore we have chosen fix the upper limit at four or five.

III. RESULTS

The present chapter exposes the results obtained from the previous analysis. I have divided the results between the two BCs types, ON and OFF, in order to be able to compare their dynamical behavior and features.

The number of experiments analyzed is 11 for a total of 136 ON terminals and 102 OFF terminals and other 29 terminals with ambiguous behavior.

1. *Primary Parameters*

At first the chapter shows the data values of the primary parameters for all the terminals at the different values of the light intensity. In order to report the results we have chosen three value of light intensity, ND00, ND20, ND40 which represent respectively the high intensity, medium one and low one; it is a concise visualization of results which allows an easy compare of the parameters between the different light intensities.

In analyzing the distribution of the parameters among the different light intensities, we have performed a normality test in order to answer the question whether these data were sampled from a Gaussian distribution or not. This information was useful to choose the indicators for describing the values distribution; if the distribution is not a Gaussian one the mean and the standard deviation are not significant, while it is better to use the median, the max and the min, the 25% and 75% percentile as descriptors. The normality test has always a P-value that represents the probability that a sample, obtained by a random sampling of a Gaussian distribution, deviates as much as the current datum does. So a small P-value indicate the data derive from a non-Gaussian distribution.

The specific normality test is the D'Agostino-Pearson one, which uses the skewness and the kurtosis values to assess how far the distribution is from the Gaussian one in term of shape and asymmetry. These two information are then combined to produce an omnibus test, the so called K^2 statistic, which has value around 2 if the data are normally distributed (D'Agostino & Belanger, 1990).

Max Average

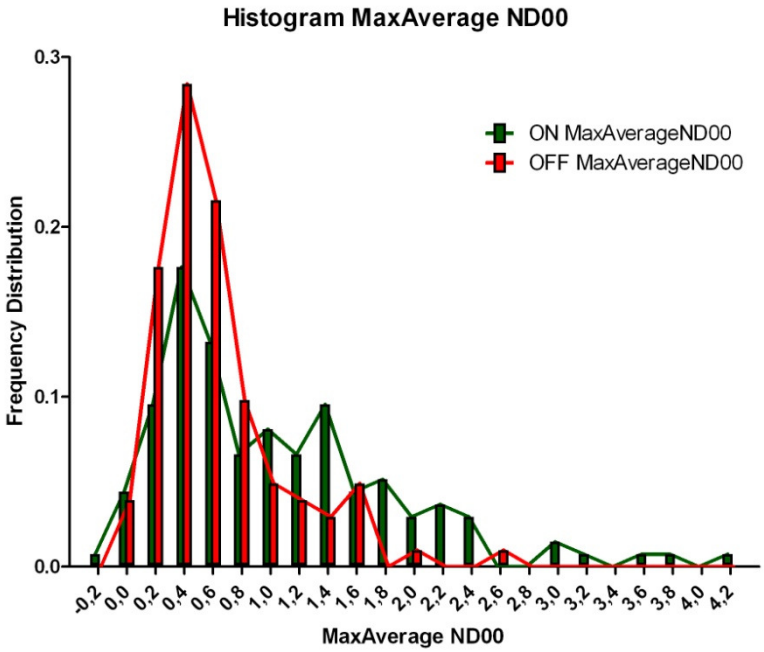

Graph 14: Histogram Max Average at ND00 for ON and OFF BCs terminals

Statistic	Value		Normality Test		
	ON	OFF		ON	OFF
Minimum	-0,113	0,005561	K2	34,90	41,27
25% Percentile	0,4358	0,3305	P value	< 0,0001	< 0,0001
Median	0,7663	0,5000	Passed normality test (alpha=0.05)?	No	No
75% Percentile	1,494	0,7419	P value summary	****	****
Maximum	4,192	2,572			

Table 2: Distribution statistics and normality test of Max Average for ON and OFF BCs terminals at ND00

At brighter light conditions, the distribution is very far from being a Gaussian one; furthermore there is a remarkable difference in the *Max Average* between the ON and OFF

population, information derived from applying a non parametric t-test which gives a p-value < 0.0001, as the graph 15 shows through a box-whiskers representation.

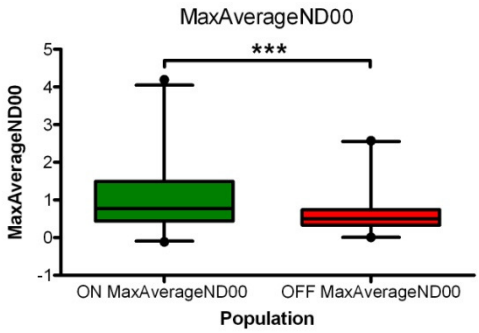

Graph 15: Box and Whiskers diagram of Max Average at ND00 for ON and OFF BCs terminals

The table 2 explicates that the ON BCs terminals have a larger $\frac{\Delta F}{F_0}$ signal, meaning there is more calcium activity and thus a larger release of neurotransmitter.

The histogram in the graph 16 shows the level of calcium inflow at dimmer light conditions.

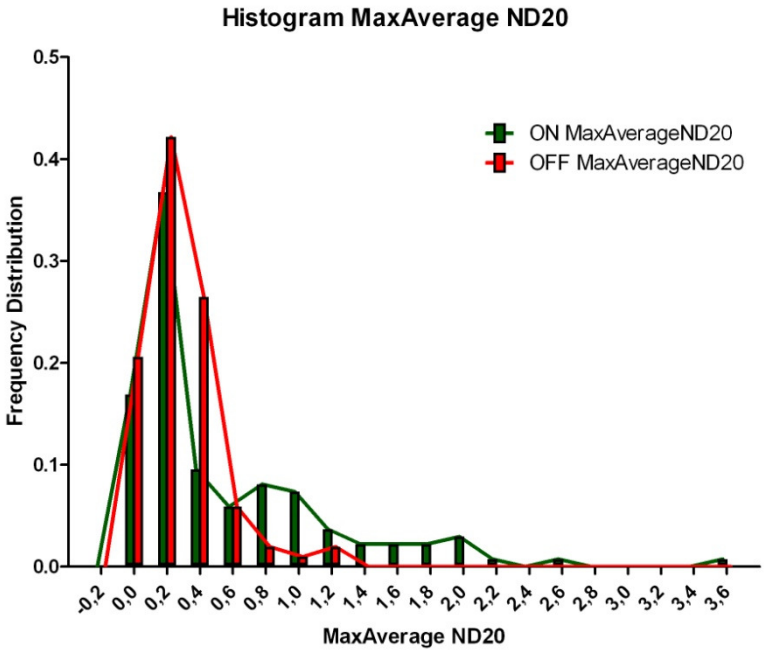

Graph 16: Histogram Max Average at ND20 for ON and OFF BCs terminals

Statistic	Value		Normality Test		
	ON	OFF		ON	OFF
Minimum	-0,035	-0,08604	K2	61,54	48,57
25% Percentile	0,1340	0,1313	P value	< 0,0001	< 0,0001
Median	0,2453	0,2218	Passed normality test (alpha=0.05)?	No	No
75% Percentile	0,8232	0,3810	P value summary	****	****
Maximum	3,528	1,223			

Table 3: Distribution statistics and normality test of Max Average for ON and OFF BCs terminals at ND20

The values between ON and OFF are still significantly different, but much less as the Box and Whisker in graph 17 depicts.

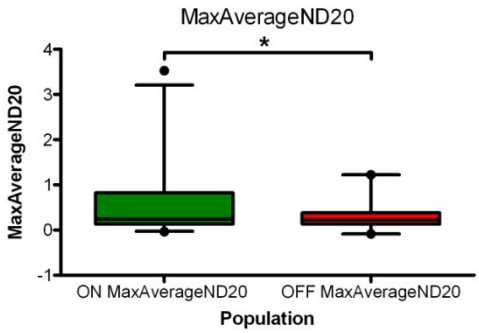

Graph 17: Box and Whiskers diagram of Max Average at ND20 for ON and OFF BCs terminals

Again the ON BCs have higher activity than the OFF BCs also for less intense light stimuli; anyway it is clear that by diminishing the stimulus intensity, the activities of ON BCs and OFF BCs get more similar.

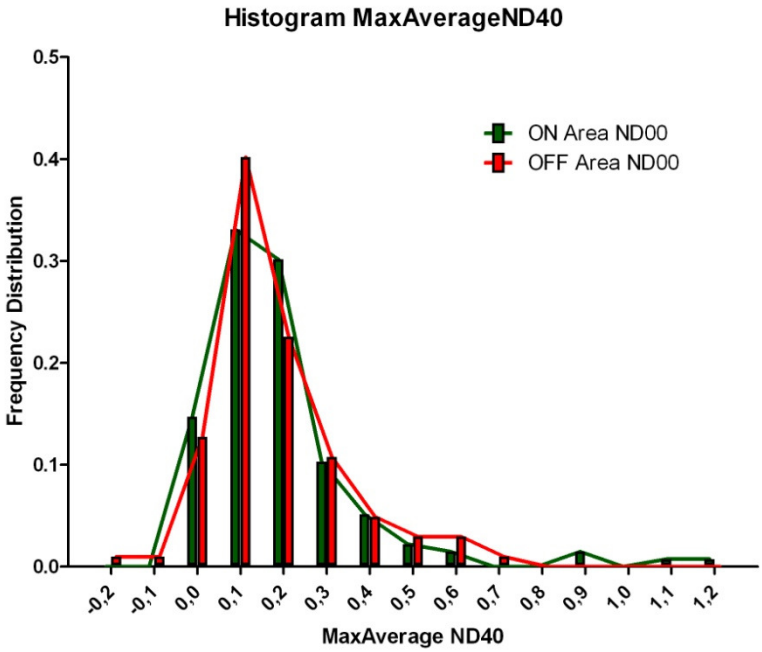

Graph 18: Histogram Max Average at ND40 for ON and OFF BCs terminals

As a matter of fact, there are not anymore significant differences in the fluorescence signal between the ON and OFF BCs terminals. At dimmer light condition the ON and OFF

terminals have the same behavior, as it is clear from the 75% percentile value, in the graph 18, that is almost the same for the two populations.

Statistic	Value		Normality Test		
	ON	OFF		ON	OFF
Minimum	0,0100	-0,1703	K2	102,3	21,88
25% Percentile	0,0851	0,08663	P value	< 0,0001	< 0,0001
Median	0.1523	0,1404	Passed normality test (alpha=0.05)?	No	No
75% Percentile	0,230	0,2368	P value summary	****	****
Maximum	1,172	0,6897			

Table 4: Distribution statistics and normality test of Max Average for ON and OFF BCs terminals at ND40

Slope Normalized

As explained in the chapter **Materials and Methods**, the *slope normalized* expresses how fast the calcium inflow mechanism is in response to a light flash and thus it is a good indicator of the overall dynamics of calcium. It is normalized for comparing terminals with different absolute intensities in their fluorescence.

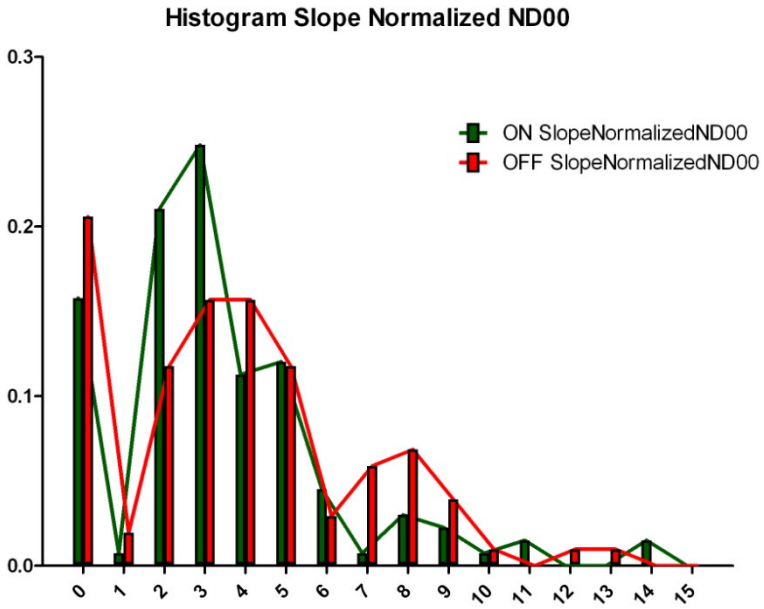

Graph 19: Histogram Slope Normalized at ND00 for ON and OFF BCs terminals

Statistic	Value		Normality Test		
	ON	OFF		ON	OFF
Minimum	0,0	0,0	K2	42,00	6,958
25% Percentile	1,917	1,911	P value	< 0,0001	0,0308
Median	2,969	3,506	Passed normality test (alpha=0.05)?	No	No
75% Percentile	4,731	5,303	P value summary	****	*
Maximum	14,32	13,01			

Table 5: Distribution statistics and normality test of Slope Normalized for ON and OFF BCs terminals at ND00

As expected the *slope normalized* values of both ON and OFF BCs terminals are not distributed Gaussian like, and they have similar values: the 25%, 50%, 75% percentiles have almost the same values, as the graph 19 and table 5 show.

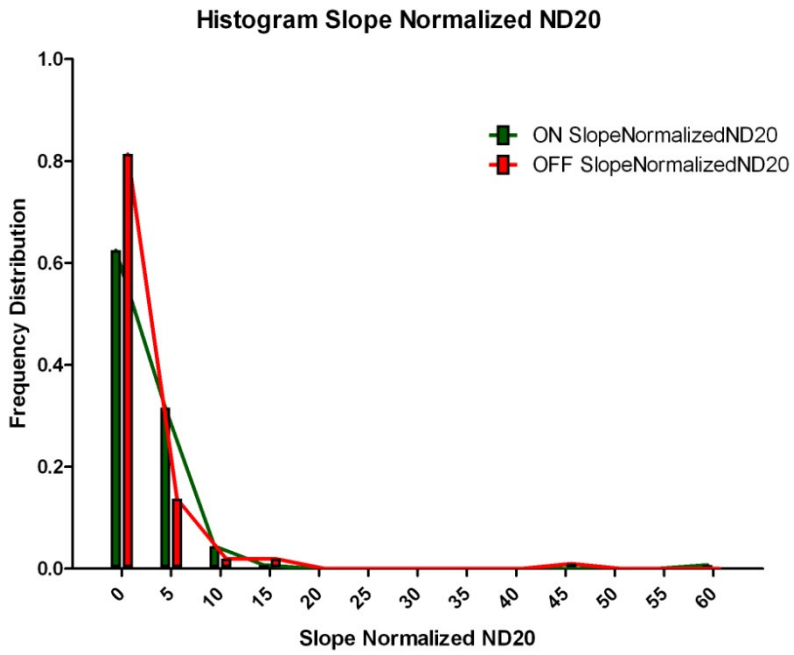

Graph 20: Histogram Slope Normalized at ND20 for ON and OFF BCs terminals

In the calculation of *slope normalized* parameter, I have set to zero the values at light intensities outside the responsive zone (*area* parameter below the threshold 0.5). Because at dimmer light intensities like the ND20 there are few terminals that have a significant response, there a lot of *slope normalized* values equal to zero.

Statistic	Value		Normality Test		
	ON	OFF		ON	OFF
Minimum	0,0	0,0	K2	233,3	161,8
25% Percentile	0,0	0,0	P value	< 0,0001	< 0,0001
Median	0,0	0,0	Passed normality test (alpha=0.05)?	No	No
75% Percentile	3,909	0,0	P value summary	****	****
Maximum	57,56	43,44			

Table 6: Distribution statistics and normality test of Slope Normalized for ON and OFF BCs terminals at ND20

Area

The *area* parameter expresses the magnitude of $\frac{\Delta F}{F_0}$ signal during the terminal response to a light flash. It is expected to have a distribution similar to the *max average* one, as confirmed by the graph 21.

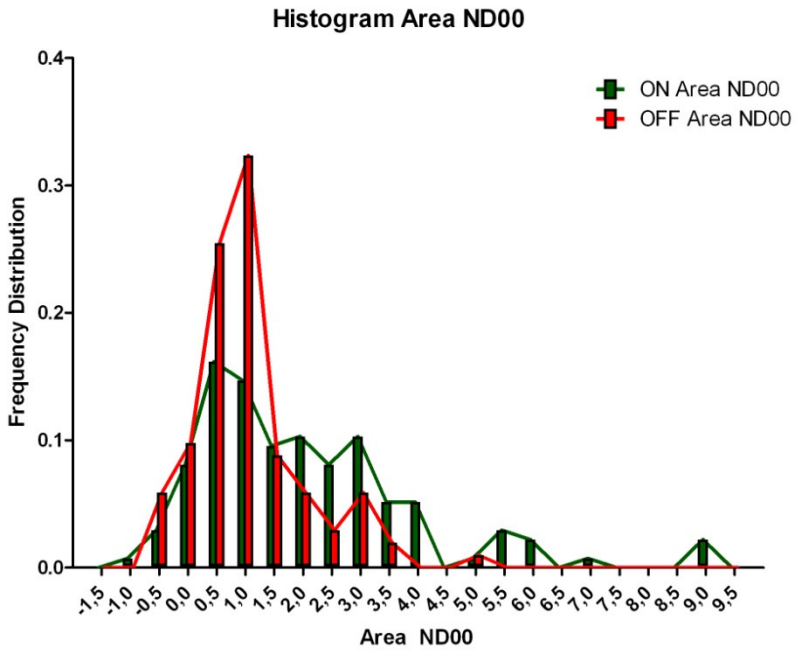

Graph 21: Histogram Area at ND00 for ON and OFF BCs terminals

Statistic	Value		Normality Test		
	ON	OFF		ON	OFF
Minimum	-1,138	-0,3960	K2	44,06	31,96
25% Percentile	0,7224	0,5012	P value	< 0,0001	< 0,0001
Median	1,588	0,9527	Passed normality test (alpha=0.05)?	No	No
75% Percentile	3,011	1,384	P value summary	****	****
Maximum	9,147	5,199			

Table 7: Distribution statistics and normality test of Area for ON and OFF BCs terminals at ND00

Again there is a statistically significant difference between the ON and OFF terminals in term of activity during a stimulation conducted at ND00 light intensity. The ON shows

larger magnitude in $\frac{\Delta F}{F_0}$ signal respect to the OFF terminals. The significance is assessed with a non parametric t-test that gives a p-value < 0.0001, as the graph 22 shows.

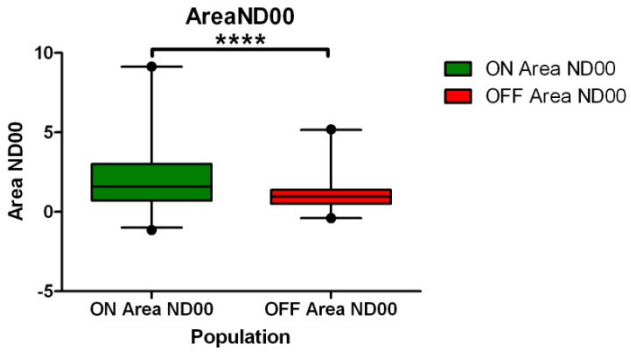

Graph 22: Box and Whiskers diagram of Area at ND00 for ON and OFF BCs terminals

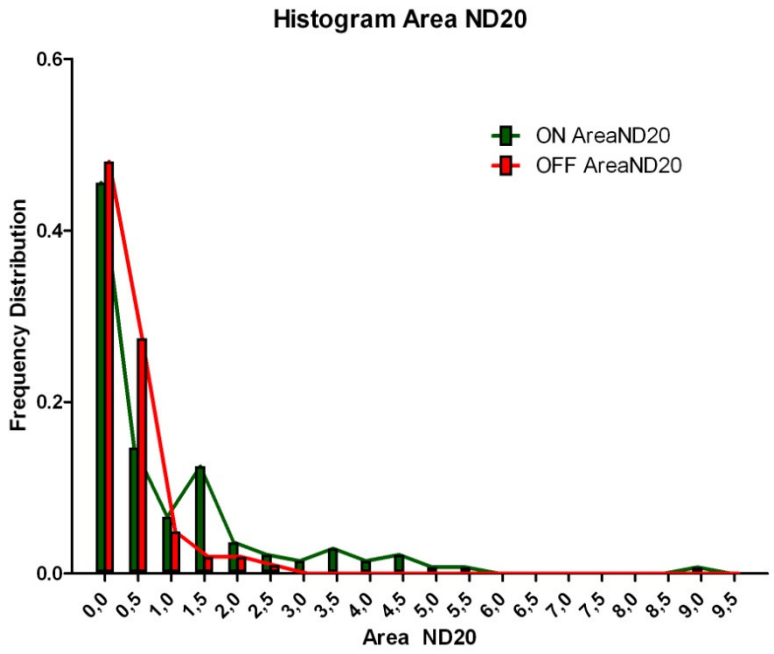

Graph 23: Histogram Area at ND20 for ON and OFF BCs terminals

Statistic	Value		Normality Test		
	ON	OFF		ON	OFF
Minimum	-0,6208	-0,8572	K2	88,46	41,92
25% Percentile	0,04479	-0,05135	P value	< 0,0001	< 0,0001
Median	0,2446	0,1323	Passed normality test (alpha=0.05)?	No	No
75% Percentile	1,419	0,3846	P value summary	****	****
Maximum	9,053	2,373			

Table 8: Distribution statistics and normality test of Area for ON and OFF BCs terminals at ND20

Statistically significant differences (p-value<0.0005) between the area of response in ON and OFF terminals are still present at dimmer light condition, as the graph 24 shows. Anyway the difference starts to be smaller, indicating how the behavior of ON and OFF gets similar by decreasing the intensity of stimulus.

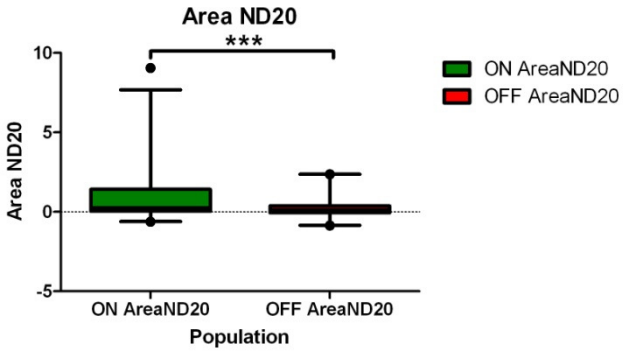

Graph 24: Box and Whiskers diagram of Area at ND00 for ON and OFF BCs terminals

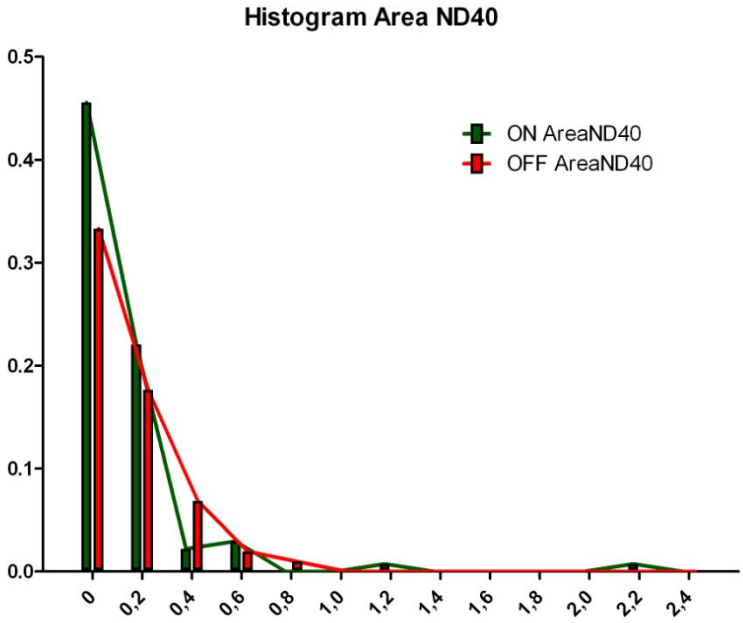

Graph 25: Histogram Area at ND40 for ON and OFF BCs terminals

Statistic	Value		Normality Test		
	ON	OFF		ON	OFF
Minimum	-0,5395	-1,255	K2	150,1	17,42
25% Percentile	-0,1046	-0,2051	P value	< 0,0001	0,0002
Median	-0,00267	-0,01157	Passed normality test (alpha=0.05)?	No	No
75% Percentile	0,1279	0,1071	P value summary	****	***
Maximum	2,247	0,7021			

Table 9: Distribution statistics and normality test of Area for ON and OFF BCs terminals at ND40

At the dimmest light conditions there are no more relevant difference in the behavior of ON and OFF BCs terminals, and they tend to express the same values of *area* parameter, as the graph 25 and the table 9 show.

Reliability

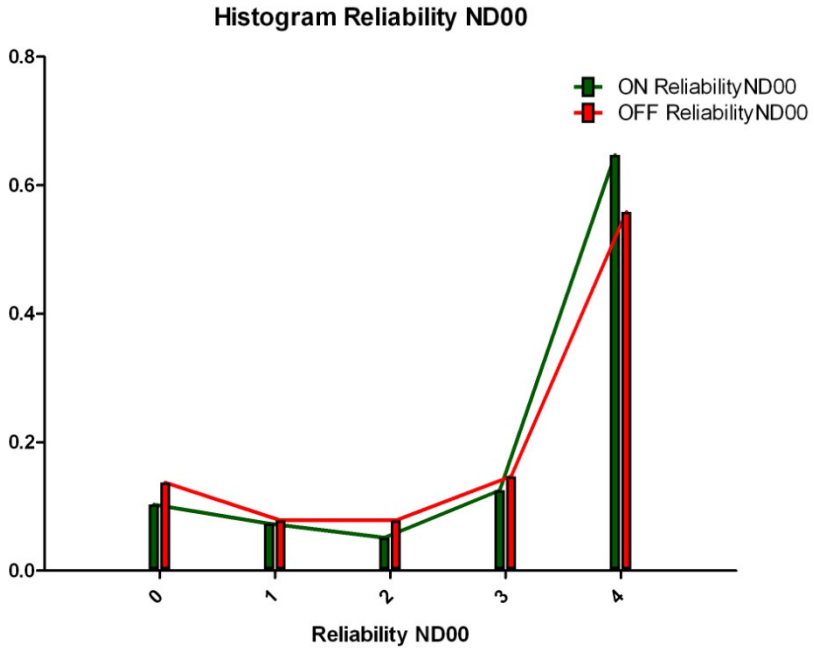

Graph 26: Histogram Reliability at ND00 for ON and OFF BCs terminals

Statistic	Value		Normality Test		
	ON	OFF		ON	OFF
Minimum	0,0	0,0	K2	29,92	16,15
25% Percentile	3,000	2,000	P value	< 0,0001	0,0003
Median	4,000	4,000	Passed normality test (alpha=0.05)?	No	No
75% Percentile	4,000	4,000	P value summary	****	***
Maximum	4,000	4,000			

Table 10: Distribution statistics and normality test of Reliability for ON and OFF BCs terminals at ND00

This parameter is very high both for ON and OFF BCs terminals: the value of the 75% percentile is equal at 4,00 which means a very large number of terminals respond to each of the four light flashes during the stimulation, as the table 100 illustrates. So at bright condition both the population are very reliable and thus transmit to the GCs.

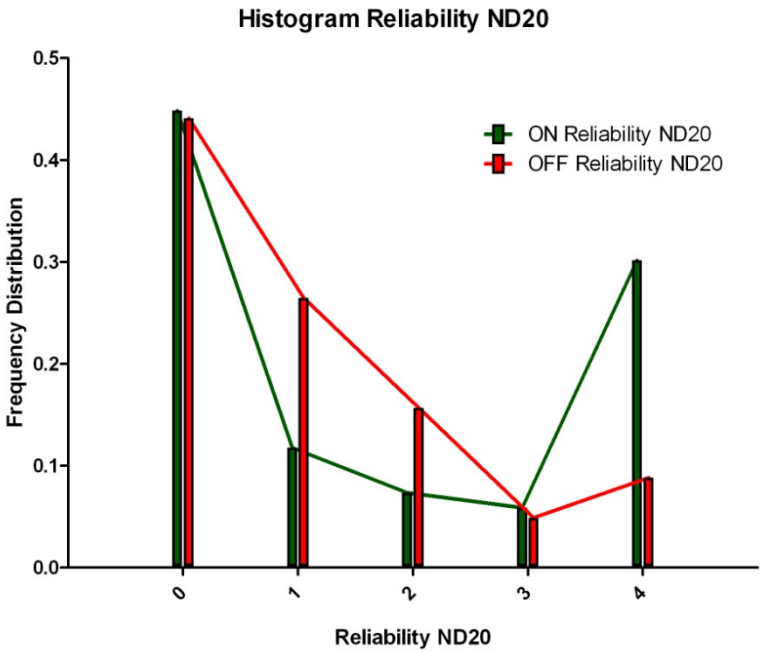

Graph 27: Histogram Reliability at ND20 for ON and OFF BCs terminals

Statistic	Value		Normality Test		
	ON	OFF		ON	OFF
Minimum	0,0	0,0	K2		16,08
25% Percentile	0,0	0,0	P value	< 0,0001	0,0003
Median	1,000	1,000	Passed normality test (alpha=0.05)?	No	No
75% Percentile	4,000	2,000	P value summary	****	***
Maximum	4,000	4,000			

Table 11: Distribution statistics and normality test of Reliability for ON and OFF BCs terminals at ND20

As the light intensity starts to become dimmer, the OFF BCs terminals tend to not respond well to each flashes of the stimulation, as showed by the high frequency of the 0 value in the graph 27. The ON terminals follow the same trend, but they seem to be more reliable than the OFF ones.

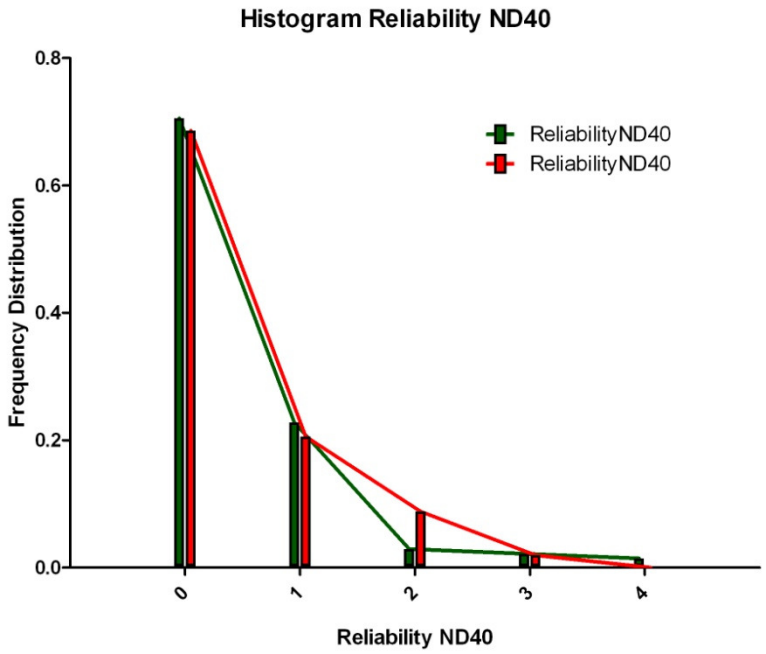

Graph 28: Histogram Reliability at ND40 for ON and OFF BCs terminals

Statistic	Value		Normality Test		
	ON	OFF		ON	OFF
Minimum	0,0	0,0	K2	88,35	35,61
25% Percentile	0,0	0,0	P value	< 0,0001	< 0,0001
Median	0,0	0,0	Passed normality test (alpha=0.05)?	No	No
75% Percentile	1,000	1,000	P value summary	****	****
Maximum	4,000	3,000			

Table 12: Distribution statistics and normality test of Reliability for ON and OFF BCs terminals at ND40

As it can be expected at four orders of magnitude lower than the original light intensity, the terminals are not any more reliable, as the graph 28 and the table 12 represent; some flashes are lost and the information they convey is not transmitted to the next stages of processing in the CNS.

It is interesting to have a look at the *reliability aligned* parameter. It is a measure of how quickly the terminal does not respond anymore after the optimal responsive zone and thus if it is robust against random events. A possible assessment is the assignment of score. A

score equal 1 is assigned to terminals ceasing their signaling after the last light intensity to which is tuned, a score equal to 0 at the others.

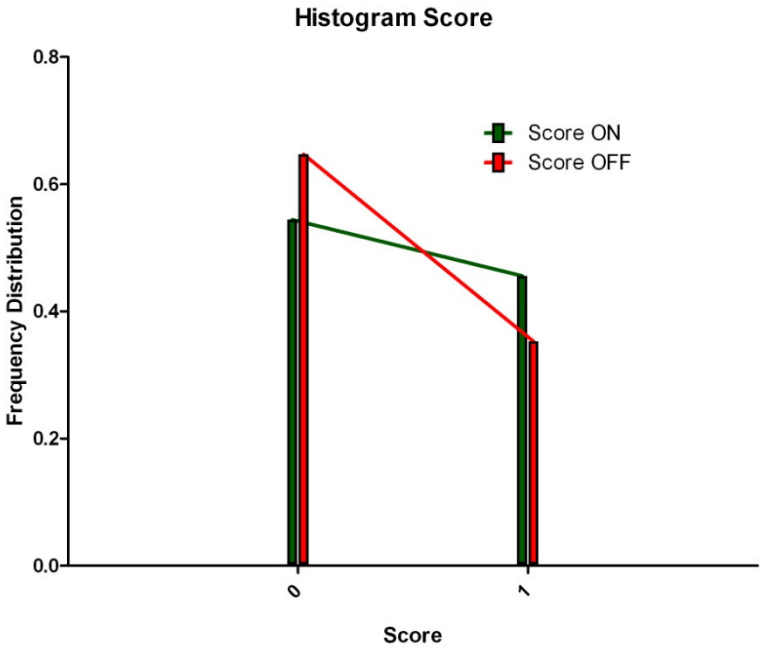

Graph 29: Histogram of the Score for the Reliability Aligned

The graph 29 shows that there are not significant differences between the score in the ON and OFF terminals; therefore both the populations have a balance between terminals strictly activated just in the responsive zone and terminals with a decreased reliability due to random events or feedback from the HCs and ACs.

2. *Derived Parameters*

It was interesting to directly compare the derived parameter between the ON and OFF population, in order to find out whether there were similarities or differences in the dynamic behavior of the two BCs populations.

I had employed various tools to carry on the differential analysis between the two groups of BCs: box and whiskers graphs, histograms and cumulative histograms, and test to compare two groups of data such as the *t*-test.

The box and whiskers graph is a representation of a dataset distribution through some statistical indexes such the median, the 25% and 75% percentile and the minimum and maximum values. It gives an immediate visualization of the difference between two dataset which are the two population ON and OFF of the BCs, in this specific context.

In order to assess whether the two BCs groups are significantly different in their dynamics or they come from the same population, the tests used are basically a Mann-Whitney test and *t*-test with Welch correction.

The Mann-Whitney test is a non parametric test that compares two unpaired groups. All the data from the two groups are mixed and ranked from the lowest to the highest value: so the former is ranked 1 while the latter is ranked as N, where N is the total number of data in two groups. Then for each groups the addition of the ranks is performed and the two total sums are compared; if they are different the P-value is small and so the null hypothesis, i.e. differences are due to a random sampling, can be rejected: the two population are significantly different (Mann & Whitney, 1947).

In some case the Mann-Whitney test gives a large P-value, because the two variances are remarkably different , a problem that is corrected by the application of the Welch correction to the *t*-test: the Welch correction is designed to provide a valid *t*-test in the presence of unequal population variances. For both the groups, the standard deviations are computed and then squared to get the variances; the larger one is then divided for the smaller one and F ratio is obtained which is very far from 1 if the two variances are remarkably different. A small P-value means that the probability that the two variances are

identical and that the difference is due to a random sampling is very little. From such a result it is possible to conclude that the two dataset are actually different.

Precision

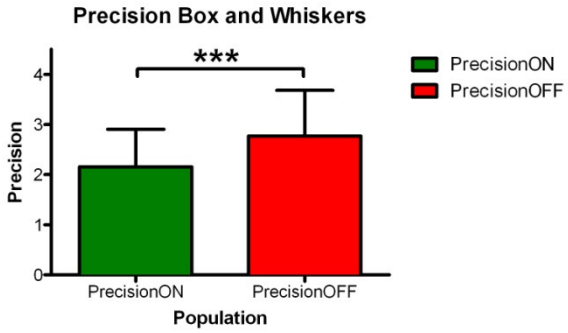

Graph 30: Box-Whiskers plot of the Precision parameter

ON and OFF populations show a significant different behavior in the *precision* feature with a P-value equal to 0.0001 for the Mann-Whitney test, as the graph 30 illustrates

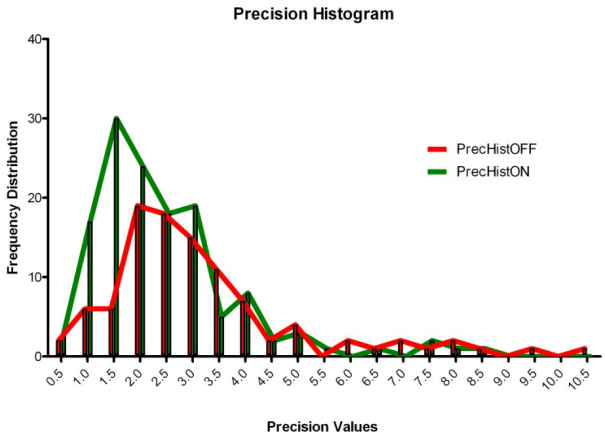

Graph 31: Histogram of the Precision parameter for ON and OFF population

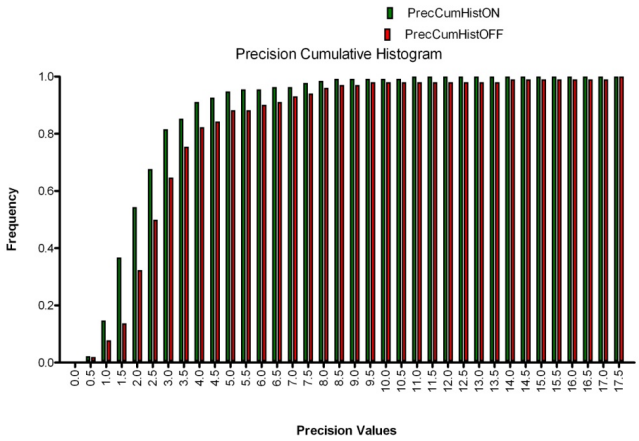

Graph 32: Cumulative histogram of the Precision parameter for the ON and OFF population

The cumulative histogram in the graph 32 allows to better appreciate the difference in *precision* between the ON and OFF BCs terminals; it is clear that the frequency distribution of the *precision* values in the ON terminals reaches its maximum before the OFF ones, and thus they have a maximum value of *precision* inferior to the one of the OFF terminals

Potentiation/Adaptation

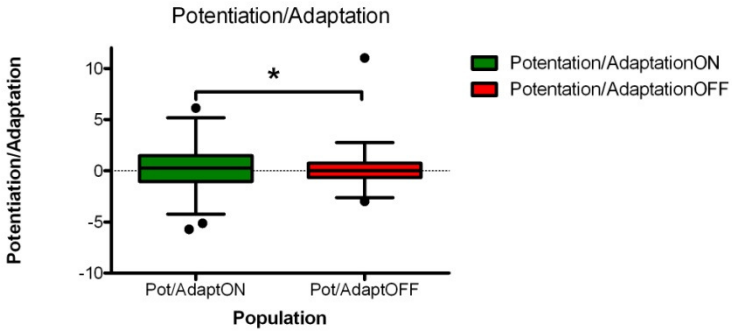

Graph 33: Box-Whiskers plot of the Potentiation/Adaptation parameter

The ON and OFF BCs have a significant difference in their variances for the *Potentiation/Adaptation* characteristic, with an F ration equal to 1.496 and a P-value equal to 0.0337 (Welch correction). It can be concluded that the two population have an actual different behavior in adapting or potentiating their vesicle release responding to a repeated stimulus, as the graph 33 shows.

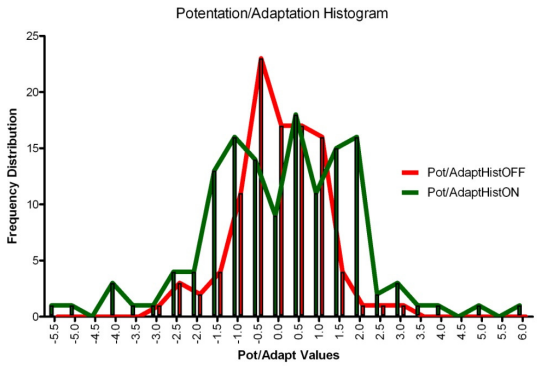

Graph 34: Histogram of the Potentiation/Adaptation parameter for ON and OFF population

The three-lobes shape of the histogram drawn in the graph 34 clarifies how both the ON and OFF BCs have a large percentage of terminals responding whit plasticity to the four light flashes following one another.

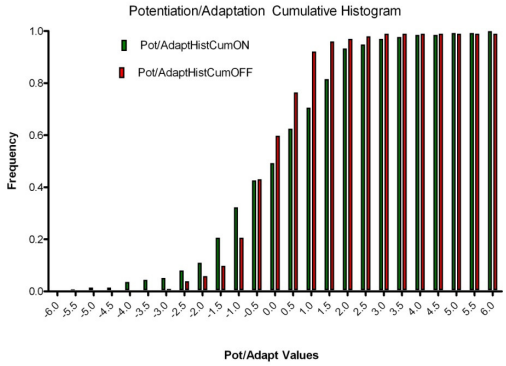

Graph 35: Cumulative histogram of the Potentiation/Adaptation parameter for the ON and OFF population

The cumulative histogram represented in the graph 35 underlines how the OFF terminals, although they have a plastic behavior, have a narrower range of plasticity than the ON terminals.

Peak Shift

The change in *Peak Shift* between the ON and OFF BCs are not significantly different.

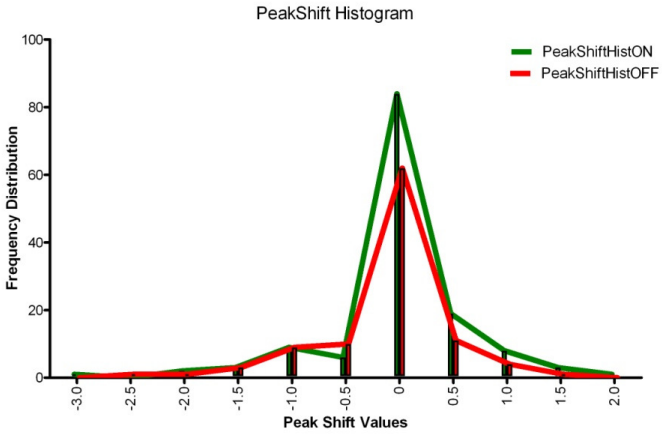

Graph 36: Histogram of the Peak Shift parameter for ON and OFF population

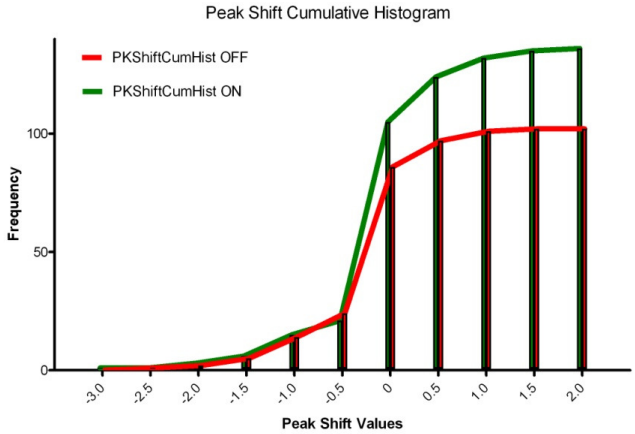

Graph 37: Cumulative histogram of the Peak Shift parameter for the ON and OFF population

The graphs 36 and 37 show how the ON and OFF terminals have the same values and distribution of values of the *peak shift* parameters.

Selectivity

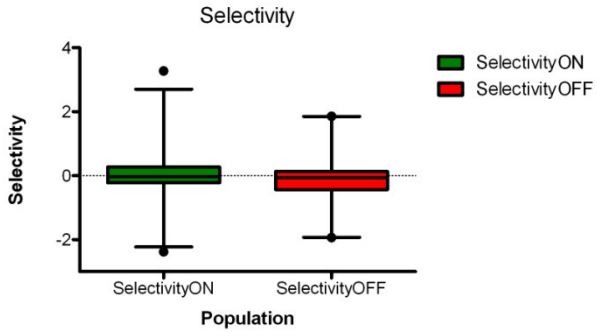

Graph 38: Box-Whiskers plot of the Selectivity parameter

There are not striking differences in the *selectivity* feature between the ON and the OFF cells and so the slight variations observed are classified as non significant, as the graph 38 illustrates.

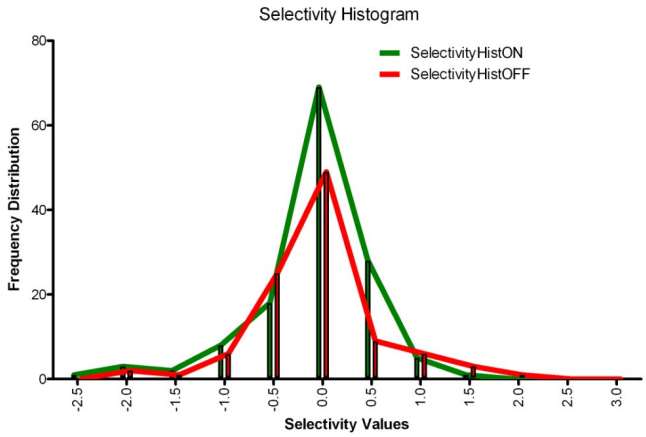

Graph 39: Histogram of the Selectivity parameter for ON and OFF population

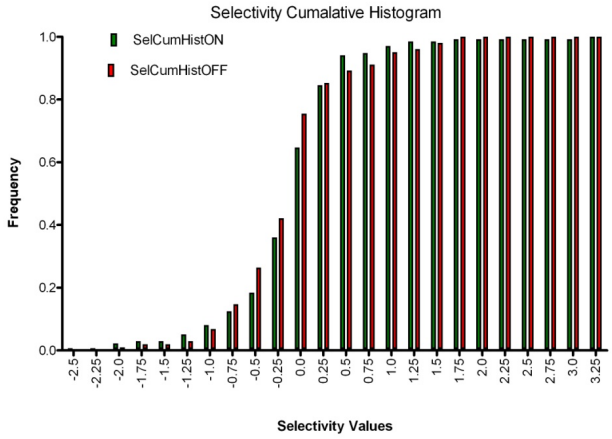

Graph 40: Cumulative histogram of the Selectivity parameter for the ON and OFF population

The ON terminals tend both to increase and decrease the range of light intensities to which they are tuned; the OFF terminals, instead, are more keen to decrease their *selectivity* and transmit a broader range of light intensities, as the graphs 39 and 40 show. However these differences are not proven to be statistically significant.

ND Start

By performing the Mann-Whitney test, the P-value is 0.0240 and thus the differences between the ON and OFF population can be considered significant from a statistical point of view.

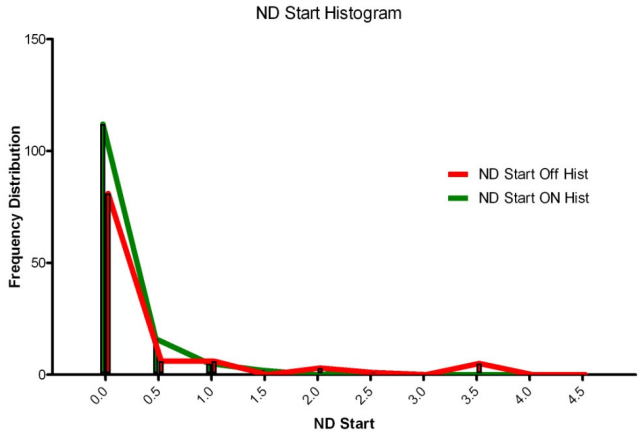

Graph 41 Histogram of the ND Start parameter for ON and OFF population

ND End

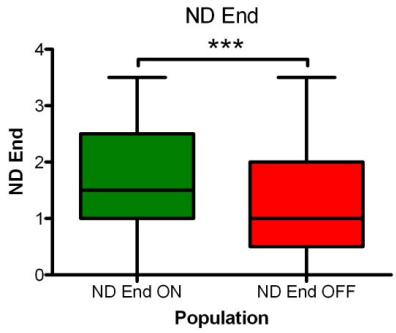

Graph 42: Box-Whiskers plot of the ND End parameter

Again the Mann-Whitney test gives a P-value equal to 0.0009 and thus allow to conclude that the ON BCs are able to respond to stimuli at intensities lower than the ones for the OFF BCs and that such difference is statistically significant, as the graph 43 depicts.

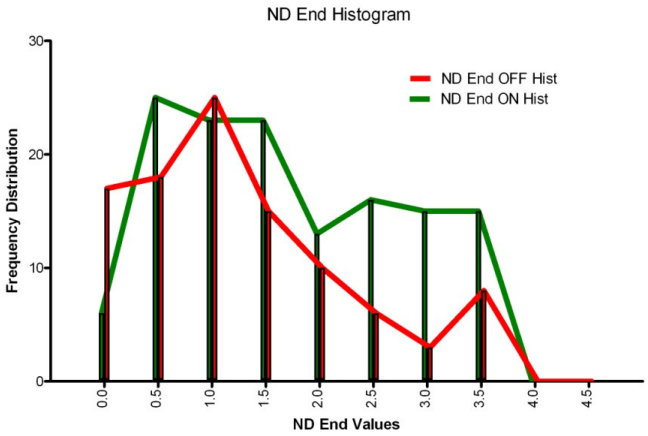

Graph 43: Histogram of the ND End parameter for ON and OFF population

The histogram in the graph 44 of the *ND End* clarifies the ON terminals are more sensitive than the OFF ones, as these ones stop responding at higher light intensities.

ND Range

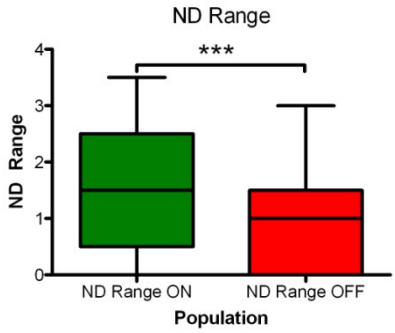

Graph 44: Box-Whiskers plot of the ND Range parameter

The values of *ND Range* are significantly different between the ON and OFF population and this is confirmed by the P-value (<0.0001) of the Mann-Whitney test, as the Box and Whisker in the graph 46 represents.

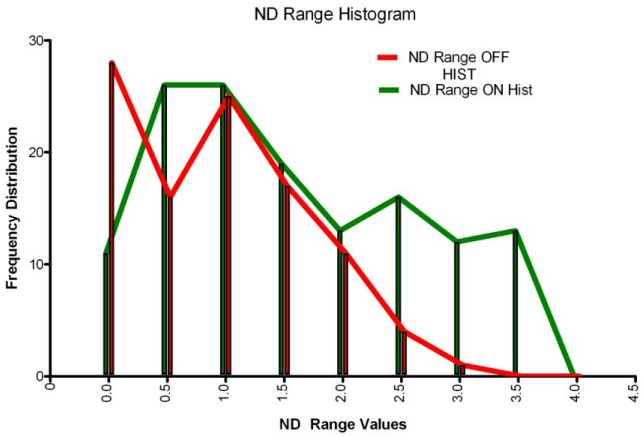

Graph 45: Histogram of the ND Range parameter for ON and OFF population

Both ON and OFF terminals respond well at ND00, but the ON terminals are more sensitive than the OFF ones: the ON cells have a broader range of light intensities to which they are responsive, as the histogram show in its right side in the graph 47.

Terminal Dimension

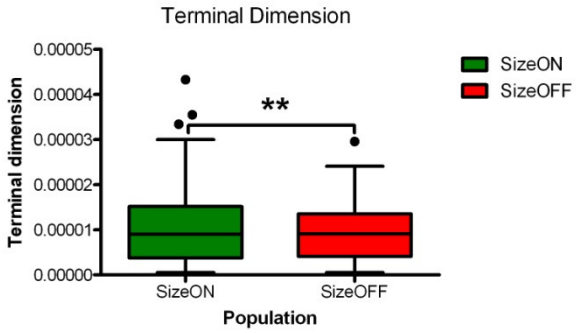

Graph 46: Box-Whiskers plot of the Dimension parameter

The ON BCs size seems to be larger than the OFF BCs one as the Mann-Whitney test highlight with a P-value equal to 0.0015, as graphs 49 and 50 illustrate.

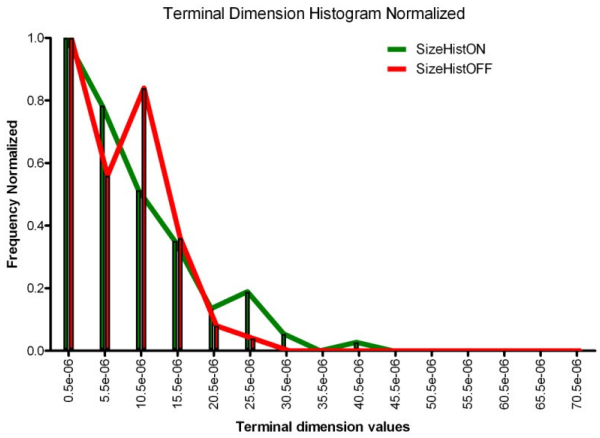

Graph 47: Histogram of the Dimension parameter for ON and OFF population

IPL Position

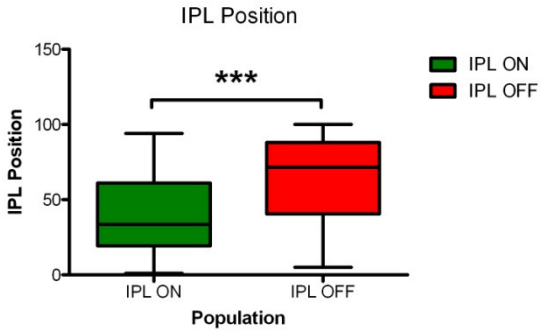

Graph 48: Box-Whiskers plot of the IPL position of the ON and OFF terminals

It is very well known the ON BCs terminals and the OFF BCs terminals occupy distinct layers in the IPL and as a matter of fact the P-value is <0.0001; a spatial segregation between the two opposite responses exists, as the graph 51 shows.

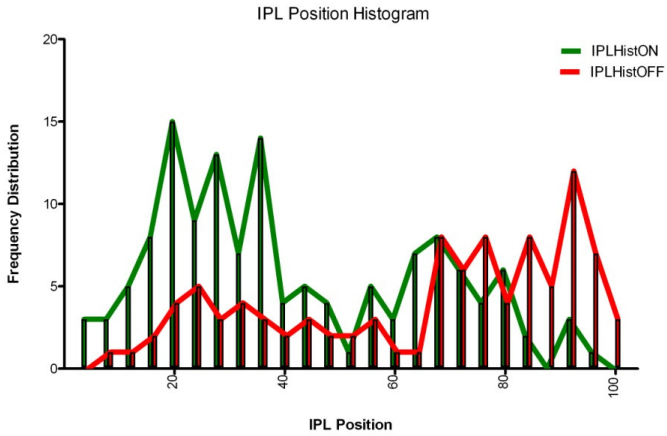

Graph 49: Histogram of the IPL position for ON and OFF population

From the histogram in the graph 52 it is noticeable there is a lack of terminals in the central zones. This zone is occupied by terminals with transient responses and as a matter of fact the terminals with this kind of response have not been found in the recordings of the experiments analyzed

3. *Clustering*

The cluster analysis is performed in order to group together terminals whose primary parameters have the similar trend over the light intensities; the K-means algorithm is thus applied just to the primary parameters. The results are the following:

- **Max Average clusters:** 7 groups
  - **1:** terminals low pass, responding just at ND00 and very low response at ND05
  - **2:** terminals low pass, responding well at ND00 and ND10 but with a notch at ND05
  - **3:** terminals low pass, with down ripple at ND10 and an up ripple at ND15
  - **4:** terminals low pass, responding until ND10
  - **5:** terminals really selective band pass with a peak at ND00 and ND10
  - **6:** terminals really selective band pass with a peak at ND10
  - **7:** terminals band pass
- **Slope clusters:** 5 groups for ON and 7 groups for OFF
  - **1:** terminals low pass on the ND range, responding just at ND00 and very low response at ND05
  - **2:** terminals low pass, with a notch at ND05
  - **3:** terminals low pass, with down ripple at ND10 and an up ripple at ND15
  - **4:** terminals low pass, responding until ND10
  - **5:** terminals really selective band pass with a peak at ND00 and ND10
  - **6:** terminals with a selective band pass with a peak at ND1.0
  - **7:** terminals band pass
- **Area clusters:** 7 groups

- **1:** terminals low, responding just at ND00 and very low response at ND05
- **2:** terminals low pass, with a notch at ND05
- **3:** terminals low pass, with down ripple at ND10 and an up ripple at ND15
- **4:** terminals low pass, responding until ND10
- **5:** terminals really selective band pass with a peak at ND00 and ND10
- **6:** terminals really selective band pass with a peak at ND10
- **7:** terminals band pass

▪ **Reliability clusters:** 7 groups

- **1:** terminals low pass reliable until ND00
- **2:** terminals low pass reliable until ND05
- **3:** terminals low pass reliable until ND10
- **4:** terminals low pass, reliable until ND15
- **5:** terminals low pass, reliable until ND20
- **6:** terminals band pass, reliable from ND05 until ND15
- **7:** terminals band pass

▪ **Reliability Aligned clusters:** 6 groups

- **1:** terminals low pass reliable just at their maximum
- **2:** terminals low pass, reliable until 05 ND unit from their maximum
- **3:** terminals low pass, reliable until 10 ND unit form their maximum
- **4:** terminals low pass, reliable until 15 ND unit from their maximum
- **5:** terminals low pass, reliable until 20 ND unit from their maximum
- **6:** terminals with oscillatory reliability

▪ **Slope Normalized clusters:** 6 groups

- **1:** terminals low pass, rapidly responding at ND00

- **2:** terminals low pass, rapidly responding until ND05
- **3:** terminals low pass, rapidly responding until ND10
- **4:** terminals low pass, rapidly responding until ND15
- **5:** terminals selective band pass, rapidly responding at ND 20
- **6:** terminals selective band pass, rapidly responding at ND30

There are three main types of the clusters as they express three main behaviors

- Low Pass: terminals respond well just at high level of light intensity; they correspond to the less sensitive terminals, because they do not produce a significant signaling for stimuli at low intensities. In figure 18 there are three clusters with low pass behavior

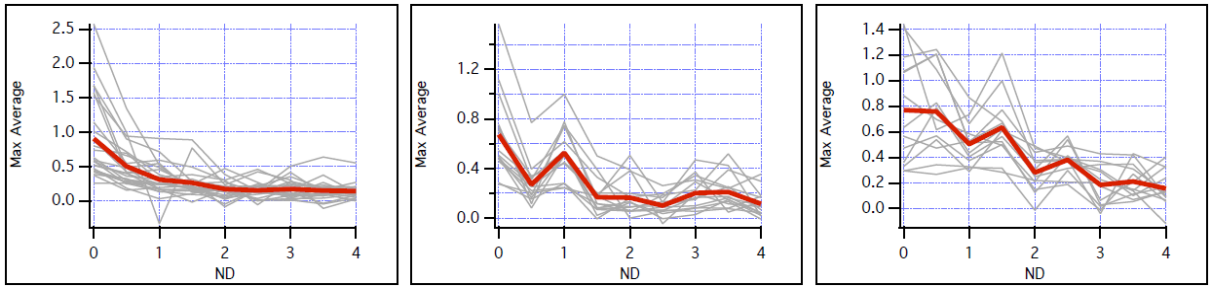

Figure 18: Clusters of the low pass intensity groups

- Band Pass: terminals respond well at broader level of light intensities so they are well performers also during dimmer light conditions. In the figure 19 there are three clusters with band pass behavior

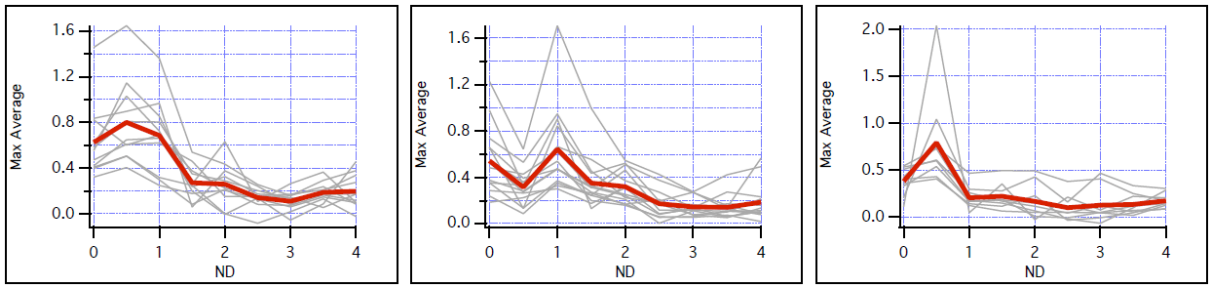

Figure 19: Clusters of the band pass intensity groups

- Band Pass / High Pass: terminal respond well at intermediate and lower level of light intensities; they correspond to the most sensitive terminals because their

activity is triggered also for small stimuli. In the figure 20 there is one cluster with band pass/ high pass behavior

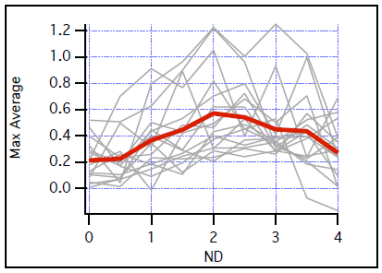

Figure 20: Cluster of the band pass/ high pass intensity group

4. *Model Identification*

The model attempts to represent the variation in the calcium concentration triggered by a light stimulation by a linear equation whose coefficients describe the dynamics of such a phenomenon. Furthermore the linear equation provides a quantitative methods for simulating the effects on different experimental conditions such as the change of the input shape.

I have taken as an example the ON terminal 53.

The figures 21, 22, 23 respectively depict the response at the light intensity ND00, ND05, ND10.

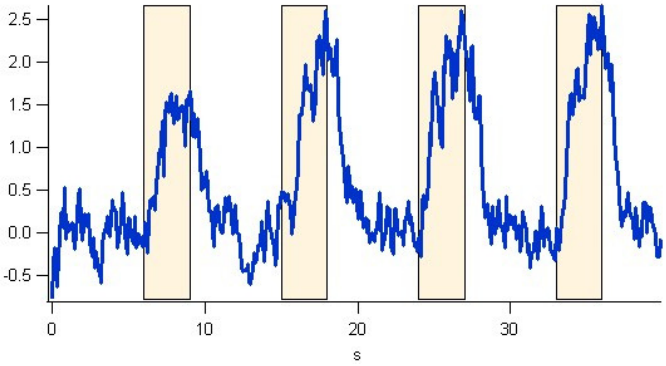

Figure 21: Fluorescence signal of the terminal 53 at ND00

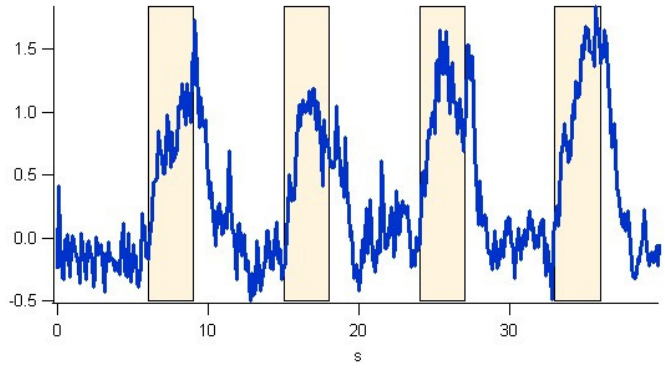

Figure 22: Fluorescence signal of the terminal 53 at ND05

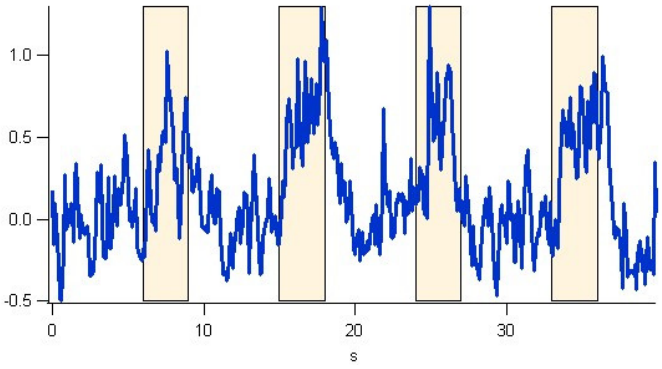

Figure 23: Fluorescence signal of the terminal 53 at ND10

The models representing the terminal behaviors are respectively:

$$y(t) = \frac{0.0856\, z^{-3} + 0.101\, z^{-4}}{1 - 0.9262\, z^{-1}} \quad (Eq\ 1)$$

$$y(t) = \frac{0.1175\, z^{-1} - 0.1107\, z^{-2}}{1 - 1.911\, z^{-1} + 0.9189\, z^{-2}} \quad (Eq2)$$

$$y(t) = \frac{0.02699\, z^{-2} + 0.005195\, z^{-3}}{1 - 1.649\, z^{-1} + 0.7031\, z^{-2}} \quad (Eq3)$$

In the current thesis three tools are chosen to present the results of the model identification: the Akaike final prediction error, the impulse response, and the linear simulation with a step input.

The Akaike FPE is used to select the best order of the model in the identification phase, by choosing the one with the smallest FPE value.

The first model (Eq1) has a FPE equal to 0.00880722, the second one (Eq2) 0.00313699 and finally the third one (Eq3) 0.00448565

The impulse response describes how the terminal would respond if the input would be an impulse, i.e. a signal of infinite energy and stimulating the entire band of frequency; the impulse response is important because its Laplace transform is the transfer function of the system, that is the mathematical representation of the relation between the input and the output. The graph 53 depicts the impulse response for the models of the T53 responses

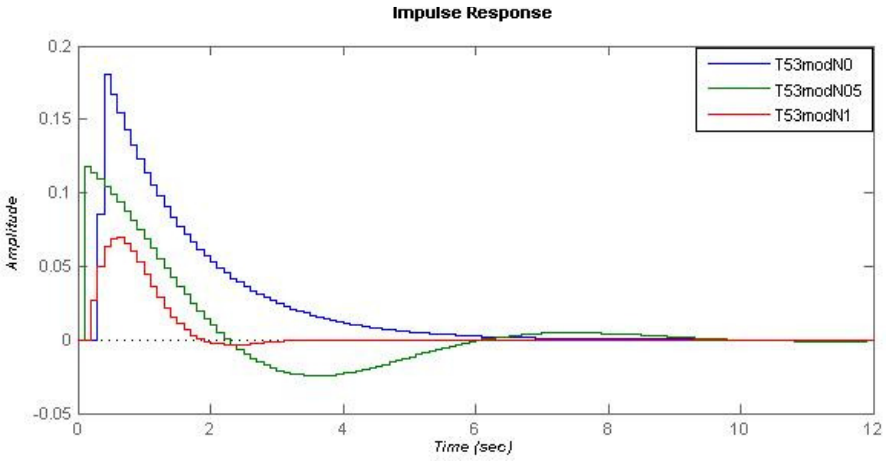

Graph 50: Impulse response of the model terminal 53 at ND00,ND05,ND10

By the linear simulation, the real experimental stimuli, the four light steps, are provided to the model and the graph 54 depicts its outputs.

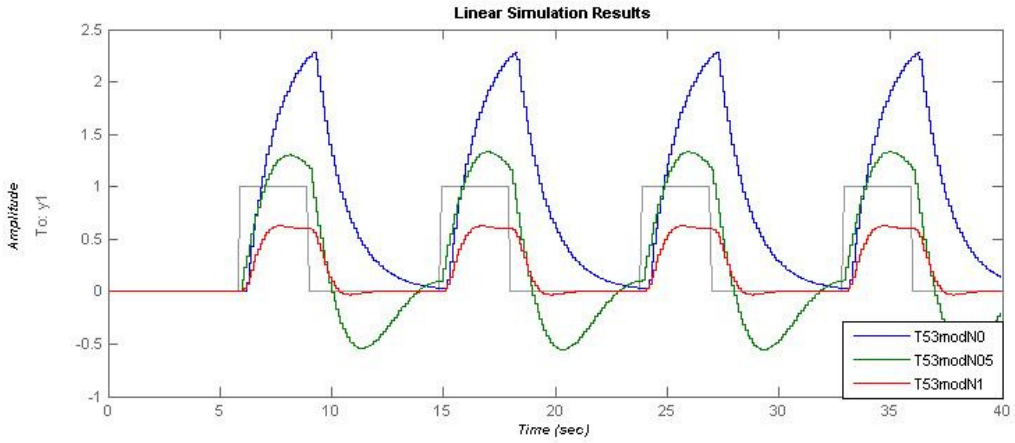

Graph 51: Linear simulation of the model terminal 53 at ND00, ND05, ND10

IV. DISCUSSION

In the discussion of the results the key points are:

- Difference in the parameters and in the dynamics between the ON BCs population and the OFF BCs one
- Significant relations between the parameters
- The spatial distribution of the parameters
- Model identification goodness

1. *Comparison between ON BCs and OFF BCs populations*

The basic difference in the behavior of the ON and OFF BCs derives from their different receptors (Masu et al., 1995).The OFF express ionotropic receptors that open the cation channels during glutamate release from the photoreceptors, whereas the ON express metabotropic and ionotropic receptors that close the cation channels. Since the photoreceptors discharge during the absence of light, the glutamate released produces a depolarization of the OFF and the hyperpolarization of the ON during the absence of light. The fundamental distinction between the two populations of BCs is due to the presence on their dendrites of excitatory (OFF) and inhibitory (ON) receptors for glutamate (Nomura & Shigemoto, 1994).

There are statistically significant differences between the ON BCs and OFF BCs on the primary parameters just at the brightest light conditions; by decreasing the amplitude of the light stimulus, the two populations tendto have similar values distribution. The primary parameters describe the basic features of response: the magnitude of the variation in the $\frac{\Delta F}{F_0}$ and the rapidity of such a variation to occur.

I have compared the ON BCs and the OFF BCs regarding the derived parameters. As explained in the **Material and Method** chapter, these parameters can be grouped in two categories, one focusing on the temporal evolution of the terminal activity during the four flashes, the other focusing on the terminal performances as an analogue sensor.

At the first category belong the *peak shift*, the increasing/ decreasing in *selectivity* and the *potentiation/adaptation*.

The ON BCs and the OFF BCs have comparable values and values distribution about the peak shift and the increasing/decreasing *selectivity*; if an ON BC and OFF BC are randomly selected, they are expected to become or more selective responding to a narrow range of light intensities or less selective responding to a broader range of light intensities. ON and OFF population have an important difference concerning the

potentiation/adaptation measures. The ON BCs terminals tend to increase/decrease the magnitude of their activity responding to a four flash train more than the OFF BCs do; it means the ON BCs terminals are more keen than the OFF BCs ones to increment/decrement the calcium level inflow and thus to run out/save the neurotransmitter to be release for further signal transmission.

Regarding the second group of derived parameters, there are more differences.

The *precision* parameter shows the OFF BCs terminals are more precise than the ON BCs ones, and thus they are able to give the same identical responses to four stimuli following each other, maintaining both the shape and the magnitude of the response.

Furthermore there is a significant difference between the two population in the value of light intensity at which their terminals stop to respond, the *ND End*. It is the minimum level of light intensity at which the terminal activity can be distinguished from the basal synaptic activity. It is a measure of the terminal sensitivity, the terminal ability to detect the slightest change in the environment illumination. The ON BCs terminals still respond to very low light levels such as ND25, ND30, ND35 which are intensities more than two-three order of magnitude less than the maximum one. Instead the OFF BCs terminals have almost stopped any activity at this low level of stimulation.

Related to the previous measure, there is the *ND Range*, an indicator of the terminal ability to respond to a broad or narrow range of light intensities. Not only the ON BCs terminal are more sensitive than the OFF BCs ones, but they are active for broader range of light intensities and thus they start responding at maximum level of stimulus amplitude and their activity lasts till low light intensities.

The terminal dimension and the position in the IPL are further features in which ON and OFF populations seem to have not negligible differences: the ON terminals are generally bigger than the OFF ones, and they are located in the IPL layers closed to the ganglion cells, while the OFF terminals are closer to the photoreceptors layers.

2. *Relation between the parameters*

I have studied whether the terminals characteristics are related between each other, to assess whether a specific value in a parameter influences the values of other parameters.

An evident relation exists between the size and the plasticity of the terminal. The relation is an inverse one: smaller terminal are more plastic than the bigger ones, because in the smaller terminals even a slight change in the calcium level inflow can modify remarkably the overall terminal activity. To highlight this relation the graph 55 represents *Adaptation/Potentiation* against *size*, the graph 56 *Peak Shift* (the absolute values) against *size* and finally the graph 57 illustrates the increase and decrease in *selectivity* against the *size*

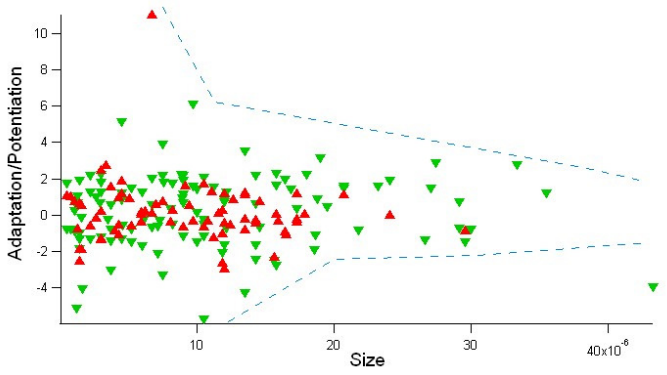

Graph 52: Relation between Adaptation/Potentiation and size for ON (green) and OFF (red) BCs

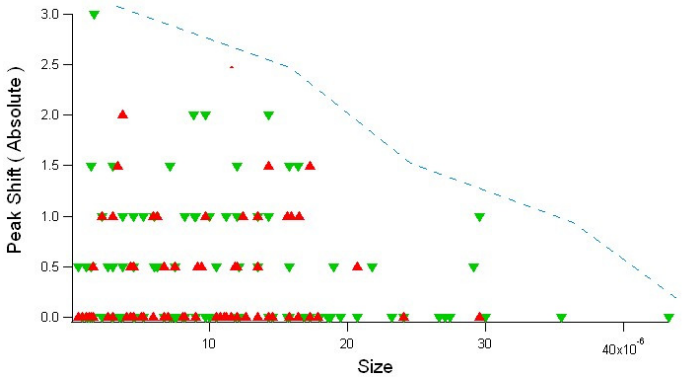

Graph 53: Relation between Peak Shift (absolute) and size for ON (green) and OFF (red) BCs

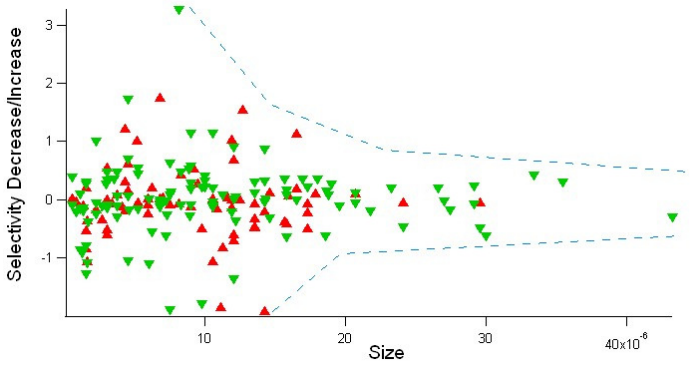

Graph 54: Relation between Selectivity and size for ON (green) and OFF (red) BCs

The magnitude in the variation of $\frac{\Delta F}{F_0}$ signal during the activation, represented by the maximum value of the *max average*, is related to plasticity: the terminals with larger variation in the $\frac{\Delta F}{F_0}$ are those whose response changes remarkably during a four light step stimulation, and so they are the more plastic. The graph 58 with the maximum values of the *max average* against the *adaptation/potentiation* and the graph 59 with maximum values of the *max average* against the increase/decrease in *selectivity* show this result.

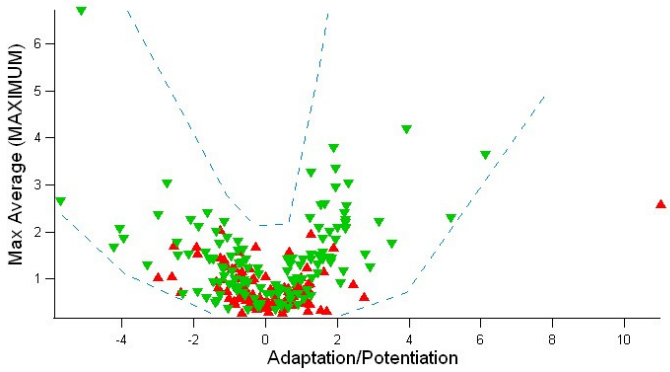

Graph 55: Relation between Max Average (Maximum) and Adaptation/Potentiation for ON (green) and OFF (red) BCs

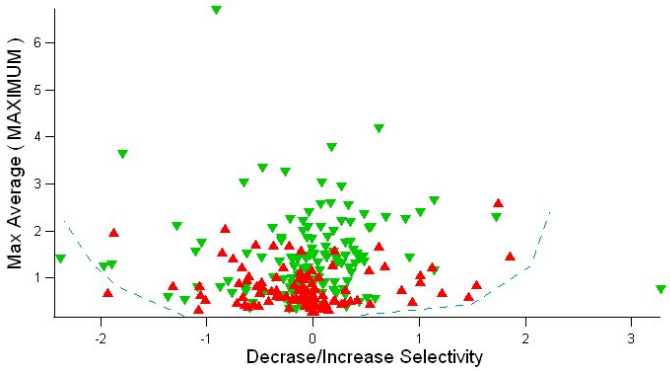

Graph 56: Relation between Max Average (Maximum) and Selectivity for ON (green) and OFF (red) BCs

The magnitude variation in $\frac{\Delta F}{F_0}$ is positively related to the plasticity indicator as well as it is negatively related to the *precision* indicator, as in graph 60.

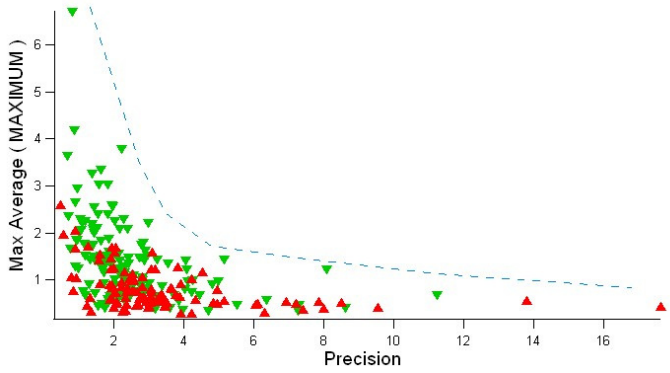

Graph 57: Relation between Max Average (Maximum) and Precision for ON (green) and OFF (red) BCs

As a matter of fact, the *precision* of a terminal indicates how well the terminal has the same response to the same stimulus repeated over the time: it is high when the terminal tends to be not plastic at all. The graph 61 depicts the *adaptation/potentiation* against the *precision*.

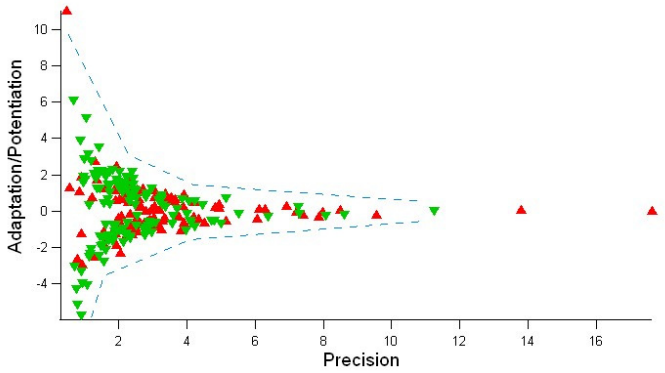

Graph 58: Relation between Adaptation/Potentiation and Precision for ON (green) and OFF (red) BCs

I have taken the maximum value of *reliability* and I have related it to the maximum value of *max average* of the same terminal: they are positively related, therefore the more is the magnitude of the $\frac{\Delta F}{F_0}$ the higher is the change that at least one value of light intensity the terminal would respond to all four the light steps, as the graph 62 shows.

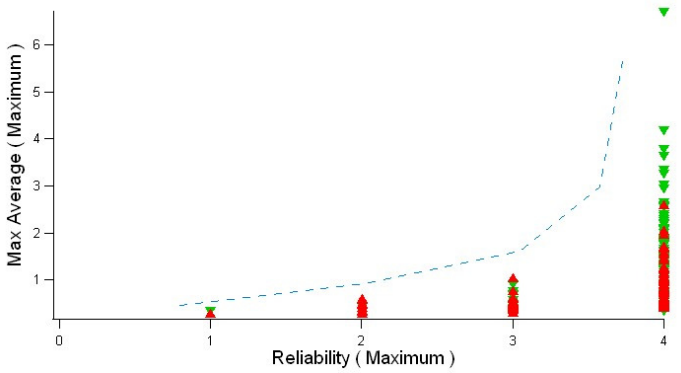

Graph 59: Relation between Max Average (Maximum) and Reliability (Maximum) for ON (green) and OFF (red) BCs

A better parameter is the *reliability aligned*, which takes into account how rapidly the terminal shuts down its activity after the optimal responsive zone. A score equal to 1 is assigned to terminals ceasing their signaling after the last light intensity of the optimal responsive zone, a score equal to 0 at the others. Representing the score against the maximum of the *max average*, it is clear this value does not affect the score: terminals characterized by a large $\frac{\Delta F}{F_0}$ signal and the ones characterized by a smaller values have no differences in their ability in not responding to random events. The graph 63 clarifies this relation.

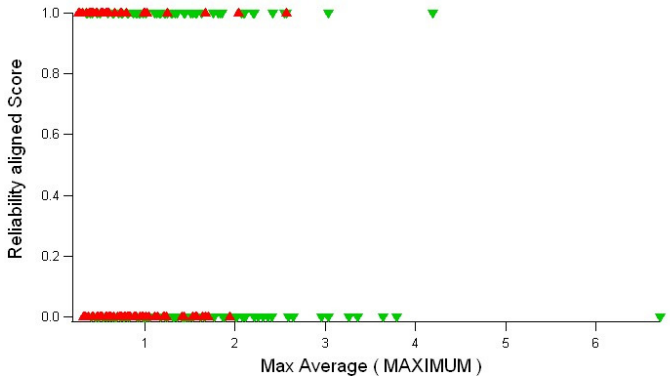

Graph 60: Relation between Score and Max Average (Maximum) for ON (green) and OFF (red) BCs

3. *Distribution of the BCs parameters on the IPL space*

From the literature it is known the spatial organization of the retina is an important feature of the visual system to provide a first step in the signal processing (S M Wu, Gao, & Maple, 2000) (Calkins, Scheln, Tsukamoto, & Sterling, 1994); as a matter of fact the layers in the IPL contain terminals responding to different frequencies in the stimulation: the terminal with transient response able to transmit high frequency visual signals occupy the central layers; the terminal with sustained response are in the lateral layers (Awatramani & M. M. Slaughter, 2000). For this reason it was interesting to explore whether the parameters and clusters had a peculiar distribution inside the IPL or were evenly distributed.

By studying the distribution of parameters expressing different characteristics of the $\frac{\Delta F}{F_0}$ signal, it is clear they are evenly distributed in the IPL. From the terminal size to its plasticity (*adaptation/potentiation*), from the terminal *precision* to its sensitivity, the various values of these measures can be founded at every layer of the IPL. It means that the all possible dynamic behaviors are associated to every frequency represented in the distinct layers; so in the layer 20-30 there can be found both big and small terminals, both precise and plastic terminals and so on. The graphs 64, 65, 66, 67, 68 depict the parameters value for each terminal against the IPL position of the terminal.

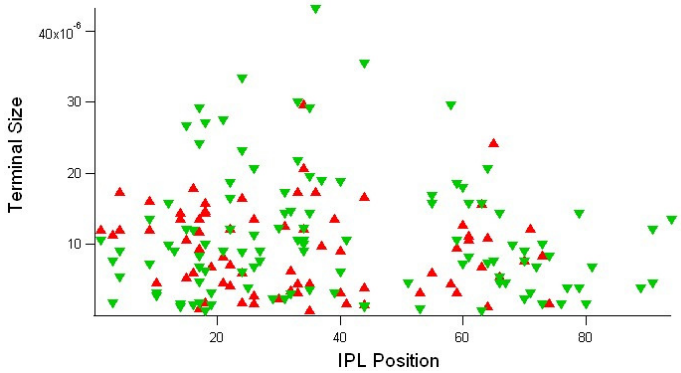

Graph 61: Spatial distribution of the terminal sizes for ON (green) and OFF (red) BCs

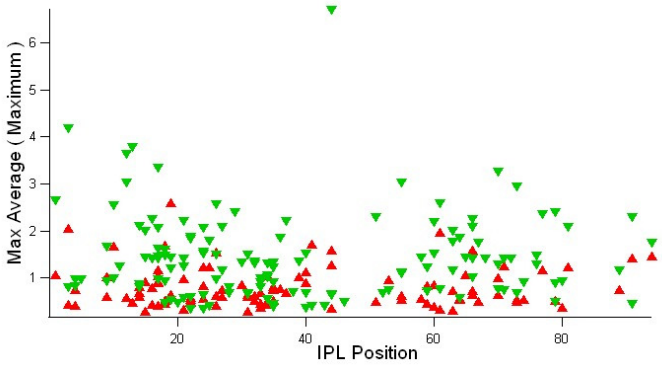

Graph 62: Spatial distribution of the Max Average (Maximum) for ON (green) and OFF (red) BCs

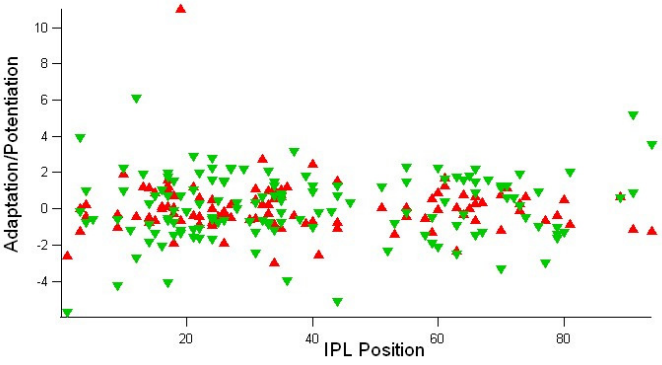

Graph 63: Spatial distribution of the Adaptation/Potentiation for ON (green) and OFF (red) BCs

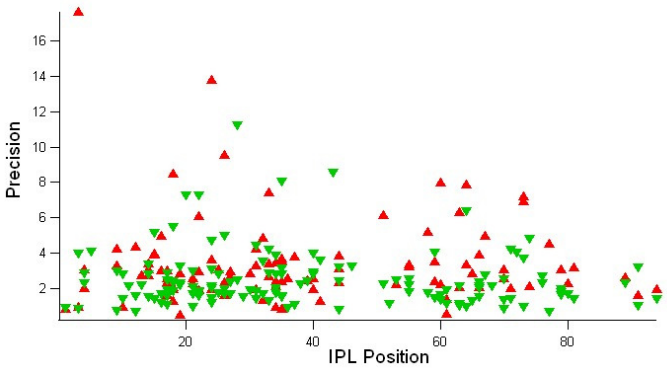

Graph 64: Spatial distribution of the Precision for ON (green) and OFF (red) BCs

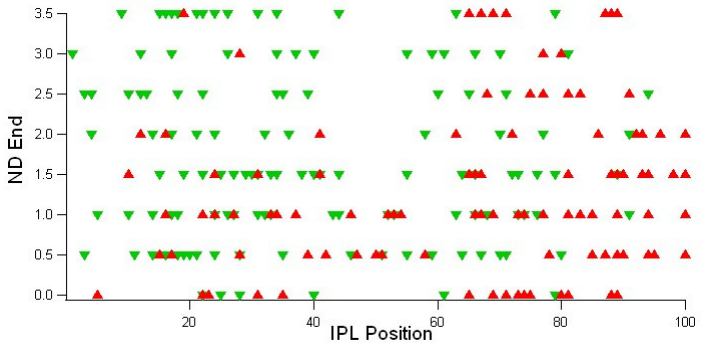

Graph 65: Spatial distribution of the ND End for ON (green) and OFF (red) BCs

The result of the clustering analysis is a set of cluster grouping together terminals with similar trend over the intensity levels of the stimuli: some act as low pass filter to the light intensity, by responding just to the brighter light stimulation, others as band pass filter by showing a calcium activity also to attenuated level of the light stimulus, finally others have a stronger $\frac{\Delta F}{F_0}$ signal at intermediate level of light intensities and tend to not respond or to weakly respond to the brightest conditions.

The graphs 69, 70, 71, 72 represent for different parameter how the clusters are distributed along the IPL layers.

The clusters evenly sample the IPL; each layer has the entire range of light intensity from the brightest to dimmest one. Again it is a significant result because it means that for each signal frequency it is represented the entire range of light intensities.

In the layers 60-70 a specific stimulation frequency is represented; in this layer there are BCs terminals responding only to the brighter light and others activated significantly for mild range of light intensity.

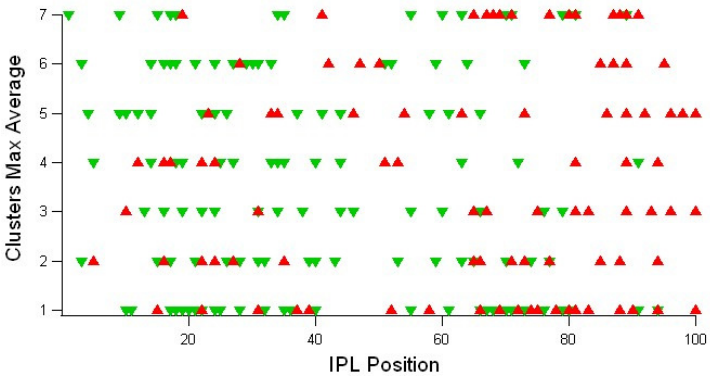

Graph 66: Spatial distribution of Max Average Clusters for ON (green) and OFF (red) BCs

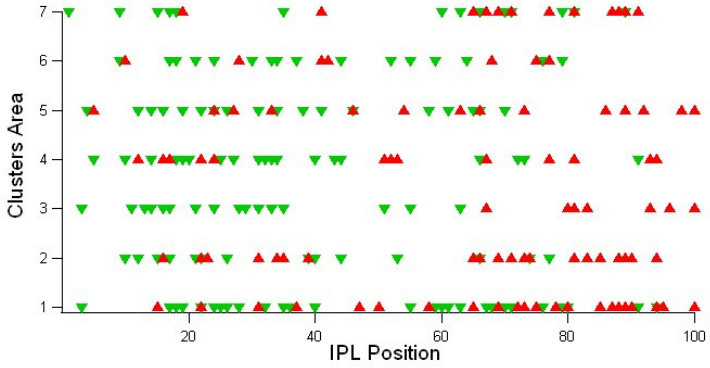

Graph 67: : Spatial distribution of Area Clusters for ON (green) and OFF (red) BCs

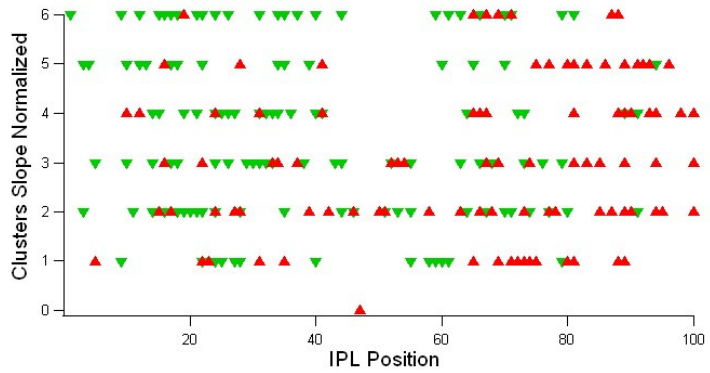

Graph 68: : Spatial distribution of Slope Normalized Clusters for ON (green) and OFF (red) BCs

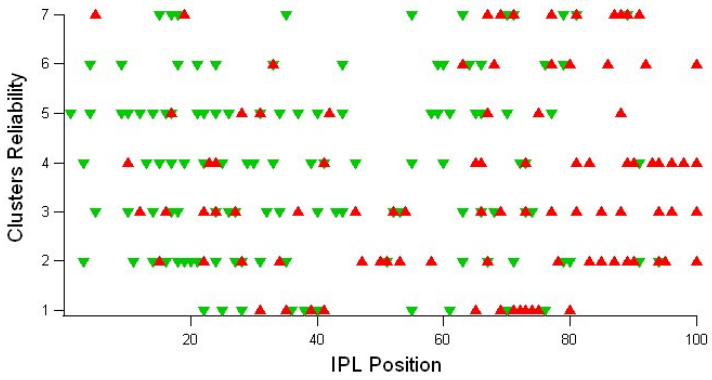

Graph 69: : Spatial distribution of Reliability Clusters for ON (green) and OFF (red) BCs

4. *The results goodness from the model identification*

The ultimate objective of a model identification is to describe a phenomenon through a mathematical equation. The Box-Jenkins is a linear method and so it assumes a linear transformation of the input to generate the output. The resulting composition of polynomial describes the system as its inner transformations are simply linear.

This is an important obstacle to the model identification. The variation in the $\frac{\Delta F}{F_0}$ is the output of the real system and it is, together with the step stimulus, the dataset for feeding the identification algorithm. However the $\frac{\Delta F}{F_0}$ signal is the potential effect of many causes and not only of the light step stimulus. ACs and HCs send signals and feedbacks to the BCs to regulate the variation in the calcium inflow for optimizing the signal transmission as well as the released vesicles (Trombley & Westbrook, 1992). Together with the light stimulus these other mechanisms are involved and they are composed through a non linear transformation to determine the calcium inflow and thus the variation in the $\frac{\Delta F}{F_0}$.

The method of model identification by a Box-Jenkins algorithm has two main problems:

The input data used to feed the identification algorithm are just referred to the light step stimulus, while the other input to the real system such as the signaling from the ACs, HCs and the feedbacks from the vesicles released are left out.

The inner process to transform the inputs in the output are assumed to be linear, whereas the real neuronal system present many non linear features, such as time delays, plasticity over the time and so on.

The results from the model identification do not simulate reliably the real terminal dynamics. The low goodness of the results demonstrate the machinery inside the synaptic terminals receives as input many signals and that these inputs are composed in non linear fashion in order to manage and regulate the calcium inflow inside the membrane.

V. CONCLUSIONS

The retina is one of the most ancient structure of the central nervous system, whose layered organization is very similar to the one of the cerebral cortex. . Retina does much more than encode the outside world in electrical signals; it process the visual information thanks to an highly organized neuronal network, in which the BCs occupy literally and figuratively a central role. The BCs importance in visual information processing is clear: there are two basic types of photoreceptors but there are many types of ganglion cells instead, which receive different types of signals and send out different types of signals. This means that BCs provide a first significant processing in the visual information from the photoreceptors to the GCs.

In this thesis, I have implemented algorithms for studying some parameters and indicators; these were useful for a quantitative description of the calcium activity, important indicator of the neurotransmitter release magnitude and dynamics in the BCs. It was interesting how their responses and behavior was spread over a wide range. There are BCs subjected to a large calcium inflow and thus providing a relevant neurotransmitter release for every stimulus, while others adapts and lower their neurotransmitter release over the repetition of the stimulus. Some BCs are high sensitive and they are able to respond at light intensities very close to the dim conditions, while other have strong and reliable responses just at high light intensities. Many BCs provides the same response over the repetition of the stimulus, while many others react to repeated stimuli adapting or potentiating their neurotransmitter release.

These results have highlighted how BCs work as a composite array of detectors endowed with different features. The different visual information components are segregated through different GC pathways and travel toward the visual cortex, where they are combined for the final processing. It is interesting that the distinct frequency components are represented in distinct substrata, while other feature detectors are evenly distributed in the substrata of the IPL. Therefore the IPL is organized to convey the whole information composition for each light frequency and thus to reliably transmit the visual signal.

Results also underlined that there are significant differences in the responses between ON and OFF BCs. These differences can have many causes. ON and OFF BCs have different receptors that can provide the terminals with different dynamics. Signals and feedbacks from HCs and ACs can be involved to optimize the signal processing and transmission in these two channels. In future research will be of interest to isolate the feedbacks from ACs and other cells for analyzing their effect on the BCs terminals responses.

Future development of the thesis may involve a new method for the model identification. Specifically a method able to take into the model the non linearity in the interaction between the many factors contributing to the terminal response. An accurate model of the BCs terminals is an useful tool for the current scientific researches about the retinal prosthesis. In this field, up to now, the scientists have addressed their attempts toward a better design of the prosthetic devices in the hardware component, by reducing dimension and increasing the number of wires (Weiland, Liu, & Humayun, 2005). The next step will be the implementation of the software with processing capacity similar to the retinal one in order to provide the most effective signal processing algorithms for improving the patients' quality of life.

VI. APPENDIX

In the following section, there is a description of the algorithms implemented and used during the thesis work. The software used have been IgorPro and Matlab. At end there are the contacts for who is interested in having the algorithms code. At first there are the two basic algorithms for the main work of the thesis, **procedure1** and **procedure2**; then there are the additional algorithms for refining the operations of data processing.

The algorithms are available in CD format at the Prof. Signorini's office, Biomedical Engineering Department, Politecnico di Milano, Milan. Please contact:

mariagabiella.signorini@polimi.it

federico.capiaghi@gmail.com

- **procedure1**: it calculates from the preprocessed recordings the primary parameters and creates graphs of the parameters trend over the light intensities
  - Input: the preprocessed recordings
  - Output: the primary parameters and the graphs about their trend
- **procedure2**: it calculates the derived parameters and organize the data in a large dataset. It carries out the studies of the populations and represents them through graphs and figures.
  - Input: the primary parameters
  - Output: the derived parameters, the terminals dataset and the graphs of the studies about the ON and OFF populations

- **align**: it aligns the signals of the parameters varying over the ND; it shift the starting point from ND00 to ND*, where ND* is the ND corresponding to the maximum value of that signal. It calculates for example the *reliability aligned*.
    - Input: the parameter
    - Output: the parameter aligned
- **cont_terminals**: it counts the number of terminals included and excluded in a certain range of values.
    - Input: the terminals dataset, and the max and min value of the range
    - Output: the number of the terminals included in the range and the number of the ones excluded
- **create_max**: it creates a vector whose elements are the maximum values of a specific parameter for each terminal.
    - Input: the terminals dataset and the parameter
    - Output: the vector containing the max values of the parameter
- **extract_clust**: it extracts from the terminals dataset and groups together the parameters of terminals belonging to the same cluster
    - Input: the terminals dataset, the subdivision in clusters
    - Output: a dataset of terminals grouped following the clustering scheme
- **extract_nd**: it creates a vector with the parameters at different NDs
    - Input: the terminals dataset, the ND desired
    - Output: the vector of the parameter at the ND desired
- **index***:* it extract the ND corresponding to the beginning and the end of the responsive zone

- Input: terminal dataset
- Output: the extreme NDs of the responsive range

- **modifyslope**: set 0 the points that are out of the responsive zone
  - Input: *slope* parameter
  - Output: the slope parameter modified
- **norm_hist**: normalize bin per bin by the total number of terminal in each bean
  - Input: the histogram to be normalized
  - Output: the histogram normalized
- **set_clust***:* takes the data from the different clusters and order them on a new column of the terminals dataset
  - Input: the clusters
  - Output: the terminals dataset with the added cluster labels
- **set_roisize**: computes the real size of terminal using the number of pixel for each terminal and the size in μm of the pixel
  - Input: the ROI mask
  - Output: the size of each terminal expressed in μm
- **set_slpnrm**: it calculates the *slope normalized* parameter:
  - Input: *slope* and *max average* parameters
  - Output: *slope normalized* parameter

VIII. **REFERENCES**

Amthor, F. R., Takahashi, E. S., & Oyster, C. W. (1989). Morphologies of rabbit retinal ganglion cells with complex receptive fields.pdf. *The Journal of Comparative Neurology*, *280*(1), 97-121.

Augustine, G. J. (2001). How does calcium trigger neurotransmitter release? *Current opinion in neurobiology*, *11*(3), 320-6. Retrieved from http://www.ncbi.nlm.nih.gov/pubmed/11399430

Awatramani, G. B., & Slaughter, M. M. (2000). Origin of transient and sustained responses in ganglion cells of the retina. *The Journal of Neuroscience*, *20*(18), 7087-95. Retrieved from http://www.ncbi.nlm.nih.gov/pubmed/10995856

Awatramani, G. B., & Slaughter, M. M. (2001). Intensity-dependent, rapid activation of presynaptic metabotropic glutamate receptors at a central synapse. *The Journal of neuroscience: the official journal of the Society for Neuroscience*, *21*(2), 741-9. Retrieved from http://www.ncbi.nlm.nih.gov/pubmed/11160453

Baier, H. (2000). Zebrafish on the move□: towards a behavior – genetic analysis of vertebrate vision. *Current Opinion in Neurobiology*, *10*, 451-455.

Belgum, J., & Copenhagen, D. (1988). Synaptic Transfer of Rod Signals to Horizontal and Bipolar Cells in the Retina of the Toad. *Journal of Physiology*, *396*, 225-245.

Boycott, B., & Wassle, H. (1974). The Morphological Types of Ganglion Cells of the Domestic Cat's Retina. *The Journal of Physiology*, *240*, 397-419. doi:10.1002/cne.903240411

Burger, W., & Burge, M. (2008). Edges Sharpening. In Springer (Ed.), *Digital Image Processing* (1st ed., pp. 130-137).

Calkins, D., Scheln, S., Tsukamoto, Y., & Sterling, P. (1994). M and L cones in macaque fovea connect to midget ganglion cells by different numbers of excitatory synapses.pdf. *Nature*, *371*, 70-72.

Chalpua, L. M., & Werner, J. S. (2004). *The Visual Neurosciences*.

Cleveland, S. (1979). Robust Locally Weighted Regression and Smoothing Scatterplots.pdf. *Journal of the American Statistical Association*, *74*(368), 829-836. Journal of the American Statistical Association.

Connaughton, V. P., Graham, D., & Nelson, R. (2004). Identification and morphological classification of horizontal, bipolar, and amacrine cells within the zebrafish retina. *The Journal of comparative neurology*, *477*(4), 371-85. doi:10.1002/cne.20261

DeVries, S. H., & Schwartz, E. a. (1999). Kainate receptors mediate synaptic transmission between cones and "Off" bipolar cells in a mammalian retina. *Nature*, *397*(6715), 157-60. doi:10.1038/16462

Dorostkar, M. M., Dreosti, E., Odermatt, B., & Lagnado, L. (2010). Computational processing of optical measurements of neuronal and synaptic activity in networks. *Journal of neuroscience methods*, *188*(1), 141-50. Elsevier B.V. doi:10.1016/j.jneumeth.2010.01.033

Dreosti, E., Odermatt, B., Dorostkar, M. M., & Lagnado, L. (2009). A genetically encoded reporter of synaptic activity in vivo. *Nature methods*, *6*(12), 883-9. Nature Publishing Group. doi:10.1038/nmeth.1399

D'Agostino, R., & Belanger, A. (1990). A Suggestion for Using Powerful and Informative Test of Normality. *The American Statistician*, *44*(4), 316-321.

Juusola, M., French, A., UUsitalo, R., & Weckstrom, M. (1996). Information processing by graded-potential transmission through tonically active synapses. *Trends in Neurosciences*, *19*, 292-297.

Kaneko, B. Y. A. (1970). Physiological and Morphological Identification of Horizontal, Bipola and Amcacrine cells in the Goldfish Retina. *Journal of Physiology*, *207*, 623-633.

Karlsson, J., von Hpfsten, J., & Olsson, P. (2001). Generating transparent zebrafish: a refined method to improve detection of gene expression during embryonic development. *Marine Biotechnlogy*, *3*, 522-527.

Lagnado, L., Gomis, A., & Job, C. (1996). Continuous Vesicle Cycling in the Synaptic Terminal of Retinal Bipolar Cells. *Neuron*, *17*, 957-967.

Ljung, L. (1999). System Identification. *The Control Handbook* (pp. 1033-1053).

Mann, H., & Whitney, D. (1947). On a Test of Whether one of Two Random Variables is Stochastically Larger than the Other. *The Annals of Mathematical Stastistics*, *18*(1), 50-60.

Masu, M., Iwakabe, H., Tagawa, Y., Miyoshi, T., Yamashita, M., Fukuda, Y., Sasaki, H., et al. (1995). Specific deficit of the ON response in visual transmission by targeted disruption of the mGluR6 gene. *Cell*, *80*(5), 757-765. Retrieved from http://www.ncbi.nlm.nih.gov/pubmed/7889569

Mollon, J., & Bowmakler, J. (1992). The spatial arrangement of cones in the primate fovea. *Nature*, *360*, 677-679.

Nakajima, Y., Iwakabe, H., Akazawa, C., Nawa, H., Shigemoto, R., Mizuno, N., & Nakanishi, S. (1993). Molecular characterization of a novel retinal metabotropic glutamate receptor mGluR6 with a high agonist selectivity for L-2-amino-4-phosphonobutyrate. *The Journal of biological chemistry*, *268*(16), 11868-73. Retrieved from http://www.ncbi.nlm.nih.gov/pubmed/8389366

Nomura, A., & Shigemoto, R. (1994). Developmentally regulated postsynaptic localization of a metabotropic glutamate receptor in rat rod bipolar cells. *Cell*, *77*(3), 361-369.

Pan, W., Lin, J., & Le, C. T. (2002). Model-based cluster analysis of microarray gene-expression data. *Genome biology*, *3*(2), 1-8. Retrieved from http://www.ncbi.nlm.nih.gov/pubmed/12926771

Parker, A. (2003). *In the blink of an eye: How vision sparked in the Big Bang of evolution* (Basic Book.).

Parsons, T. D., & Sterling, P. (2003). Synaptic ribbon. Conveyor belt or safety belt? *Neuron*, *37*(3), 379-82. Retrieved from http://www.ncbi.nlm.nih.gov/pubmed/12575947

Pologruto, T. a, Sabatini, B. L., & Svoboda, K. (2003). ScanImage: flexible software for operating laser scanning microscopes. *Biomedical engineering online*, *2*, 1-9. doi:10.1186/1475-925X-2-13

Slaughter, M., & Miller, F. (1985). CHARACTERIZATION OF THE ON BIPOLAR OF AN EXTENDED NEURON VERTEBRATE RECEPTOR RETINA. *The Journal of Neuroscience*, *5*(1), 224-233.

Sprague, J., Doerry, E., Douglas, S., & Westerfield, M. (2001). The Zebrafish Information Network (ZFIN): a resource for genetic, genomic and developmental research. *Nucleic acids research*, *29*(1), 87-90. Retrieved from http://www.pubmedcentral.nih.gov/articlerender.fcgi?artid=29808&tool=pmcentrez&rendertype=abstract

Tallini, Y. N., Ohkura, M., Choi, B.-R., Ji, G., Imoto, K., Doran, R., Lee, J., et al. (2006). Imaging cellular signals in the heart in vivo: Cardiac expression of the high-signal Ca2+ indicator GCaMP2. *Proceedings of the National Academy of Sciences of the United States of America*, *103*(12), 4753-8. doi:10.1073/pnas.0509378103

Trombley, Q., & Westbrook, L. (1992). L-AP4 Inhibits Calcium Currents and Synaptic Glutamate Receptor Transmission via a G-Protein-coupled Glutamate Receptor. *The Jouronal of Neuroscience*, *12*(6), 2043-2050.

Tsai, P. S., Nishimura, N., Yoder, E. J., Dolnick, E. M., White, G. A., & Kleinfeld, D. (2002). In vivo optical imaging of brain function. *In vivo optical imagin of brain function* (pp. 115-119).

Weiland, J. D., Liu, W., & Humayun, M. S. (2005). Retinal prosthesis. *Annual review of biomedical engineering*, *7*, 361-401. doi:10.1146/annurev.bioeng.7.060804.100435

Werblin, S., & Dowling, E. (1969). Organization of the Retina of the Mudpuppy , Recording Necturus macubsus . II . Intracellular. *Journal of Neurophysiology*, *32*, 339-355.

Williams, R. W., Cavada, C., & Reinoso-Suárez, F. (1993). Rapid evolution of the visual system: a cellular assay of the retina and dorsal lateral geniculate nucleus of the Spanish wildcat and the domestic cat. *The Journal of neuroscience:the official journal of the Society for Neuroscience*, *13*(1), 208-28. Retrieved from http://www.ncbi.nlm.nih.gov/pubmed/8423469

Wu, S M, Gao, F., & Maple, B. R. (2000). Functional architecture of synapses in the inner retina: segregation of visual signals by stratification of bipolar cell axon terminals. *The Journal of neuroscience: the official journal of the Society for Neuroscience*, *20*(12), 4462-70. Retrieved from http://www.ncbi.nlm.nih.gov/pubmed/10844015

Wu, Samuel M. (2010). Synaptic organization of the vertebrate retina: general principles and species-specific variations. *Investigative ophthalmology & visual science*, *51*(3), 1263-74. doi:10.1167/iovs.09-4396